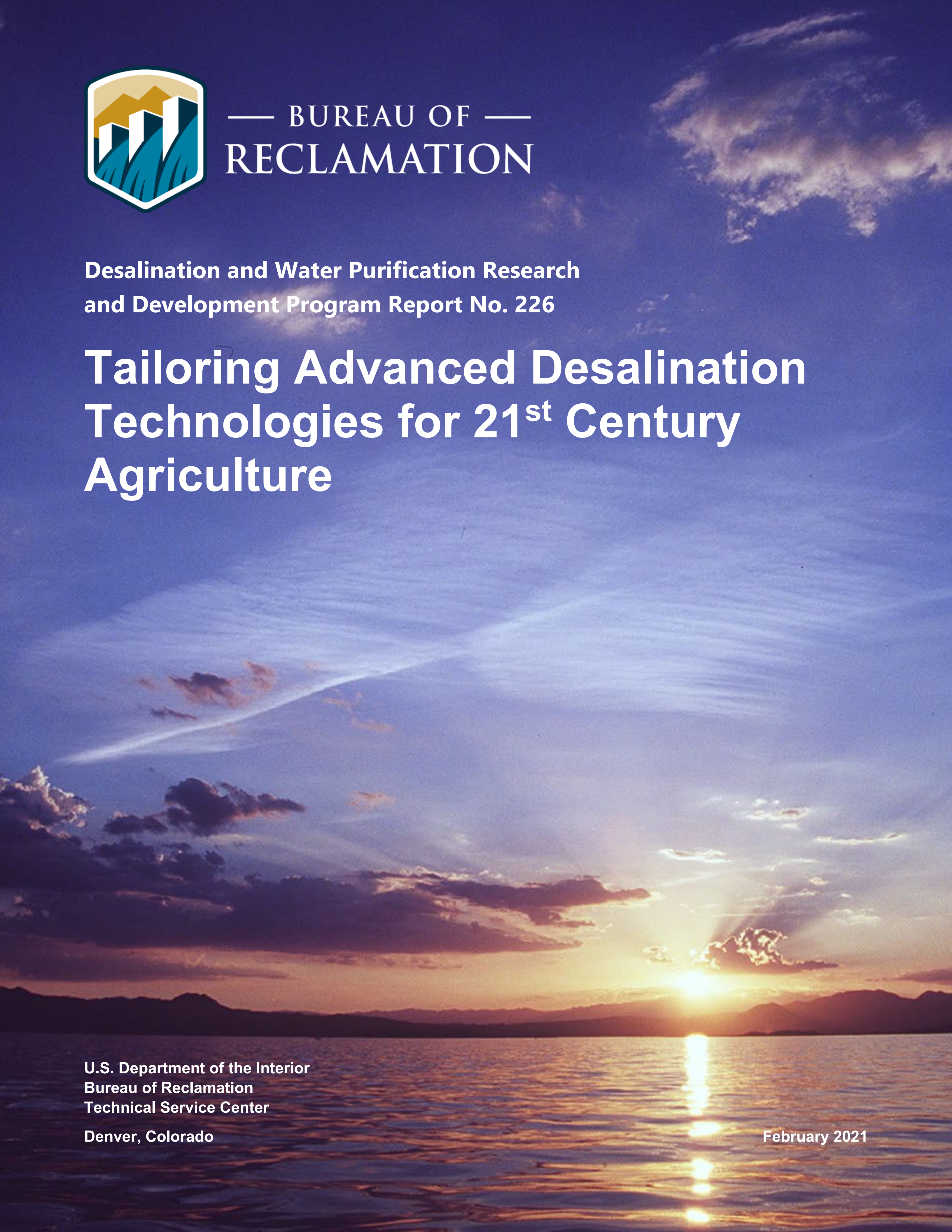

BUREAU OF RECLAMATION

Desalination and Water Purification Research
and Development Program Report No. 226

Tailoring Advanced Desalination Technologies for 21st Century Agriculture

U.S. Department of the Interior
Bureau of Reclamation
Technical Service Center

Denver, Colorado

February 2021

REPORT DOCUMENTATION PAGE	*Form Approved* *OMB No. 0704-0188*

1. REPORT DATE *(DD-MM-YYYY)* 31-09-2020	2. REPORT TYPE Final	3. DATES COVERED *(From - To)* 01-02-2018 to 30-06-2020

4. TITLE AND SUBTITLE Tailoring Advanced Desalination Technologies for 21st Century Agriculture	5a. CONTRACT NUMBER Agreement No. R17AC00135
	5b. GRANT NUMBER
	5c. PROGRAM ELEMENT NUMBER
6. AUTHOR(S) Y.D. Ahdab (Graduate Student) D. Rehman (Graduate Student) K.G. Nayar (Postdoctoral Researcher) J.H. Lienhard, V (Professor)	5d. PROJECT NUMBER
	5e. TASK NUMBER
	5f. WORK UNIT NUMBER
7. PERFORMING ORGANIZATION NAME(S) AND ADDRESS(ES) Massachusetts Institute of Technology 77 Massachusetts Ave., Cambridge, MA 02139-4307	8. PERFORMING ORGANIZATION REPORT NUMBER
9. SPONSORING/MONITORING AGENCY NAME(S) AND ADDRESS(ES) Bureau of Reclamation U.S. Department of the Interior Denver Federal Center PO Box 25007, Denver, CO 80225-0007	10. SPONSOR/MONITOR'S ACRONYM(S) Reclamation
	11. SPONSOR/MONITOR'S REPORT NUMBER(S) DWPR Report No. 226

12. DISTRIBUTION/AVAILABILITY STATEMENT
Available from https://www.usbr.gov/research/dwpr/DWPR_Reports.html

13. SUPPLEMENTARY NOTES

14. ABSTRACT

Substantial parts of the U.S., particularly drier landlocked regions, are facing acute water shortages and water quality issues that decrease agricultural productivity. Reduced crop yields cause billions of dollars in losses annually, affecting the livelihoods of thousands. A combination of population growth, inefficient agricultural practices, and resource demanding consumption trends is only expected to increase pressure on our water supplies. This research proposal seeks to address water and food security issues by cost-effectively and energy-efficiently enhancing water quality and water supply in greenhouses; a $22.93 billion dollar industry in 2017 that is rapidly growing at an annual rate of 8.92%. Greenhouses widely practice desalination of salty irrigation water to improve their operations. However, currently used desalination methods do not tailor greenhouse waters based on crop requirements. This work investigates a fully integrated desalination solution that treats and tailors brackish source waters in greenhouses to save fertilizer and water. Specifically, this project experimentally studies multi-ion transport in and assesses the economic viable of monovalent selective electrodialysis (MSED). MSED allows for the selective removal of monovalent ions damaging to crops and the retention of divalent ions beneficial for crops, unlike the widely used reverse osmosis (RO), which removes all ions from greenhouse source water. First, we evaluate the techno-economic feasibility of MSED compared to other brackish desalination technologies for agricultural applications, based on primary market research we conduct with over 70 greenhouses. These include conventional technologies, such as reverse osmosis (RO) and electrodialysis (ED), and advanced technologies, such as closed circuit reverse osmosis (CCRO). The analysis determines the levelized costs of water, the capital costs and energy requirements of these technologies, and how these vary with feed salinity, system capacity and recovery ratio. Then, we build a bench-scale setup to experientially characterize MSED membrane properties, including monovalent selectivity, ion transport, limiting current and resistance, for multiple brackish feedwaters and for two sets of MSED membranes: the widely used Neosepta ACS/CMS membranes and the new Fujifilm Type 16 membranes. Both MSED membranes show notable monovalent selectivity for all tested compositions, reflecting the potential of the technology for selective desalination in greenhouses. The measurements are compared to a model for MSED in multi-ion solutions. The model predicts multi-ion transport for the Neosepta and Fujifilm MSED systems within 6% and 8%, respectively.

15. SUBJECT TERMS Brackish water, desalination, agriculture, monovalent selective electrodialysis (MSED), reverse osmosis (RO), electrodialysis (ED), membrane selectivity					
16. SECURITY CLASSIFICATION OF:			17. LIMITATION OF ABSTRACT	18. NUMBER OF PAGES	19a. NAME OF RESPONSIBLE PERSON Saied Delegah, Chemical Engineer Bureau of Reclamation, Water Treatment Group P.O. Box 25007, MS-86-68190 Denver, Colorado 80225 sdelagah@usbr.gov
a. REPORT U	b. ABSTRACT U	THIS PAGE U			19b. TELEPHONE NUMBER *(Include area code)* 303-445-2248

Desalination and Water Purification Research
and Development Program Report No. 226

Tailoring Advanced Desalination Technologies for 21st Century Agriculture

Prepared for the Bureau of Reclamation Under Agreement No. R17AC00135

by

Y.D. Ahdab, D. Rehman, K.G. Nayar, J.H. Lienhard, V

**Massachusetts Institute of Technology, 77 Massachusetts Avenue,
Cambridge, MA 02139-4307**

**U.S. Department of the Interior
Bureau of Reclamation
Technical Service Center
Denver, Colorado**

February 2021

Mission Statements

The Department of the Interior (DOI) conserves and manages the Nation's natural resources and cultural heritage for the benefit and enjoyment of the American people, provides scientific and other information about natural resources and natural hazards to address societal challenges and create opportunities for the American people, and honors the Nation's trust responsibilities or special commitments to American Indians, Alaska Natives, and affiliated island communities to help them prosper.

The mission of the Bureau of Reclamation is to manage, develop, and protect water and related resources in an environmentally and economically sound manner in the interest of the American public.

Disclaimer

The views, analysis, recommendations, and conclusions in this report are those of the authors and do not represent official or unofficial policies or opinions of the United States Government, and the United States takes no position with regard to any findings, conclusions, or recommendations made. As such, mention of trade names or commercial products does not constitute their endorsement by the United States Government.

Acknowledgments

The Desalination and Water Purification Research and Development Program at the Bureau of Reclamation sponsored this research. This report was prepared by Yvana D. Ahdab, Danyal Rehman, Kishor G. Nayar, and John H. Lienhard V. We thank Amit Kumar for helpful discussions, as well as Georg Schüking, Flora Klise, and Maria Barbosa for crucial contributions to this work.

Acronyms and Abbreviations

Acronym or Abbreviation	Description
AEM	anion-exchange membrane
BGW	brackish groundwater
CapEx	capital cost
CCRO	closed-circuit reverse osmosis
CEM	cation-exchange membrane
CP	concentration polarization
ED	electrodialysis
EDR	electrodialysis reversal
ERD	energy recovery device
gpm	gallons per minute
ha	hectare
LCOE	levelized cost of electricity
LWS	least work of separation
MED	multiple-effect distillation
MENA	Middle East and North Africa
MSED	monovalent selective electrodialysis
MSF	multi-stage flash distillation
NF	nanofiltration
OpEx	operating cost
ppm	parts per million
PV	photovoltaics

Acronym or Abbreviation	Description
RO	reverse osmosis
RPP	relative payback period
SAR	sodium adsorption ratio
SEC	specific energy consumption
SpCapEx	specific capital costs
SPP	simple payback period
TDS	total dissolved solids
ZLD	Zero Liquid Discharge

Contents

Figures

Tables

Executive Summary

Substantial parts of the United States, particularly drier, landlocked regions, are facing acute water shortages and water quality issues that decrease agricultural productivity. Reduced crop yields cause billions of dollars in losses annually, affecting the livelihoods of thousands. A combination of population growth, inefficient agricultural practices, and resource-demanding consumption trends is only expected to increase pressure on our water supplies. This research proposal seeks to address water and food security issues by cost-effectively and energy-efficiently enhancing water quality and water supply in greenhouses, a $22.93 billion industry in 2017 that is rapidly growing at an annual rate of 8.92 percent. Greenhouses widely practice desalination of salty irrigation water to improve their operations. However, currently used desalination methods do not tailor greenhouse waters based on crop requirements. This work investigates a fully integrated desalination solution that treats and tailors brackish-source waters in greenhouses to save fertilizer and water. Specifically, this project experimentally studies multi-ion transport in, and assesses the economic viability of, monovalent selective electrodialysis (MSED). MSED allows for the selective removal of monovalent ions damaging to crops and the retention of divalent ions beneficial for crops, unlike the widely used reverse osmosis (RO), which removes all ions from greenhouse source water. First, we evaluate the techno-economic feasibility of MSED compared to other brackish desalination technologies for agricultural applications, based on primary market research we conduct with more than 70 greenhouses. These include conventional technologies, such as RO and electrodialysis (ED), and advanced technologies, such as closed-circuit reverse osmosis (CCRO). The analysis determines the levelized costs of water, the capital costs and energy requirements of these technologies, and how these vary with feed salinity, system capacity, and recovery ratio. Then, we build a bench-scale set-up to experientially characterize MSED membrane properties, including monovalent selectivity, ion transport, limiting current and resistance, for multiple brackish feedwaters and for two sets of MSED membranes: the widely used Neosepta ACS/CMS membranes and the new Fujifilm Type 16 membranes. Both MSED membranes show notable monovalent selectivity for all tested compositions, reflecting the potential of the technology for selective desalination in greenhouses. The measurements are compared to a model for MSED in multi-ion solutions. The model predicts multi-ion transport for the Neosepta and Fujifilm MSED systems within 6 percent and 8 percent, respectively.

1. Introduction

Substantial parts of the United States, particularly drier, landlocked regions, are facing acute water shortages and water quality issues that decrease agricultural productivity. Reduced crop yields cause billions of dollars in losses annually, affecting the livelihoods of thousands. A combination of population growth, inefficient agricultural practices, and resource-demanding consumption trends is only expected to increase pressure on our water supplies. This research seeks to address water and food security issues by cost-effectively and energy-efficiently enhancing water quality and water supply in greenhouses. Greenhouses widely practice desalination of salty irrigation water to improve their operations. However, currently used desalination methods do not tailor greenhouse waters based on crop requirements.

This work investigates a fully integrated desalination solution that treats and tailors brackish-source waters in greenhouses to save fertilizer and water. Specifically, this project experimentally studies multi-ion transport in and assesses the economic viable of monovalent selective electrodialysis (MSED). MSED allows for the selective removal of monovalent ions damaging to crops and the retention of divalent ions beneficial for crops, unlike the widely used reverse osmosis (RO), which removes all ions from greenhouse source water.

First, we evaluate the techno-economic feasibility of MSED compared to other brackish desalination technologies for agricultural applications, based on primary market research we conduct with more than 70 greenhouses. These include conventional technologies, such as RO and electrodialysis (ED), and advanced technologies, such as closed-circuit reverse osmosis (CCRO). The analysis determines the levelized costs of water, the capital costs and energy requirements of these technologies, and how these vary with feed salinity, system capacity and recovery ratio. Second, we build a bench-scale set-up to experientially characterize MSED membrane properties, including monovalent selectivity, ion transport, limiting current and resistance, for multiple brackish feedwaters and for two sets of MSED membranes: the widely used Neosepta ACS/CMS membranes and the new Fujifilm Type 16 membranes. Both MSED membranes show notable monovalent selectivity for all tested compositions, reflecting the potential of the technology for selective desalination in greenhouses. The measurements are compared to a model for MSED in multi-ion solutions. The model predicts multi-ion transport for the Neosepta and Fujifilm MSED systems within 6 percent and 8 percent, respectively.

1.1. Project Overview

By 2050, based on current consumption patterns and farming practices, it is projected that there will not be enough water available to current croplands for producing enough food to feed all 9.5 billion people on the planet at that time [1]. Population growth, coupled with climate change, is also causing the availability of freshwater resources around the world to vary substantially in both space and time [2, 3], which is leading to an increased reliance on groundwater withdrawal

[4-6]. However, around half the groundwater resources in the world are brackish ($0.5 \leq S \leq 5$ g/kg) [7]. When brackish water is used for irrigation purposes, there can be significant yield reductions in crops. It is estimated that globally, around 20 to 30 million hectares (ha) of agricultural land have experienced productivity losses due to irrigation with brackish water [7]. Annually, this translates to around $12 billion in revenue losses. Desalination is thus increasingly becoming relevant for agriculture. Global trends around food consumption and water usage are also leading to the adoption of more efficient and high-yielding forms of agriculture, such as greenhouse-based production and hydroponics. These high-yielding agriculture sectors are also early adopters of desalination technologies, with greenhouse and hydroponic growers around the world beginning to use RO to treat their water.

Figure 1-1 shows the sub-systems involved in desalinating brackish water to provide irrigation water for agriculture. These include sub-systems for pumping, desalination, brine disposal, nutrient addition, and the plants themselves. For groundwater-sourced farms, pumping systems lift brackish water from the water table to the surface, where a desalination system removes the salt content in the water, producing saltier brine and product water. The product water must be tailored to have an appropriate pH and nutrient content. The nutrients are either directly added to the water, like in hydroponic systems, or the nutrients are added to the soil in conventional field farming, primarily through the addition of fertilizer. Crops then respond appropriately to the desalinated and tailored water. For this research project, we will be looking at the sub-systems marked by dashed boxes in Figure 1-1: desalination system and the crop system. We will determine whether MSED can selectively remove monovalent ions detrimental to crops, while retaining divalent ions that are nutrients for crops in irrigation water. This selective removal would reduce the fertilizer costs for greenhouses, while the higher recovery of MSED would increase the water savings in greenhouses.

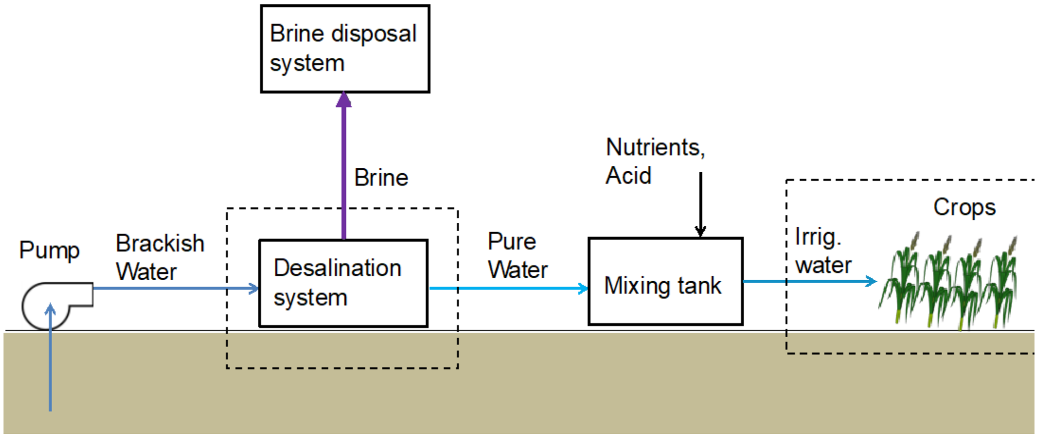

Figure 1-1. Diagram showing key systems used for providing desalinated irrigation water, with dashed boxes representing aspects of the system that this proposal focuses on.

1.1.1. Techno-economic Comparison of MSED, ED, RO, CCRO, Including Primary Market Research

While there are some early adopters of desalination within the agriculture industry, our interviews with more than 70 hydroponic growers in the Unites States, Mexico, and South America show that desalination has not yet been customized to meet all of the requirements of the agriculture end-user. Within agriculture, the problem of brackish irrigation water is encountered in two irrigation settings: groundwater-based open-loop irrigation systems and closed-water-loop systems (may be either surface-water fed or groundwater fed). Currently, sophisticated farmers use conventional RO systems to address the salinity problem encountered in these irrigation settings. These RO systems were originally designed for providing drinking water and are largely used without customizing the design for agriculture. The following problems are encountered currently with conventional RO systems:

- Low water recoveries, with typically just 50 percent of the brackish water recovered
- Over-designed systems for peak capacity production, with limited ability to dynamically vary the quantity of desalinated water
- Removal also of ions beneficial for plant growth such as Calcium (Ca^{2+}) and Magnesium (Mg^{2+}), which farmers have to pay for to add back to water.

While some sectors of agriculture have started using desalination systems (8), the design requirements and constraints for farmers in the United States have not been reported well in the literature. The market is also quite fragmented with several sectors: high-yielding hydroponic farms, orchard farms and conventional field farms, using either open-loop or closed-loop systems with different salt removal needs. There is a need to synthesize the design requirements and tailor desalination systems for agriculture. Furthermore, for brackish water desalination, there are alternatives to conventional RO. These include: a novel variant of RO that operates in a semi-batch fashion called closed-circuit reverse osmosis (CCRO) [9-11] (shown in Figure 1-2(a)), conventional electrodialysis (ED) [9], and a variant of ED called monovalent selective electrodialysis (MSED) [12] that selectively desalinates just monovalent ions (shown in Figure 1-2(b)). While several works have compared RO and ED [13, 14], to the best of our knowledge, one of our previous studies is the only one to compare CCRO with RO and ED [9]. However, the earlier analysis was restricted to just energy consumption and did not examine all the factors that are relevant for agriculture, particularly capital costs. Furthermore, there are significant cost differences between ED and MSED. MSED also provides additional value in that, since it removes only monovalent ions, there could be significant reductions in fertilizing costs or, alternatively, increases in yields due to the presence of ions such as Calcium (Ca^{2+}) and Magnesium (Mg^{2+}).

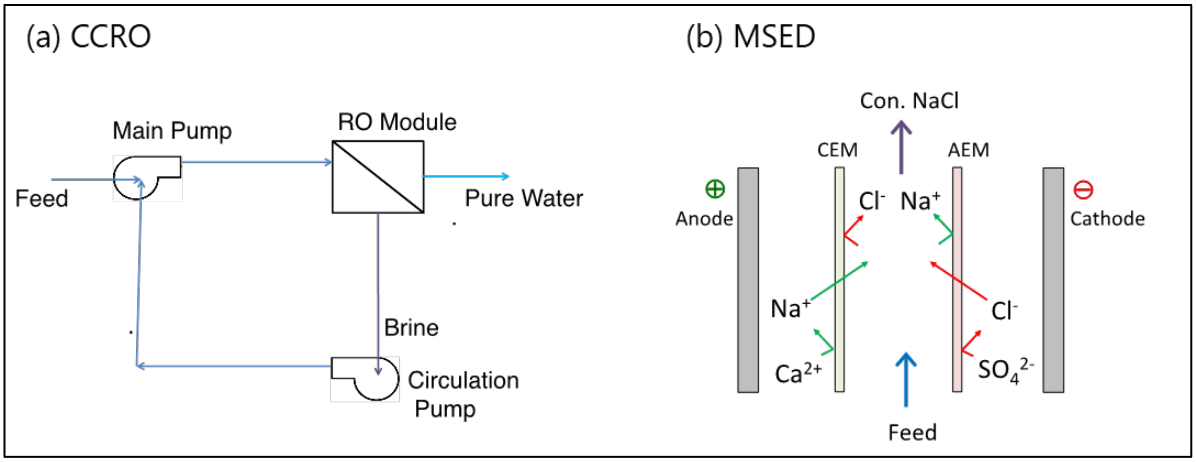

Figure 1-2. Diagram showing (a) CCRO and (b) MSED.

Specific research questions that we address can be summarized as:

- What are the key priorities, design requirements and design constraints for a desalination system that meets the needs of the average famer? Design variables to be characterized include water recovery, fertilizer savings, desired yield increases in plants, desired water quality, energy consumption, and capital cost.
- What is the relative commercial potential of CCRO, ED, and MSED for use in agriculture? What are the levelized costs of water, capital, and energy for these technologies? How do these costs vary with system size, feed salinities, and water recovery ratios? Which technologies offer the lowest overall costs or the most value (from increased crop yields, fertilizer savings, etc.) for agricultural applications?
- Can MSED be designed to meet the requirements for agriculture? What would the capital costs, operating costs, energy requirements, and performance characteristics be of MSED?

1.1.2. Experimental Characterization of MSED Membranes

Primary market research indicates that high-recovery, brackish water desalination technologies (more than 80 percent water recovery), such as MSED, are better aligned with the needs of greenhouses. We experimentally characterize MSED performance for multiple brackish feedwaters, due to the large variations in brackish groundwater (BGW) composition with location and the fact that greenhouses typically use groundwater as source water for irrigation. We test two types of MSED membranes: the Neosepta ACS/CMS membranes and the Fujifilm Type 16 membranes. Aside from the studies we have conducted [15, 16], only two other studies examine MSED membrane selectivity in brackish waters to our knowledge [17, 18]. The experimental measurements are compared to a multi-ion model for MSED we develop.

Specific research questions that we address can be summarized as:

- Does MSED selectively remove monovalent ions that are detrimental to crops while retaining divalent ions that are beneficial for crops in solutions? Does MSED show potential for adoption in greenhouses to save fertilizer and water?
- How does this selective removal vary with water composition? How do other membrane parameters, such as limiting current and membrane resistance vary with water composition?
- How does the performance of the Neosepta and Fujifilm membranes compare?

1.1.3. Overarching Problem Statement

The aim of this work is to determine whether MSED may serve as a more sustainable and cost-effective desalination alternative to the widely used RO for the treatment of brackish source water in greenhouses, which primarily depend on groundwater for irrigation. Water quality is central to greenhouse operations. Because most groundwater is brackish (0.5 g/kg < S < 5 g/kg), desalination is required to reduce the concentration of salts and toxic solutes, which would otherwise threaten crop productivity. In the United States, for example, annual fresh groundwater usage is more than 30 times less than the availability of BGW (1,000 parts per million (ppm) < total dissolved solids (TDS) < 10,000 ppm) [5] and BGW is the most readily accessible water source for irrigation in some regions, such as New Mexico [6]. As a result, greenhouses increasingly rely on RO, the most widely adopted and cost-effective desalination technology, to improve their source water quality. However, the technology poses two main disadvantages in agricultural applications. First, RO removes all ions from solution, including monovalent ions (Na^+, Cl^-) damaging to crops and divalent ions (Ca^{2+}, Mg^{2+}, SO_4^{2-}) favorable for crop growth [7]. These nutrients must then be re-added to the desalinated water, typically through fertilizer, which incurs additional associated costs. Second, RO's water recovery of approximately 80 percent is lower than other brackish water technologies, resulting in lesser water savings.

MSED, a variant of ED, provides an alternative to RO for greenhouses. Most notably, the technology selectively extracts harmful monovalent ions, while retaining divalent ions beneficial for crop growth in the desalinated water. This selective separation decreases fertilizer requirements and related costs. Moreover, MSED can operate at a water recovery greater than 90 percent [9], saving more water and reducing the amount of brine for disposal and/or reuse. Other advantages of MSED include its superior chemical and mechanical membrane stability, resulting in a 2- to 3-year increase in membrane lifetime relative to RO [9], and its process reversal, making the membranes less susceptible to fouling or scaling.

Despite the development of MSED in the 1960s, the technology has not been implemented to desalinate brackish water at the commercial scale. Instead, MSED membranes have historically been manufactured to concentrate seawater for salt production (i.e., for much higher salinities than those of brackish water) [10]. Only recently were MSED membranes developed specifically for brackish water applications by Fujifilm. Consequently, the literature widely investigates MSED membrane selectivity in seawater and concentrated seawater [11-13], while, to our knowledge, only two studies [7,14] prior to our published work examine MSED membrane selectivity in brackish waters.

This work addresses this gap in the literature by experimentally characterizing and developing a multi-ion transport model for the widely used Neosepta and novel Fujifilm MSED membranes, in order to determine the technology's potential for adoption in place of RO in greenhouses. Greenhouses are considered because they constitute a technologically advanced agricultural sector that depends on desalination. However, the results in this report can be extended to irrigation reliant on brackish water more broadly.

1.2. Format of Report

This report first outlines the background regarding the global status of brackish groundwater desalination. It then summarizes the experimental and modelling methods used to investigate MSED for brackish groundwater treatment for irrigation. The last part of this report discusses the results on MSED performance for this particular greenhouse application. The content in this report is based on three published journal papers, a conference paper, and a book chapter:

- The brackish groundwater desalination status globally corresponds to the book chapter: Y. Ahdab, J. Lienhard, "Desalination of brackish groundwater to improve water quality and water supply." Global Groundwater: Source, Scarcity, Sustainability, Security, and Solutions. Elsevier, 2020, 1st Ed.
- The techno-economic comparison of MSED and various technologies corresponds to the paper: K.G. Nayar and J.H. Lienhard, "Brackish water desalination for greenhouse agriculture: comparing the costs of RO, CCRO, EDR, and monovalent-selective EDR." *Desalination*, online 8 November 2019, 475:114188, 1 February 2020.
- The experimental characterization and modelling of the Neosepta ACS/CMS MSED membranes corresponds to the paper: Y.D. Ahdab, D. Rehman, G. Schücking, M. Barbosa, and J.H. Lienhard V, "Treating irrigation water using high-performance membranes for monovalent selective electrodialysis." ACS ES&T—Water, online 15 September 2020.
- The experimental characterization and modelling of the Fujifilm Type 16 membranes corresponds to the paper: Y.D. Ahdab, D. Rehman, and J.H. Lienhard, "Brackish water desalination for greenhouses: improving groundwater quality using monovalent selective electrodialysis reversal." *J. Membrane Sci.*, online 26 March 2020, 610:118072, 1 September 2020.
- Comparison between model and experiments also corresponds to the conference paper: D. Rehman, Y. Ahdab, J. Lienhard, "Improving groundwater quality for irrigation using monovalent selective electrodialysis." The International Desalination Association World Congress, Dubai, October 2019.

1.3. References

[1] A. Jägerskog, T. Jønch Clausen. Feeding a Thirsty World – Challenges and Opportunities for a Water and Food Secure Future. Report, 2012.

[2] G.L. Barbosa, F.D. Almeida Gadelha, N. Kublik, A. Proctor, L. Reichelm, E. Weissinger, G.M. Wohlleb, R.U. Halden. Comparison of land, water, and energy requirements of lettuce grown using hydroponic vs. Conventional agricultural methods. *Int. J. Environ. Res. Public Health*. 12 (2015) 6879–6891. doi:10.3390/ijerph120606879.

[3] HTF Market Intelligence Consulting Pvt Ltd. 2018-2023 Global and Regional Commercial Greenhouse Industry Production, Sales and Consumption Status and Prospects Professional Market Research Report. Edison, New Jersey, USA, 2017.

[4] D. Zarzo, E. Campos, P. Terrero. Spanish experience in desalination for agriculture. *Desalin. Water Treat.* 51 (2013) 53–66. doi:10.1080/19443994.2012.708155.

[5] E.A. Laate. The Economics of Production and Marketing of Greenhouse Crops in Alberta. 2011.

[6] J.B. Jones. Tomato Plant Culture: In the field, greenhouse and home garden. 1999.

[7] P.H. Gleick. The World's Water 2000–2001: The Biennial Report on Freshwater Resources. Island Press, Washington DC, 2001

[8] K.G. Nayar, N.C. Wright, G.P. Thiel, A.G. Winter, J.H. Lienhard. Energy Requirement of Alternative Technologies for Desalinating Groundwater for Irrigation. in: Int. Desalin. Assoc. World Congr. 2015, San Diego, USA, 2015.

[9] D.M. Warsinger, E.W. Tow, K.G. Nayar, L.A. Maswadeh, J.H. Lienhard. Energy efficiency of batch and semi-batch (CCRO) reverse osmosis desalination. *Water Res.* 106 (2016). doi:10.1016/j.watres.2016.09.029.

[10] W.E. Katz. The electrodialysis reversal (EDR) process. *Desalination*. 28 (1979) 31–40. doi:10.1016/S0011-9164(00)88124-2.

[11] H. Strathmann. Electrodialysis, a mature technology with a multitude of new applications. *Desalination*. 264 (2010) 268–288. doi:10.1016/j.desal.2010.04.069.

[12] K.M. Chehayeb, D.M. Farhat, K.G. Nayar, J.H. Lienhard. Optimal design and operation of electrodialysis for brackish-water desalination and for high-salinity brine concentration. *Desalination*. 420 (2017) 167–182. doi:10.1016/j.desal.2017.07.003.

[13] D.W. Bian, S.M. Watson, N.C. Wright, S.R. Shah, T. Buonassisi, D. Ramanujan, I.M. Peters, A.G. Winter. Optimization and design of a low-cost, village-scale, photovoltaic-powered, electrodialysis reversal desalination system for rural India. *Desalination*. 452 (2019) 265–278. doi:10.1016/j.desal.2018.09.004.

[14] G. Saracco, M.C. Zanetti, M. Onofrio. Novel application of monovalent-ion-permselective membranes to the recovery treatment of an industrial wastewater by electrodialysis. *Ind. Eng. Chem. Res.* 32 (1993) 657–662. doi:10.1021/ie00016a012.

[15] Y. Ahdab, D. Rehman, J. Lienhard. Brackish water desalination for greenhouses, Improving groundwater quality for irrigation using monovalent selective electrodialysis reversal. *J. Membr. Sci.* 610 (2020) 118072. doi: 10.106/j.memsci.2020.118072.

[16] Y. Ahdab, D. Rehman. G. Schuking, M. Barbosa, J. Lienhard. Treating irrigation water using high-performance membranes for monovalent selective electrodialysis. ACS ES&T Water. In-press.

[17] Jiang, W.; Lin, L.; Xu, X.; Wang, H.; Xu, P. Physicochemical and electrochemical characterization of cation-exchange membranes modified with polyethyleneimine for elucidating enhanced monovalent permselectivity of electrodialysis. *J. Membr. Sci.* 572 (2019), 545−556. doi: 10.1016/j.memsci.2018.11.038.

[18] B. Cohen, N. Lazarovitch, J. Gilron. Upgrading groundwater for irrigation using monovalent selective electrodialysis. *Desalination.* 431 (2018): 126-239. doi: 10.1016/j.desal.2017.10.030.

2. Background: The State of Brackish Groundwater Desalination Globally

Water scarcity around the world is leading to a greater dependence on groundwater to meet freshwater demand [1]. Despite the fact that most groundwater resources are brackish (500 mg/L ≤ TDS ≤ 5,000 mg/L) [2], brackish groundwater remains a largely untapped resource in many parts of the world. In the United States, for example, the volume of BGW (1,000 mg/L ≤ TDS ≤ 10,000 mg/L) was measured to be more than 35 times the amount of fresh groundwater used annually [3]. Increased exploitation of brackish groundwater may relieve some of the mounting pressure on freshwater supplies, particularly in drier, landlocked regions. Desalination can be employed to reduce the salt concentration in brackish groundwater to meet the needs of freshwater applications.

2.1. Brackish Groundwater Composition

All naturally occurring waters contain some level of total dissolved solids (TDS), a measure of the concentration of all inorganic and organic dissolved substances, including salts, minerals, and metals. TDS determines whether a surface water or groundwater resource is fresh or brackish. Brackish groundwater contains a TDS greater than freshwater but less than seawater. A variety of classification schemes are used to categorize waters with different TDS. Brackish groundwater falls within the 500-to-20,000 mg/L TDS range, with some classifications placing the upper TDS limit at 10,000 mg/L [3]. In comparison, seawater typically contains a TDS greater than 25,000 mg/L.

Unlike seawater, both the TDS and major ion constituents of brackish water vary greatly with depth of the well below the land surface and with geographic location, as a result of local geologic, hydrologic, and climactic conditions. Groundwaters containing higher TDS are more often drawn from greater depth below the land surface [3]. These variations are critical in determining the feasibility, required treatment, and associated cost of brackish groundwater usage. Because a specific location may correspond to a particular BGW composition, location is crucial in water resource planning and treatment system selection and design.

Brackish groundwater must be treated before use in applications that require high water quality, such as drinking water and irrigation. Water used for public supply, which fulfills the majority of the population’s daily water needs, must not include high dissolved solids concentration or significant concentrations of specific constituents. The U.S. Environmental Protection Agency recommends that drinking water contain less than 500 mg/L of TDS to ensure public health [4]. Water used for irrigation of agricultural crops, the largest consumer of our water supplies globally, is limited by dissolved solids concentration, the relative amount of solutes, and specific constituents that can be damaging to crops.

2.2. Desalination

Desalination is a water treatment that removes dissolved solids and other minerals from a water resource that would otherwise be unsuitable for use in freshwater applications. Desalination has been on the rise since the 1960s, and this trend is expected to continue into the 2020s (Figure 2-1). Today, the global desalination operating capacity is approximately 70 million m^3/day [5]. It is primarily used in treating seawater (61 percent of desalinated water) and brackish water (21 percent of desalinated water), the majority of which is groundwater [5, 6]. Its various end uses include municipal (e.g., drinking water), industry, power, and irrigation. Brackish water desalination requires less energy and can recover more product water for a given amount of feedwater than seawater desalination.

Commercial desalination technologies can be divided into two main categories: thermal and membrane. Thermal technologies, most commonly multi-stage flash distillation (MSF) and multiple-effect distillation (MED), mimic the hydrological cycle of evaporation and condensation by heating salty water to form water vapor that is then condensed into fresh water. Membrane processes, such as RO and ED or electrodialysis reversal (EDR), use a semi-permeable membrane that prevents or allows the passage of certain salt ions. The driving force for transport can be a pressure, electrical potential, temperature, or concentration gradient. Due to their increased energy efficiency and cost effectiveness, membrane processes have surpassed the once dominant thermal processes in terms of desalination capacity (Figure 2-1).

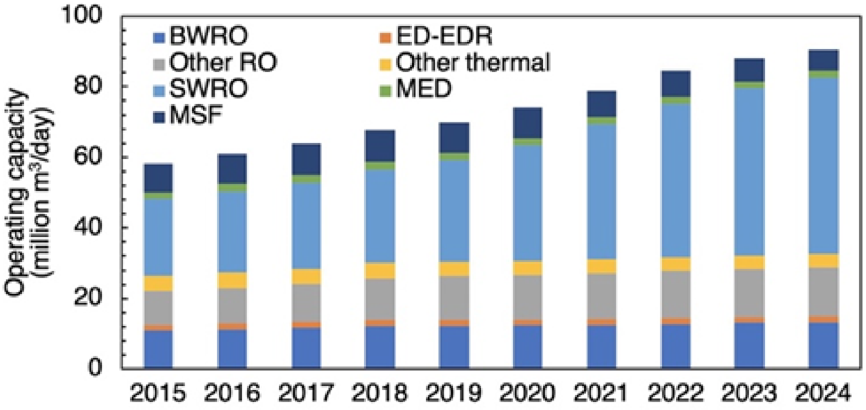

Figure 2-1. Operating desalination capacity from 2015 to 2019 and expected operating desalination capacity from 2020 to 2024. A breakdown of operating capacity by plant (RO, ED or EDR, MSF, MED, Other) and feedwater (brackish water = BW, seawater = SW) is shown. Data are from the DesalData online database [5].

To treat brackish groundwater, membrane desalination technologies, primarily RO and ED, are used without exception [7, 8, 9]. Thermal processes are not used, primarily because their energy requirements are independent of salinity, unlike membrane processes in which energy requirements decrease with salinity. RO is overwhelmingly the dominant desalination technology, including for brackish water treatment. In 2019, RO and ED produced 76 percent and 2.4 percent, respectively, of desalinated water globally [5]. Around one-quarter of RO generated water and well over half of ED generated water originated from brackish water [5, 6].

The remainder of this section is divided into two parts. The first part focuses on brackish groundwater desalination technologies, including associated energy consumption, cost, and environmental impact. The second part examines regional and national variations in desalination capacity, technology, feedwater type, and expenditure. In particular, trends in the United States, Saudi Arabia, Australia, China, Spain, and India are investigated.

2.3. Desalination Process

A brackish groundwater desalination plant is typically composed of six key stages, as shown in Figure 2-2: 1) groundwater is pumped from wells; 2) the raw water undergoes pretreatment, depending on its composition, to reduce membrane fouling; 3) the pretreated water is fed into the desalination stage (RO, ED), which yields desalinated water (low in salinity) and brine (concentrated in salinity); 4) the brine is disposed of or further concentrated and dried to achieve Zero Liquid Discharge; 5) the desalinated water is post-treated; and 6) final product water is distributed to the end consumer or a storage tank using service pumps.

This section provides a detailed overview of these desalination plant stages. Membrane fouling; RO and ED systems, including corresponding pre-treatment and post-treatment plant energy consumption and cost data; brine management; emerging desalination technologies; and renewable coupled desalination are discussed.

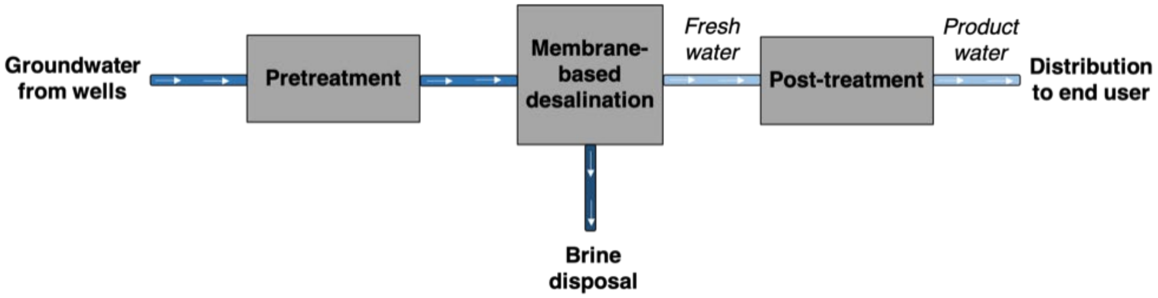

Figure 2-2. A process diagram for a typical brackish groundwater plant comprises groundwater pumping, pretreatment, electricity-driven (e.g., pump or power supply) desalination, brine disposal, post-treatment, and distribution stages.

2.3.1. Membrane Fouling and Pre-treatment

Depending on feedwater composition and membrane type, several constituents can result in membrane contamination, which is referred to as fouling. Fouling reduces membrane efficiency, resulting in a shorter membrane lifetime, more frequent cleaning, and a decrease in recovery rate. Recovery rate is defined as the fraction of freshwater produced from a given amount of feedwater. The primary types of fouling in membrane desalination systems are scaling and biofouling. Scaling occurs due to the precipitation of inorganic salts, such as carbonate, sulfates, and silica, from the feedwater onto the membrane surface. Brackish water RO is especially prone to membrane scaling [7, 9]. Biofouling arises from the growth of bacteria on the membranes, which depends on temperature, pH, dissolved oxygen, and composition of feedwater. In some cases, high concentrations of suspended and colloidal matter in the feedwater block the feed flow channels in the membrane elements. Pretreatment of desalination source water before it enters a membrane is required to minimize the fouling potential, extend membrane life and maximize recovery rate. Pretreatment can involve chemical processes, physical processes, or a combination of the two. The extent of pretreatment required in brackish desalination facilities is less than that of seawater, due to the lower fouling potential of many groundwater sources.

2.3.2. Reverse Osmosis

RO uses a semipermeable membrane that enables the passage of water, while rejecting salts, under an applied pressure. It represents the state-of-the-art desalination technology for brackish water applications, because it can reject a variety of contaminants in a single process with lower energy consumption. Aside from raw water intake and product water conveyance, an RO facility is composed of pretreatment; desalination modules with RO membranes; a high-pressure pump to drive desalination; post-treatment; and, in some cases, an energy recovery device that depressurizes the brine leaving the system.

Pretreatment. RO membranes are sensitive to pH, oxidizers, a wide range of organics, algae, bacteria, particulates, and other foulants. The most common pretreatment method is the chemical addition of antiscalants and acid to prevent the formation of pH-dependent membrane scaling, followed by cartridge filters to remove particulates that will plug or foul membranes. In some cases, more pretreatment may be necessary to control iron and manganese using oxidation/filtration pretreatment, or to reduce sand loading from wells using sand separators or strainers.

Desalination mechanism. A schematic drawing of the RO desalination mechanism is shown in Figure 2-3. The natural osmotic pressure of a saline solution will drive water from the low to high solute (salt) concentration side of a semipermeable membrane. RO uses a high-pressure pump to apply a hydraulic pressure greater than the osmotic pressure to the saltier side. The applied pressure required for brackish water typically ranges from 17to 27 bars (seawater requires pressure of 55 to 82 bars) [8]; water higher in salinity will require a higher hydraulic pressure and will consume more energy to overcome the osmotic pressure. Under the applied pressure, water is forced through the membrane to the low solute concentration side. Salt ions almost entirely remain on the high concentration side, although some salt leakage from high to low solute concentration will occur due to diffusion that results from the salinity gradient across the membrane. RO yields a freshwater stream (permeate) and a concentrated solution (brine or concentrate) on the high-pressure side of the membrane.

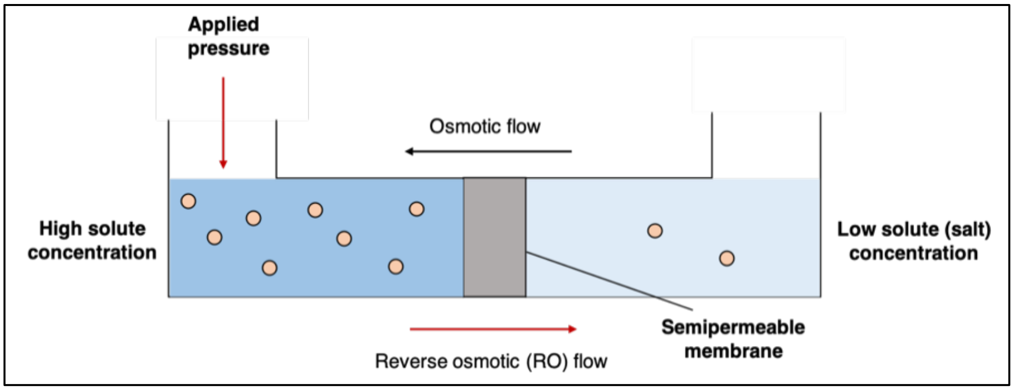

Figure 2-3. A schematic drawing of the RO desalination mechanism. An applied pressure forces water to flow from the high to the low solute concentration side.

Membranes. RO membranes can be broadly categorized as low-pressure elements (brackish water) and high-pressure elements (seawater). Several types of membranes are available on the market. The two most commonly used membrane configurations are hollow fiber and spiral-wound in a cross-flow filtration. In cross-flow, the pressurized water flows parallel to, rather than perpendicular to, the membrane surface in order to assist in the removal of concentrated salts from the surface; this configuration reduces the rate of fouling and salt leakage into the permeate from diffusion. Key RO membrane parameters include permeability (i.e., the rate of salt diffusion across the membrane) and rejection (i.e., the quantity of salt rejected from the feedwater). These vary significantly with membrane type. Current brackish RO membranes remove between 98 and 99.2 percent of TDS from the feedwater and are designed to produce a permeate of approximately 500 mg/L [9]. They have a life expectancy of 2 to 5 years [7, 9]. Improvements in these membranes continue to simultaneously reduce desalination energy requirements and the rate of fouling.

System design. Typically, six to eight membrane modules are placed in series within a fiberglass pressure vessel. RO plants are often composed of two to three stages in order to maximize recovery rate. In these multi-stage configurations, the brine from two first-stage pressure vessels will serve as feedwater to a single second stage and so on. The recovery rate of brackish water RO systems ranges from 75 to 85 percent [11], resulting in a concentrated brine stream that must be disposed of (see Section 2.3.6 for details). Almost all systems are single pass (i.e., the feedwater is sent through the RO unit once), with the exception of facilities treating highly brackish water.

Energy recovery devices. Applying an external pressure in excess of the osmotic pressure requires a significant amount of energy, some of which remains in the pressurized brine stream leaving the last RO stage. Energy recovery devices (ERDs) can be used to recover energy from this pressurized brine. While ERDs are used in almost all seawater facilities, their implementation in brackish facilities is not commonplace. Brackish water RO has a lower pressure requirement and a higher recovery rate than seawater RO, which results in a smaller amount of recoverable energy in the brine stream. However, recent developments in ERDs for low-pressure applications suggest that even a small amount of energy recovery would result in positive returns for brackish RO plants [7].

Consequently, ERDs are increasingly incorporated into brackish water facilities. The devices are either positive displacement (e.g., pressure exchangers), or centrifugal (e.g., the directly coupled turbocharger), which is the most widely adopted ERD in brackish water facilities.

Post-treatment. Following the desalination process, the product water is often low in alkalinity, hardness, and pH. Post-treatment may be required to remove dissolved gases (e.g., hydrogen sulfide), stabilize the product water, and/or further disinfect the product water. pH control minimizes corrosion of piping, tanks, and pumps in distribution networks. Air-stripping towers, also known as degasifiers or decarbonators, increase pH through the removal of dissolved carbon dioxide and remaining sulfides. The addition of lime or calcium chloride or blending with raw water provides stable hardness in the product water. Chlorine gas is used for primary disinfection and sodium hypochlorite for secondary disinfection.

2.3.3. Electrodialysis

Electrodialysis reversal (referred to as ED or EDR throughout this chapter) is an electrochemical separation process that removes salt ions from a given feedwater, unlike RO, which strives to keep salt ions in the feedwater. It relies on semipermeable, ion-exchange membranes that enable the passage of ions with a particular charge. Aside from source water intake and product water distribution, an EDR plant consists of pretreatment, a membrane stack for desalination, a direct-current power supply to drive desalination, a low-pressure circulation pump to flow water through the desalination system, and post-treatment. While RO is used across the brackish groundwater salinity range, EDR is typically limited to brackish waters containing a TDS that is less than 5,000 mg/L for cost reasons [7, 8]. In recent years, the market share of EDR brackish water desalination has diminished due to improvements in RO performance and decreases in RO membrane cost.

Pretreatment. Because EDR systems allow for salt transport and the reversal of the direction of such transport, they are generally more robust to fouling than RO. The polarity of the applied voltage potential, which determines the direction of ion transport, is periodically reversed (three to four times per hour) to flush scalants from the membrane surface on the concentrating side. This reversal lessens the need for continuous chemical feeds and cleanses alternating electrodes (during anodic operation) of acid formation. EDR can also tolerate high concentrations of silica, which are present in many brackish groundwaters, without a significant effect on recovery, unlike RO. However, the addition of antiscalants are still required to control the formation of inorganic scale and cartridge filters to remove suspended solids that can foul the membranes. Depending on source water quality, there may be a need for additional pretreatment, such as conventional coagulation, sedimentation, and filtration.

Desalination mechanism. Figure 2-4 shows an EDR membrane stack comprising two membrane pairs (the number of membrane pairs in an actual EDR system is usually much larger than two). Each pair consists of two types of ion-exchange membranes in order of alternating charge between two electrodes. Cation-exchange membranes (CEMs) enable the passage of cations, or positively charged ions such as calcium and sodium. Conversely, anion-exchange membranes (AEMs) enable the passage of anions, or negatively charged ions such as sulfate and chloride. Spacers are placed between the membranes, as well as the membranes and electrodes.

A voltage potential difference, rather than a pressure difference as in RO, drives the desalination process. Ion transport through the membrane is induced, with cations and anions migrating towards the cathode and anode, respectively. The alternating membranes trap cations and anions in the brine channel. Caution must be taken in choosing an operating voltage and current for an EDR process below the operating limit that will cause water dissociation.

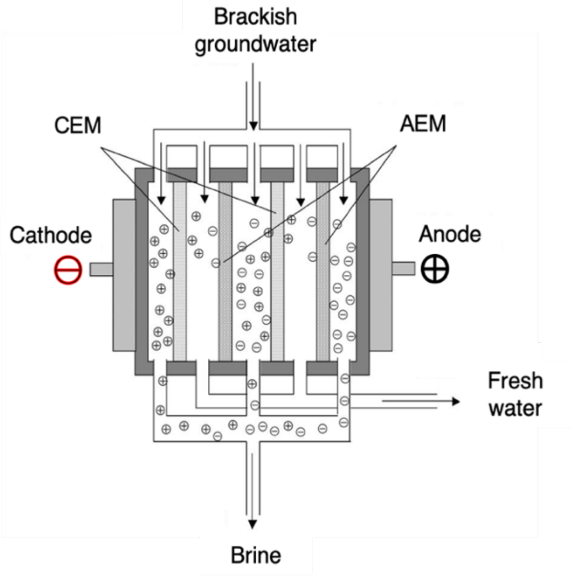

Figure 2-4. A simplified EDR stack comprising two electrodes, two CEMs, and two AEMs, with brackish groundwater as the feedwater. An applied voltage across the electrodes yields a brine stream and a freshwater stream.

Membranes. EDR systems use flat sheet membranes, reinforced with synthetic fiber, that are stacked in a module between electrodes. The number of membranes varies depending on the target membrane area for a given application. The key EDR membrane properties are charge-based ion selectivity (i.e., selection of specific ions for removal) and electrical conductivity. The membranes have a particularly high removal efficiency for multivalent ions, such as calcium and magnesium, although they also remove monovalent ions, such as sodium and chloride under a sufficient applied voltage. Ion selectivity is best at lower salinities (greater than 90 percent removal of TDS) and decreases at higher salinities, which hampers EDR performance for more saline feedwaters. Membranes with low electrical resistance are desired in order to consume less energy during the desalination process. The life expectancy of EDR membranes far exceeds that of RO, with an average of 10 years for AEMs and 15 years for CEMs [7].

System design. Similar to RO, staging provides the opportunity to achieve the desired level of desalination and to increase recovery rate. ED typically operates with three stages, in which brine from the first stage serves as feed to the subsequent stage. The first stack achieves approximately 60 percent salt removal, the second achieves 85 percent removal, and the third achieves up to 94 percent removal [7]. ED systems can operate at high water recoveries of 85 to 94 percent [11].

Post-treatment. Post-treatment requirements for EDR depend on whether the product water will be used for industrial or potable purposes. In industrial applications, mixed-bed ion exchange units serve as polishers by removing any remaining ions in the product water. In municipal or potable water applications, disinfection through a small chlorinator or corrosion control is often implemented.

2.3.4. Energy Consumption Using Conventional Energy Sources

Electricity is the only form of energy required in RO and EDR. Table 2-1 compiles specific energy consumption (SEC) data in kWh/m^3 of produced water for RO and EDR brackish water facilities. SEC includes the energy required for groundwater pumping, pretreatment, desalination, post-treatment, and conveyance. SEC depends on feedwater salinity and temperature, membrane properties, age of the facility, conveyance of the raw and treated water, and pretreatment requirements. For example, higher salinities require a greater energy consumption to achieve desalination. For groundwaters containing a TDS of less than 10,000 mg/L and conventional energy sources, the SEC range for RO in the surveyed literature is 0.26 to 3 kWh/m^3 and for ED is 0.5 to 7 kWh/m^3. The SEC of ED for lower salinity groundwaters (1,000 to 5,000 mg/L) ranges from 0.5 to 5.5 kWh/m^3, with recent sources [7, 12] reporting an SEC of 0.5 to 1.8 kWh/m^3. SEC greatly increases with TDS in EDR systems. Up to a TDS of 1,500 mg/L, EDR SEC is comparable to that of RO. At higher TDS concentrations, EDR energy consumption is significantly greater than that of RO. As a result, EDR is not typically used for brackish waters containing a TDS greater than 5,000 mg/L. Conversely, RO can be used across salinities spanning the brackish and seawater ranges.

Table 2-1. Specific energy consumption in kWh/m^3 of produced water for RO and ED desalination of brackish groundwater containing 1,000 ≤ TDS ≤ 10,000 mg/L. The data were obtained from review papers and reports that compile these values from numerous sources [7, 8, 12, 13, 14, 15, 16, 17, 18, 19, 20, 21, 22, 23, 24]

Desalination Type	SEC (kWh/m^3)	Feedwater (mg/L)
RO	0.26-3	1,000-10,000
ED	0.5-5.5	1,000-5,000
	3-7	1,000-10,000

The breakdown of desalination plant SEC varies on a case-by-case basis depending on plant parameters, such as system design and size and fouling propensity of feedwater. Figure 2-5 reflects the differences in the SEC breakdown of two brackish groundwater RO plants in California. Pretreatment, RO, and post-treatment, which are lumped together in available datasets, dominate SEC relative to pumping and conveyance. Groundwater pumping energy requirements may increase as fresher and shallower groundwater sources continue to be over-extracted, demanding that wells be deeper. Moreover, conveyance SEC will vary depending on the distance the water must be pumped to the end user.

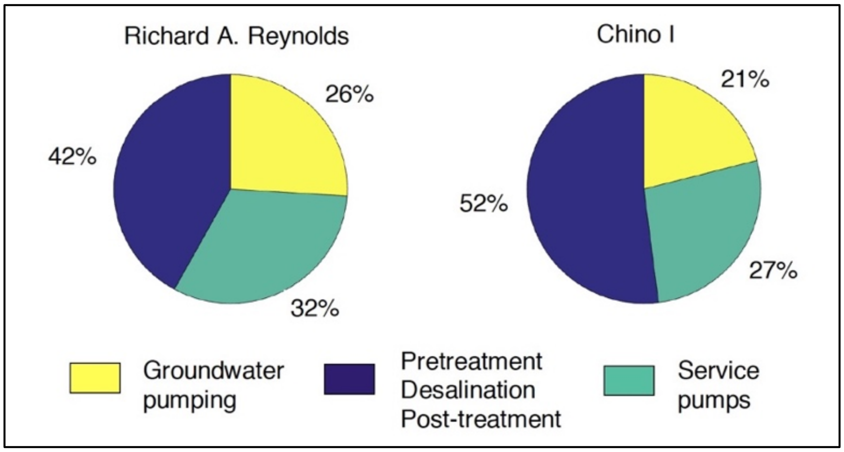

Figure 2-5. SEC breakdown of the Richard A. Reynolds and Chino I brackish groundwater RO plants in California (data from [7]).

The typical SEC of brackish water plants far exceeds the theoretical minimum energy required for desalination. Depending on the desalination process used, SEC is usually 5 to 26 times greater than the theoretical minimum [25]. Figure 2-6 shows a comparison between least work of separation (LWS), which is equivalent to the theoretical minimum energy required for desalination based on a given input water, and plant SEC for various brackish water RO plants in the United States. Because LWS accounts for the minimum energy required by only the desalination phase, the differences in plant SEC and LWS are likely overestimated. Nonetheless, the disparity shows that much room still remains for improvement in terms of desalination energy efficiency.

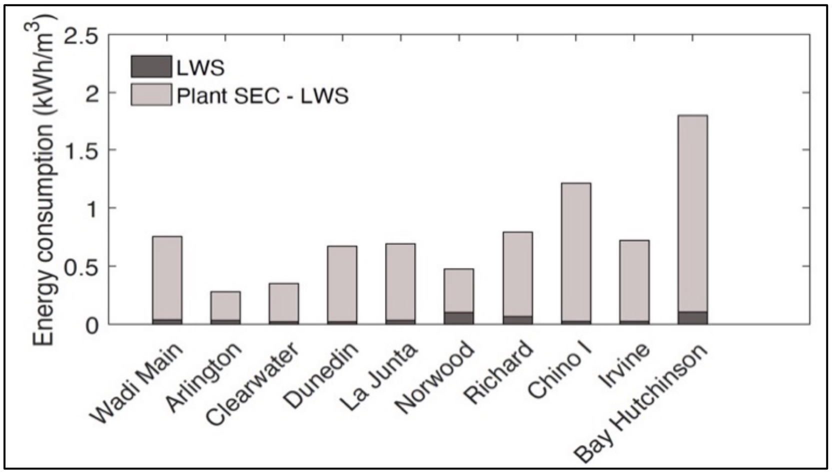

Figure 2-6. LWS compared to SEC of 10 brackish groundwater RO plants with complete feedwater composition data [7].

2.3.5. Economics of Desalination

The total desalination cost (\$/m^3 of produced water) is a function of the capital cost (CapEx) and operating cost (OpEx) needed to produce one unit (1 m^3) of freshwater. CapEx comprises construction (direct capital) and non-construction (indirect capital) project costs. OpEx includes costs for operation and maintenance, energy, labor, chemicals, brine disposal, and plant management. As mentioned previously, RO production costs have decreased in recent years due to membrane advancements, and ED is generally not believed to be cost-effective in treating feedwater with TDS greater than 5,000 mg/L unless maximizing recovery rate is the priority. ED has some economic potential for partially desalting high-salinity feeds if a pure product is not required [26] or in hybrid RO-ED arrangements [27].

Table 2-2 includes cost data for brackish water RO and ED from the literature. Cost largely depends on feedwater salinity and desalination production capacity. Total RO plant expenses range from \$0.20 to \$1.33/m^3 in the surveyed literature. Large RO systems (capacity of 40,000 m^3/day) cost \$0.26 to \$0.54/m^3. Small RO systems (capacity of 20 to 1,200 m^3/day) cost \$0.78 to \$1.33/m^3. This cost increases drastically for RO systems operating at a capacity less than 20 m^3/day. Total ED plant expenses range from \$0.60 to \$1.05/m^3, where larger-capacity plants also correspond to lower cost.

Table 2-2. Total cost of brackish groundwater (1,000 ≤ TDS ≤ 10,000 mg/L) desalination in \$/m³ of produced water, using RO and ED and conventional energy sources for a comprehensive range of desalination capacities unless otherwise specified in the capacity column [7, 8, 12-22, 28-32].

Desalination Type	Total Cost (\$/m³)	Capacity (m³/day)
RO	0.10-1.33	Typical range
	0.26-0.54	40,000
	0.78-1.33	20-1,200
	0.56-12.99	Few (<20)
ED	0.60-1.05	Typical range

Fixed costs (e.g., capital amortization and insurance) dominate the total cost to produce water from brackish groundwater, whereas SEC dominates the cost to produce water from seawater. Greenlee et al. [30] outline a typical cost distribution of brackish water RO plants: capital recovery (54 percent), SEC (11 percent, compared to seawater 44 percent); maintenance (9 percent), membrane replacement (7 percent), labor (9 percent), and chemicals (10 percent). Veerapaneni et al. [7] report the following cost breakdown: capital recovery (27 percent), SEC (17 percent), maintenance (17 percent), membrane replacement (11 percent), labor (17 percent) and chemicals (10 percent). A key cost driver for inland brackish desalination plants is brine disposal (see Section 2.3.6 for details). A comparison of these cost breakdowns is shown in Figure 2-7.

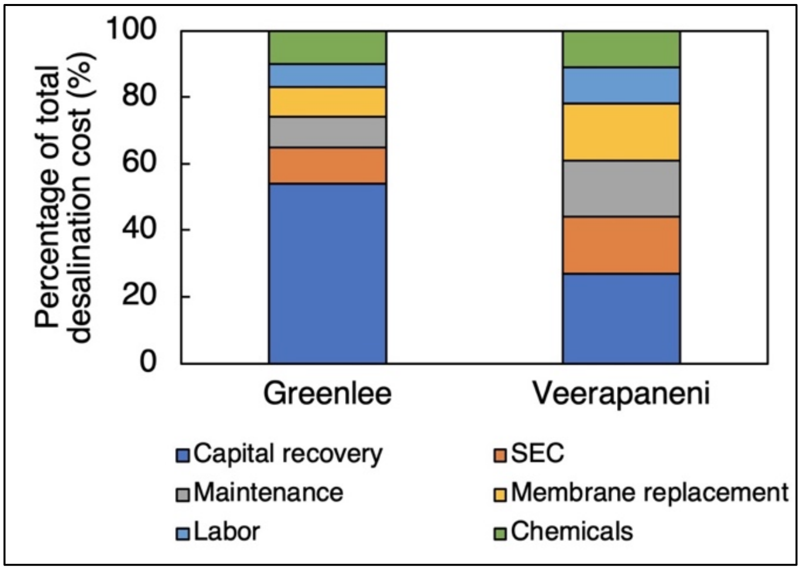

Figure 2-7. Typical brackish water RO plant cost breakdown from studies conducted by Veerpaneni et al. [7] and Greenlee et al. [30].

2.3.6. Brine Management

Brine is the high-salinity byproduct of the desalination process. Its characteristics and volume depend on source water and desalination technology used. For example, RO brackish groundwater desalination generates a brine stream that is 4 to 10 times as concentrated in salinity as the feedwater. Current brine disposal methods negatively impact the environment and are limited by high capital costs. The cost of brine disposal is 5 to 33 percent of the total cost of desalination, with inland brackish desalination plants lying in the upper echelon of this range [6, 33]. Consequently, cost-effective and efficient brine management is critical to address environmental pollution. A desirable alternative to liquid brine disposal is fully dewatering the brine to a solid product, so as to achieve Zero Liquid Discharge (ZLD). Table 2-3 includes information on these disposal and treatment methods, including the treatment principle and the cost. This section elaborates on the results in this table.

Table 2-3. Brine disposal and treatment principles and cost ($/m^3 of rejected brine) [30, 31, 34].

Method	Principle	Cost ($/m^3)
Surface water discharge	Discharged into surface water	0.03-0.30
Sewer discharge	Discharged into existing sewage collection system	0.30-0.66
Deep-well injection	Injected into porous subsurface rock formations	0.33-2.65
Evaporation ponds	Evaporated, resulting in salt accumulation at pond bottom	1.18-10.04
Land application	Irrigates salt-tolerant crops and grasses	0.74-1.95
ZLD	Concentrated and evaporated to yield freshwater and solid	0.66-26.41

2.3.6.1. Brine Disposal

Current methods for disposing of desalination brine are surface water discharge, sewer discharge, deep-well injection, evaporation ponds, and land application. A method is selected depending on a variety of factors, including brine composition and quantity; geographic location; availability of receiving site (e.g., surface body); and capital and operating costs. More than 90 percent of seawater desalination plants use surface water discharge back into the ocean, while sewer discharge, deep-injection wells, and land application are almost exclusively used by brackish water desalination plants.

The most common practice for inland brackish groundwater facilities is to dispose to surface water bodies (47 percent), sewer discharge (42 percent) and deep-well injection (9 percent) [7]. The remaining 1 percent includes other methods, such as evaporation ponds and thermal treatment. Surface water discharge is proving to have very detrimental environmental effects.

For example, annual economic damage due to increased salinity from brine disposal in the Central Arizona Valley and Southern California coastal plain basin has been estimated to be \$15 to \$30 million and \$95 million, respectively, for each 100 mg/L increase in product water TDS [7]. Even if the brine is diluted using large wastewater effluent flows prior to discharge, the increase in surface water salinity over time results in salinization of surrounding land, which has economic and environmental repercussions. Deep-well injection, land application, and evaporation ponds may be suitable alternatives to surface water discharge, largely depending on the local climate and brine volume. Deep well-injection is cost-effective but risks groundwater pollution. Evaporation ponds are very pricey and can only be used in dry climates with high evaporation rates and land availability. For example, this approach has been used in the United Arab Emirates and Oman [33]. Land application may be useful for the disposal of small brine volumes to irrigate plants and grasses with high salinity tolerance [34].

2.3.6.2. Brine Treatment

ZLD combines desalination technologies to produce freshwater and achieve zero liquid waste from a desalination plant. This approach consists of a concentration stage (membrane technologies), as well as evaporation and crystallization stages (thermal technologies). Together, they yield a pure water stream that can be used for drinking water, irrigation, etc., and a compressed solid waste for environmentally friendly disposal or further processing into a useful material. However, as shown in Table 2-3, the ZLD approach is by far the most costly method and may have indirect environmental impact as a result of its large energy requirements. Further research is being conducted on reducing energy consumption of and incorporating renewable energy sources and low-grade waste heat in ZLD.

2.3.7. Desalination Using Renewable Energy Sources

Desalination processes typically rely on fossil fuel power plants, which emit greenhouse gases, to meet their energy intensive needs. Rahuy et al. reports that energy consumption accounts for 89 to 99 percent of desalination's total environmental load [7]. Renewable energy sources (wind, solar thermal, geothermal) provide alternatives to mitigate the environmental impact of desalination.

Despite its promise, renewable energy-powered desalination accounted for 1 percent of the total global installed desalination capacity as of 2016 [36], with photovoltaics (PV) leading at 43 percent, followed by solar thermal (27 percent), wind turbine (20 percent) and hybrid (10 percent) of sources [37]. The biggest barrier to adoption has historically been the high capital cost of renewable energy systems in comparison to conventional energy systems. A 2011 study [38] reports water production costs of \$2.17 to \$2.41/m^3 for select brackish PV-RO systems (10 m^3/day) in Australia, Tunisia, Jordan, and the United States. A 2013 review paper [8] finds that PV-RO (less than 100 m^3/day), PV-ED (less than 100 m^3/day) and wind-RO (50 to 2,000 m^3/day) systems require an SEC of 1.5 to 4 kWh/m^3 and water production costs of \$6.50 to \$9.10/m^3, \$10.40 to \$11.70/m^3, and \$1.92 to \$5.20/m^3, respectively. In comparison, RO (20 to 1,200 m^3/day) powered by fossil fuels required an SEC of 1.5 to 2.5 kWh/m^3 and water production cost of \$0.78 to \$1.33/m^3. ED (small capacity) required an SEC of 2.64 to 5.5

kWh/m^3 and cost of \$0.60/m^3 [8]. According to a 2014 study [39], PV-ED can cost significantly less than PV-RO for small-scale systems (6 to 15 m^3/day) using lower salinity feedwater (e.g., 50 percent cost reduction for 2,000 mg/L feedwater). However, the variability of energy prices over the past decade is quickly changing the desalination landscape, as the electricity generated by new solar and wind power projects is becoming cheaper than the electricity generated by new coal and gas power plants around the world.

According to a 2019 report from the business intelligence company Bloomberg NEF [40], recent onshore wind and solar power plants have achieved parity with average wholesale prices in parts of Europe, California, and China, some of the world's largest markets. The expected levelized cost of electricity (LCOE) of recently financed solar projects ranges from \$0.027 to \$0.036/kWh in India, Chile, and Australia [40] and is less than \$0.020/kWh in California, the United Arab Emirates, and Portugal [41]. In the United States, the average LCOE of wind power dropped from \$0.070/kWh in 2009 to less than \$0.020/kWh in 2017 [42]. The cost-competitiveness of wind and solar power has motivated increased development of large-scale desalination plants powered by renewable energy, in addition to the already implemented small-scale systems [35]. Brazil's Agua Doce Program consists of brackish water desalination systems powered by PV that aim to provide high-quality water to 500,000 people in the semi-arid region of Brazil [37]. The Arabian Gulf is increasingly shifting its entire desalination infrastructure to PV, with such RO plants operating at up to 100,000 m^3/day in Saudi Arabia [36]. Australia contains wind-powered RO plants with even larger desalination capacities (e.g., Kurnell-Sydney seawater RO plant with a capacity of 250,000 m^3/day [36]).

Renewable-energy-coupled desalination at small and large scales is expected to only become more economically attractive as the price of fossil fuels continues to increase and that of renewable technologies continues to decline. The International Desalination Association has set a 2020–2025 target of using renewable energy in 20 percent of new desalination plants [43].

2.3.8. Emerging Desalination Techniques

In addition to the development of new-generation membrane materials for desalination, several desalination technologies that improve water recovery and/or energy consumption are emerging. These technologies are typically variations of RO, including nanofiltration and semi-batch RO.

2.3.8.1. Nanofiltration

Nanofiltration (NF) membranes and RO membranes are similar in many ways. Both are pressure-driven membrane desalination technologies that foul easily. Their differences stem from the size and charge of contaminants that each technology is capable of removing. RO membranes effectively remove most ions from product water, with the exception of dissolved gases and some weakly charged molecules that are low in molecular weight. NF is able to reject larger, strongly charged ions (e.g., 90 percent calcium removal), but it enables more passage of monovalent and smaller molecular weight ions (e.g., 70 percent sodium removal). The salt rejection of NF membranes is often inadequate in treating brackish groundwater. However, NF requires less energy than RO and consequently has been widely adopted in some parts of the

United States for brackish groundwater desalination. NF is also often used for softening (i.e., to remove calcium and magnesium [hardness] from a given solution).

2.3.8.2. Semi-batch Reverse Osmosis

The RO systems discussed thus far operate in a continuous mode. In other words, the membranes are treating the same feedwater, so the applied pressure to overcome the osmotic pressure is fixed. In semi-batch RO, also known as closed-circuit RO, the brine is recirculated and mixed with the pressurized feedwater in order to reduce the osmotic pressure of the feed over time and the overall energy consumption required for desalination. A variable operating pressure is applied as the feed pressure changes. Brine recirculation allows for over 90 percent recovery rate for brackish water desalination systems. An SEC of 0.64 to 0.76 kWh/m^3 has been reported in the literature [44]. Desalitech, LLC, which has commercialized this technology, claims a 20 percent energy consumption reduction in semi-batch RO compared to continuous RO [44].

2.4. Global and National Trends in Desalination

Location is of the utmost importance in desalination system design and selection for a variety of reasons, including the geographic variation in BGW composition and differences in regional water needs and in local costs of energy or electricity. For example, in much of the Middle East (e.g., Saudi Arabia, Israel), desalination is the primary, if not only, option to provide the required water supply. In other countries (e.g., China, Australia, United States), desalination provides a water supply that is more reliable, albeit more expensive, than traditional river and aquifer systems. For island users of desalination, such as in the Caribbean, energy is often very expensive compared to the energy costs in large oil-producing countries. This section explores global and national differences in operating and contracted desalination capacities by plant type, feedwater type, and target end use and in capital and operating desalination expenditures annually. Results are based on the most up-to-date data from the Global Water Intelligence desalination database [5].

2.4.1. Global Trends

Figure 2-8 shows annual operating capacity and contracted capacity by plant type from 2015 to 2024. The desalination market as a whole is expected to continue on an upward trajectory. Brackish water RO (BWRO) and ED-EDR together comprised 20 percent of the total operating desalination capacity in 2019. BWRO operating capacity has been and is expected to continue growing from year to year, although 2019 experienced a decrease in the annual growth rate from 4.3 percent (2018 vs. 2017) to 0.9 percent (2019 vs. 2018). Similarly, BWRO contracted capacity in 2019 reached the lowest level since 2015 (0.37 million m^3/day). This drop may be caused by market changes in China and Saudi Arabia, which are both major players in the desalination space; China is pivoting toward wastewater reuse, while Saudi Arabia is pivoting toward enhanced transmission and storage infrastructure. ED-EDR annual growth rate in terms of operating capacity was positive in 2015 through 2018 and negative in 2018 through 2019. Its growth rate is expected to remain negative as RO becomes more energy efficient and cost-effective.

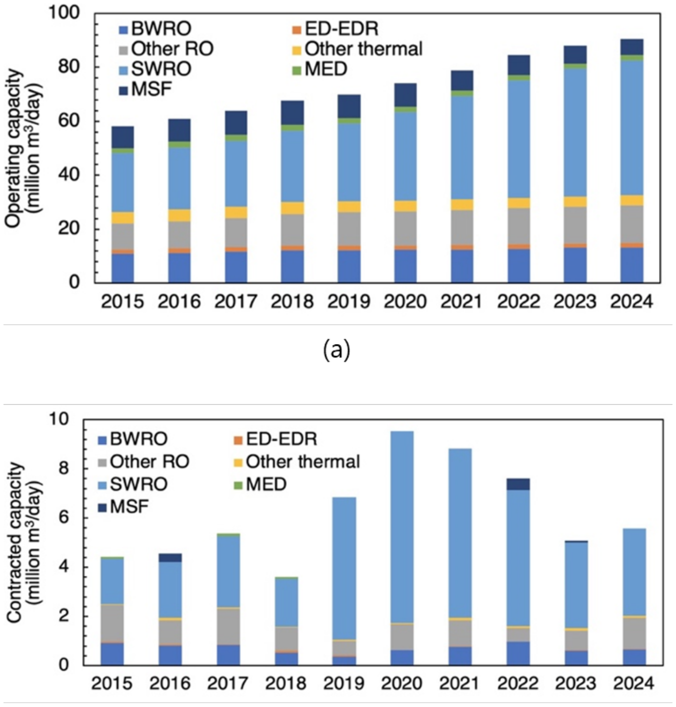

(a)

(b)

Figure 2-8. Annual desalination (a) operating capacity and (b) contracted capacity by plant type from 2015 to 2024.

2.4.1.1. Annual Desalination Expenditures

Annual desalination capital and operating expenditures by plant type from 2015 to 2024 can be found in Figure 2-9. In 2019, BWRO and ED CapEx were $276 million and $54.8 million, respectively; BWRO and ED OpEx were $1,455 million and $216 million, respectively. The OpEx of both technologies remains relatively constant, while the CapEx varies across the surveyed time period.

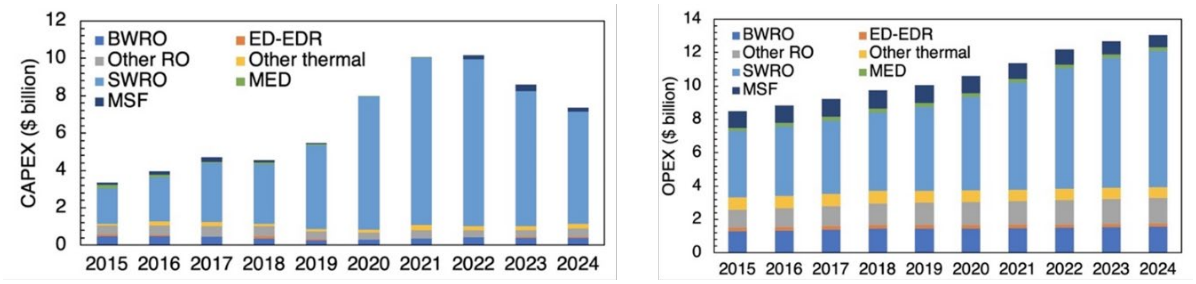

(a)

(b)

Figure 2-9. Annual desalination (a) capital expenditures and (b) operating expenditures by plant type from 2015 to 2024.

2.4.1.2. Geographic Region

Large numbers of desalination facilities are located in the Middle East and North Africa (MENA), Arab States of the Gulf, Asia/Pacific, Europe, and North America, while relatively few are based in Latin America, Caribbean, and Sub-Saharan Africa (Figure 2-10). Desalination plants are concentrated on or near the coastline for seawater desalination. Inland desalination plants tend to be smaller in capacity than coastal desalination plants. Today, the MENA and Arab States of the Gulf contain almost half of global desalination capacity, with Saudi Arabia, United Arab Emirates, and Kuwait serving as major regional and global leaders. The Asia/Pacific region has the next largest desalination regional capacity as a result of China's market share, followed by North America (almost entirely due to U.S. capacity), and Europe, where Spain is the leader.

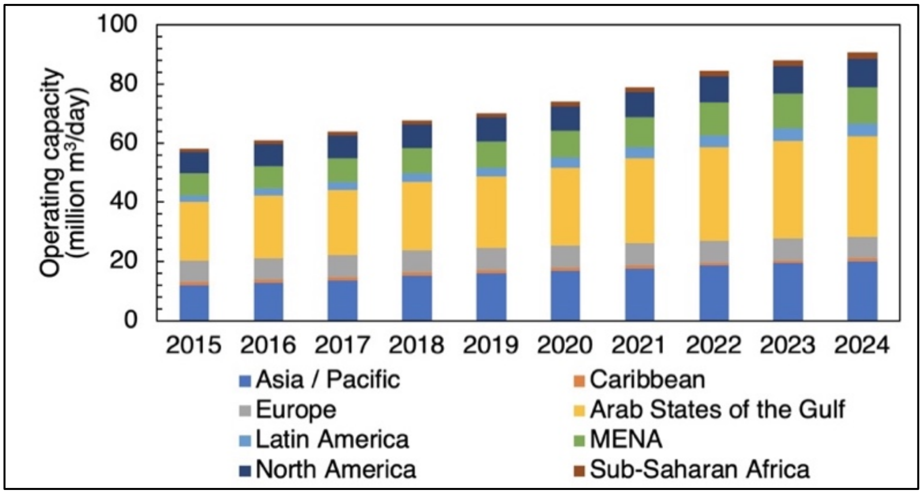

Figure 2-10. The breakdown of operating desalination capacity by geographic region from 2015 to 2024.

2.4.1.3. Target End Use

Desalination provides water for the following sectors in decreasing order: municipal (e.g., drinking water), industry, power, irrigation, and military. Municipal desalination plants are located worldwide, particularly in MENA. Compared to MENA, North America, Western Europe, and East Asia and Pacific regions contain a larger proportion of non-municipal desalination plants, because industrial and power sectors constitute large market shares. The few desalination plants in South America and Africa are primarily for industrial use. In Eastern Europe and Central Asia, Sub-Saharan Africa, and Southern Asia, desalination plants are predominantly designed to produce water for industrial and private applications. Figure 2-11 demonstrates the sectoral use of desalinated water annually from 2015 to 2024 in terms of industry and utility/other, which includes municipal, power, irrigation, and military.

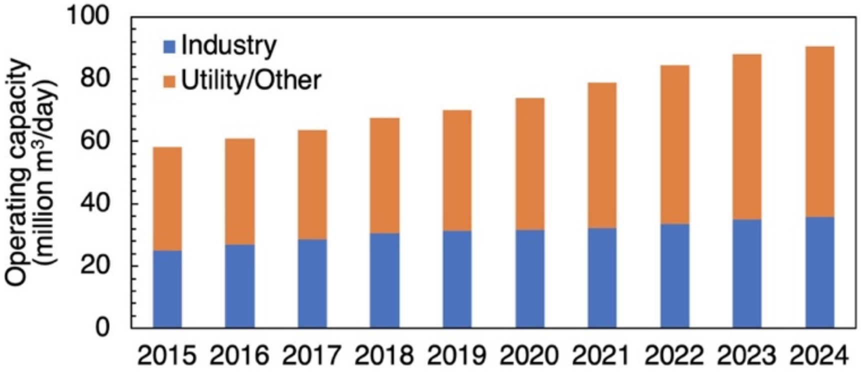

Figure 2-11. Sectoral use of desalinated water annually from 2015 to 2024 in terms of industry and utility/other, which includes municipal, power, irrigation, and military.

2.4.1.4. National Trends

The U.S., China, Saudi Arabia, Australia, and India are the top markets by contracted brackish water capacity (Figure 2-12(a)), while the United States, Saudi Arabia, China, Spain, and Australia are the top markets by brackish water desalination expenditure (Figure 2-12(b)). Consequently, these six countries are considered leaders in brackish water desalination. The contracted brackish water capacity is expected to decrease in India, Saudi Arabia, and China and increase in Australia and the United States, with the largest projected capacity in the United States. The annual OpEx from 2020 to 2024 is projected to range from 67 to 97 percent of the total annual desalination expenditure for brackish water desalination in Australia, Spain, China, Saudi Arabia, and the United States.

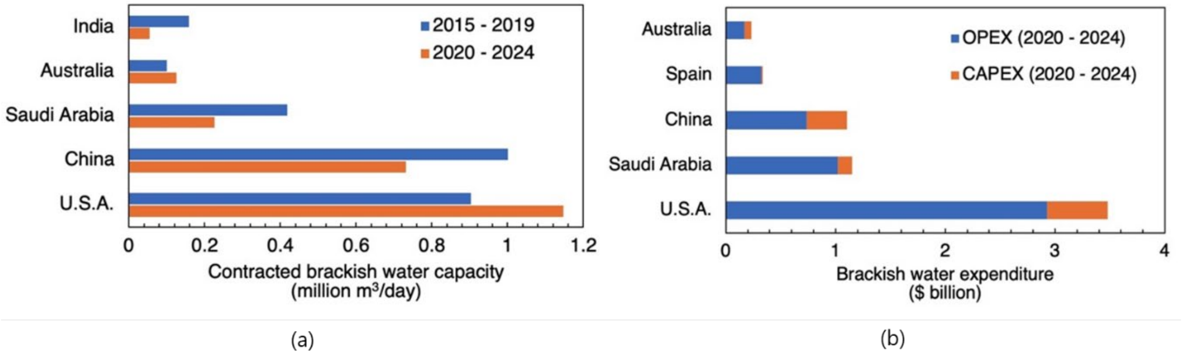

Figure 2-12. Top national markets by (a) contracted brackish water desalination capacity and (b) brackish water desalination CapEx and OpEx.

Figure 2-13 shows the national operating desalination capacities of Australia, Spain, China, Saudi Arabia, United States, and India as a function of (a) feedwater type, (b) plant type and (c) target end use in 2019. Together, the desalination capacity of these nations (independent of feedwater) constitutes more than 45 percent of the global capacity: Saudi Arabia (15.8 percent), United States (11.4 percent), China (98.8 percent), Spain (6.1 percent), India (2.9 percent) and Australia (1.2 percent). Feedwater type is divided into three categories: seawater (20,000 to 50,000 mg/L), brackish water (3,000 to 20,000 mg/L), and other (less than 3,000 mg/L). The "other" category includes freshwater (less than 500 mg/L), wastewater, and low-salinity brackish water (500 to 3,000 mg/L). The desalination feedwater breakdown varies from country to country. For instance, desalinated water in the United States predominantly originates from brackish water (500 to 20,000 mg/L), the majority of which is groundwater, while desalinated water in Saudi Arabia primarily originates from seawater. Across the considered countries, RO is overwhelmingly the dominant technology for both brackish water and seawater, with the exception of Saudi Arabia, in which thermal systems play a substantial role. India, China, and Australia primarily use their desalinated water for industrial purposes, while Spain, Saudi Arabia and the United States primarily use it for other purposes (e.g., municipal, agriculture).

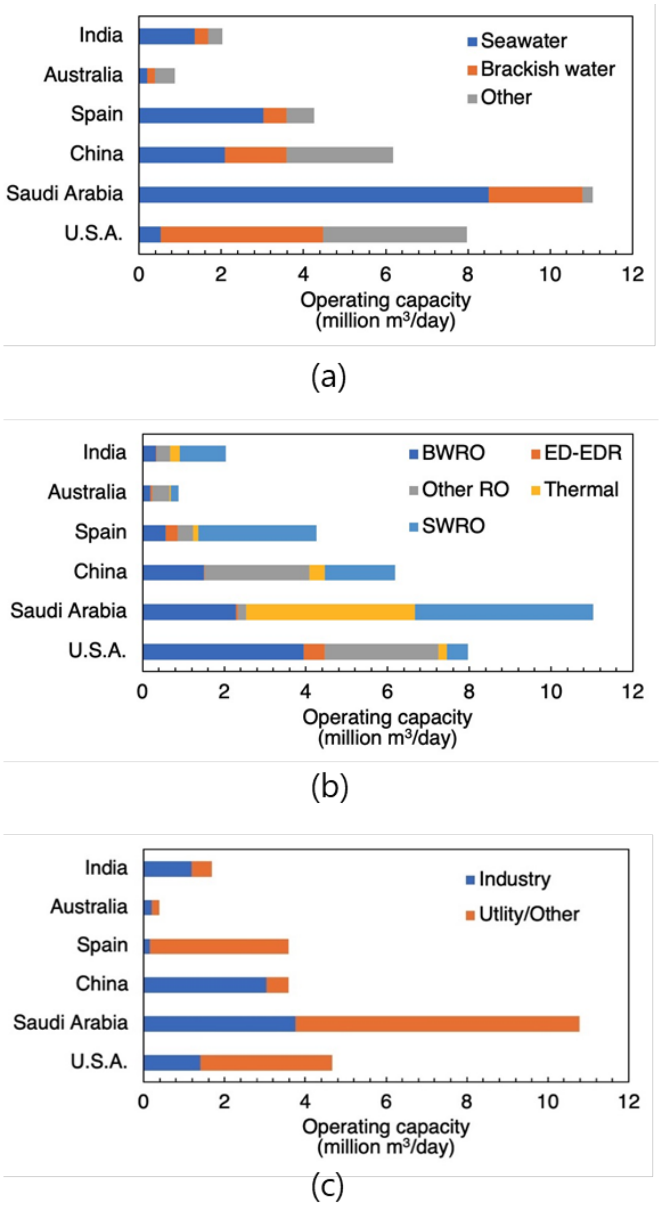

Figure 2-13. The national operating desalination capacities of the United States China, Saudi Arabia, Spain, India, and Australia as a function of (a) feedwater type, (b) plant type and (c) target end use in 2019.

2.5. References

[1] A. Mukherjee, B. Scanlon, A. Aureli, S. Langan, H. Guo, A. McKenzie. Global Groundwater: Source, Scarcity, Sustainability, Security and Solutions. 1st Edition, Elsevier. 2020. ISBN 9780128181720.

[2] Y. D. Ahdab, G. P. Thiel, J. Böhlke, J. Stanton, J. H. Lienhard. Minimum energy requirements for desalination of brackish groundwater in the United States with comparison to international datasets. *Water Research* 141 (2018) 387–404. doi:https://doi.org/10.1016/j.watres.2018.04.015. URL http://www.sciencedirect.com/science/article/pii/S0043135418302999

[3] J. S. Stanton, D. W. Anning, C. J. Brown, R. B. Moore, V. L. McGuire, S. L. Qi, A. C. Harris, K. F. Dennehy, P. B. McMahon, J. R. Degnan, et al. Brackish groundwater in the United States. Tech. rep., U.S. Geological Survey (2017).

[4] Office of Water of the U.S. Environmental Protection Agency, 2018 edition of the drinking water standards and health advisories. Tech. rep., EPA 822-F-18-001, Washington, DC. 2018.

[5] Global Water Intelligence. Desaldata online database (2020). URL https://www.desaldata.com/

[6] E. Jones, M. Qadir, M. T. van Vliet, V. Smakhtin, S. mu Kang. The state of desalination and brine production: A global outlook. *Science of The Total Environment* 657 (2019) 1343–1356. doi:https://doi.org/10.1016/j.scitotenv.2018.12.076.

[7] S. Veerapaneni, B. Klayman, S. Wang, R. Bond. Desalination Facility Design and Operation for Maximum Efficiency. Water Research Foundation. Denver, Colorado. 2011.

[8] A. Al-Karaghouli, L. L. Kazmerski. Energy consumption and water production cost of conventional and renewable-energy-powered desalination processes. *Renewable and Sustainable Energy Reviews* 24 (2013) 343–356. doi:https://doi.org/10.1016/j.rser.2012.12.064. URL http://www.sciencedirect.com/science/article/pii/S1364032113000208

[9] C. Q. He, R. G. Bond. Inland desalination and concentrate management. American Water Works Association. 2019.

[10] C.-C. Ho. Chapter 7 - Membranes for Bioseparations, in: S.T. Yang (Ed.), Bioprocessing for Value-Added Products from Renewable Resources. pp. 163–183. Elsevier. Amsterdam, The Netherlands. 2007. doi:https://doi.org/10.1016/B978-044452114-9/50008-6.

[11] S. D. Faust, O. M. Aly. Chemistry of Water Treatment. CRC Press. 2018.

[12] P. Rao, A. Aghajanzadeh, P. Sheaffer, W. R. Morrow, S. Brueske, C. Dollinger, K. Price, P. Sarker, N. Ward, J. Cresko. Volume 1: Survey of Available Information in Support of

the Energy-Water Bandwidth Study of Desalination Systems. Tech. rep. Lawrence Berkeley National Laboratory. 2016.

[13] R. Semiat. Energy issues in desalination processes. *Environmental Science & Technology* 42 (22): 8193–8201. (2008) pMID: 19068794. doi:10.1021/ es801330u.

[14] T. Mezher, H. Fath, Z. Abbas, A. Khaled. Techno-economic assessment and environmental impacts of desalination technologies. *Desalination* 266 (1-3): 263–273. (2011). doi:10.1016/j.desal.2010.08.035.

[15] S. Avlonitis, K. Kouroumbas, N. Vlachakis. Energy consumption and membrane replacement cost for seawater ro desalination plants. *Desalination* 157 (1) (2003) 151–158, desalination and the Environment: Fresh Water for all. doi:https://doi.org/10.1016/S0011-9164(03)00395-3. URL http://www.sciencedirect.com/science/article/pii/ S0011916403003953

[16] J. R. Ziolkowska, Desalination leaders in the global market – current trends and future perspectives, Water Supply 16 (3) (2015)563–578. doi:10.2166/ws.2015.184.

[17] United Nations, Escwa water development report 3 role of desalination in addressing water scarcity (2009).

[18] K. Quteishat, Desalination and water affordability, in: SITeau International Conference, Casablanca, Morocco, 2009.

[19] A. M. Lopez, M. Williams, M. Paiva, D. Demydov, T. D. Do, J. L. Fairey, Y. J. Lin, J. A. Hestekin, Potential of electrodialytic techniques in brackish desalination and recovery of industrial process water for reuse, Desalination 409 (2017) 108–114. doi:https://doi.org/10.1016/j.desal.2017.01.010.

[20] A. Al-Karaghouli, L. Kazmerski, Economic and technical analysis of a reverse-osmosis water desalination plant using deep-3. 2 software, Journal of Environmental Science and Engineering, A 1 (3) (2012) 318–328.

[21] E. Fatima, M. Elazhar, M. Hafsi, A. Elmidaoui, Performances of electrodialysis process in desalination of brackish waters at various salinities and voltage, International Journal of Advanced Chemistry 2 (2) (2014) 49–52. doi:10.14419/ijac.v2i2.1741.

[22] R. Singh, Analysis of energy usage at membrane water treatment plants, Desalination and Water Treatment 29 (1-3) (2011) 63–72. doi:10.5004/ dwt.2011.2988.

[23] J. P. MacHarg, Energy optimization of brackish groundwater reverse osmosis desalination, Texas Water Development Board, 2011.

[24] T. Qiu, P. A. Davies, Comparison of configurations for high-recovery inland desalination systems, Water 4 (3) (2012) 690–706. doi:https://doi.org/ 10.3390/w4030690.

[25] G. Gude, Sustainable desalination handbook: plant selection, design and implementation, Butterworth-Heinemann, 2018.

[26] R. K. McGovern, S. M. Zubair, J. H. Lienhard, The cost effectiveness of electrodialysis for diverse salinity applications, Desalination 348 (2014) 57–65. doi:https://doi.org/10.1016/j.desal.2014.06.010.

[27] R. K. McGovern, S. M. Zubair, J. H. Lienhard, The benefits of hybridising electrodialysis with reverse osmosis, Journal of Membrane Science 469 (2014) 326–335. doi:https://doi.org/10.1016/j.memsci.2014.06.

[28] K. Zotalis, E. G. Dialynas, N. Mamassis, A. N. Angelakis, Desalination technologies: Hellenic experience, Water 6 (5) (2014) 1134–1150. doi: https://doi.org/10.3390/w6051134.

[29] I. C. Karagiannis, P. G. Soldatos, Water desalination cost literature: review and assessment, Desalination 223 (1-3) (2008) 448–456.

[30] L. F. Greenlee, D. F. Lawler, B. D. Freeman, B. Marrot, P. Moulin, Reverse osmosis desalination: Water sources, technology, and today's challenges, Water Research 43 (9) (2009) 2317–2348. doi:https://doi.org/10.1016/j.watres.2009.03.010.

[31] J. E. Miller, et al., Review of water resources and desalination technologies, Sandia National Laboratories, Albuquerque, NM 49 (2003) 2003–0800. doi:10.2172/809106.

[32] J. Arroyo, S. Shirazi, Cost of brackish groundwater desalination in Texas, Tech. rep. (2012).

[33] M. Ahmed, W. H. Shayya, D. Hoey, J. Al-Handaly, Brine disposal from reverse osmosis desalination plants in oman and the united arab emirates, Desalination 133 (2) (2001) 135–147. doi:https://doi.org/10.1016/S0011-9164(01)80004-7.

[34] A. Panagopoulos, K.-J. Haralambous, M. Loizidou, Desalination brine disposal methods and treatment technologies - a review, Science of The Total Environment 693 (2019) 133545. doi:https://doi.org/10.1016/j.scitotenv.2019.07.351.

[35] R. Klaimi, S. Y. Alnouri, M. Al-Hindi, F. Azizi, Optimization techniques for coupling renewable/hybrid energy options with desalination systems for carbon footprint reduction, Chemical Engineering Research and Design 151 (2019) 270 – 290. doi:https://doi.org/10.1016/j.cherd.2019.09.010.

[36] G. Gude, Renewable Energy Powered Desalination Handbook: Application and Thermodynamics, Butterworth-Heinemann, 2018.

[37] R. G. Cavalcante Ju´nior, M. A. Vasconcelos Freitas, N. F. da Silva, F. R. de Azevedo Filho, Sustainable groundwater exploitation aiming at the reduction of water vulnerability in the brazilian semi-arid region, Energies 12 (5) (2019) 904. doi:https://doi.org/10.3390/en12050904.

[38] A. M. Bilton, R. Wiesman, A. Arif, S. M. Zubair, S. Dubowsky, On the feasibility of community-scale photovoltaic-powered reverse osmosis desalination systems for remote locations, Renewable Energy 36 (12) (2011) 3246–3256. doi:https://doi.org/10.1016/j.renene.2011.03.040.

[39] N. C. Wright, A. G. Winter, Justification for community-scale photovoltaic-powered electrodialysis desalination systems for inland rural villages in india, Desalination 352 (2014) 82–91. doi:https://doi.org/10.1016/j.desal.2014.07.035.

[40] M. Maisch, Solar electricity can retail for $0.027–0.036/kwh as renewables close in on global grid parity (2019). URL https://www.pv-magazine.com/2019/11/01/solar-electricity-can-retail-for-0-027-0-036-kwh-as-renewables-close-in-on-global-grid

[41] D. Dudley, Race heats up for title of cheapest solar energy in the world (2019). URL https://www.forbes.com/sites/dominicdudley/2019/10/17/ cheapest-solar-energy-in-the-world/#1a1418c34772

[42] R. Wiser, M. Bolinger, 2017 wind technologies market report, Tech. rep., U.S. Department of Energy's Office of Energy Efficiency and Renewable Energy (2017).

[43] M. Isaka, Water desalination using renewable energy, Tech. rep., International Renewable Energy Agency (2013).

[44] A. Subramani, J. G. Jacangelo, Emerging desalination technologies for water treatment: A critical review, Water Research 75 (2015) 164–187. doi:https://doi.org/10.1016/j.watres.2015.02.032.

3. Technical Approach and Methods

This section discusses the experimental and modeling approaches used to determine key MSED system parameters, as well as the market research and cost methods used for comparing MSED to other brackish desalination technologies.

3.1. MSED Operating Principles

In an MSED system, two types of monovalent selective ion-exchange membranes, arranged in alternating order between two electrodes, separate a feed stream into a product (or diluate) stream and a concentrate stream. Anion exchange membranes (AEMs) and cation exchange membranes (CEMs) contain positively charged and negatively charged groups, respectively, fixed to their polymer matrix [7]. The membranes employ Donnan exclusion to enable the selective charge-based migration of ionic species [14]: AEMs allow the transport of monovalent anions, while rejecting divalent anions and all cations. Similarly, CEMs enable the transport of monovalent cations while rejecting divalent cations and all anions. The effectiveness of ion-exchange membranes depends on various parameters, such as the type and concentration of the fixed charges in the polymer, the hydrophobic nature of the matrix polymer, the membrane morphology, and the polymer network density [7].

Spacers are placed between the membranes and electrodes, as well as between the membranes themselves, in order to configure the flow. An applied potential difference across the electrodes induces ion transport across the membranes. Anions migrate towards the anode, while cations migrate toward the cathode.

Figure 3-1 demonstrates this process for an MSED system with two membranes treating brackish groundwater, typically source water for irrigation. The primary groundwater constituents are calcium, magnesium, sulfate, sodium, and chloride [15]. Sodium and chloride, which are monovalent ions, are damaging to crops. Calcium, magnesium, and sulfate, which are divalent ions, act as nutrients to crops. The MSED desalination process generates a diluate stream containing low salinity and high nutrient concentrations for irrigation, and a concentrate stream containing high salinity and high sodium chloride concentration for disposal or reuse after treatment.

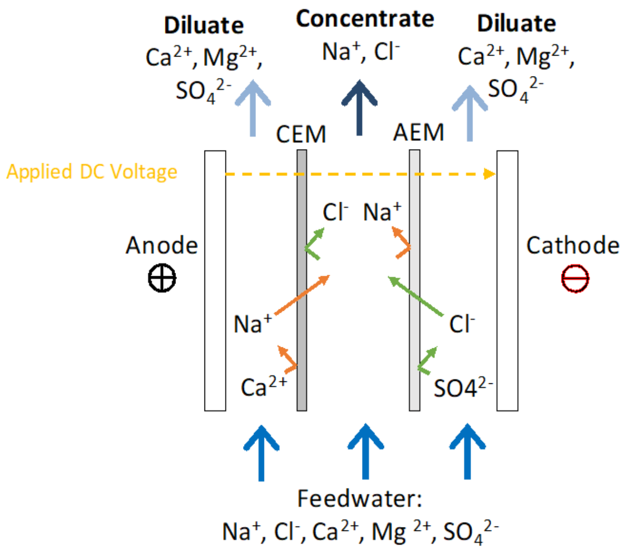

Figure 3-1. A simplified MSED stack consisting of two electrodes, a CEM, and an AEM. In reality, the number of membrane cell pairs is much greater. Groundwater serves as the feedwater. An applied voltage across the electrodes yields a diluate stream, high in nutrients and low in NaCl, for irrigation and a concentrate stream for disposal. Magnesium, not shown here, will show similar behavior as calcium.

We may express the net salt and water transport across the membrane in each compartment of the MSED stack as:

$$J_{s,j} = \frac{T^{s}_{cp,j}i}{zF} - L_j(C_{j,c,m} - C_{j,d,m}) \tag{1}$$

$$J_w = \frac{T^{w}_{cp}i}{F} + L_w(\pi_{s,c,m} - \pi_{s,d.m}) \tag{2}$$

where J is flux in $mol \cdot m^{-2} \cdot s^{-1}$, *s* denotes salt, *w* denotes water, *T* is a transport number, *F* is Faraday's constant, *L* is the membrane permeability in $m \cdot s^{-1}$ for the salts and in $s \cdot m^{-1}$ for the water, *z* is the ion valence, *c* denotes concentrate, *d* denotes diluate, *m* is membrane, and *C* is a concentration in $mol \cdot m^{-3}$. The subscript *j* represents an ion species in the groundwater that travels across the series of ion-exchange membranes. The applied current density *i* is a function of Donnan potentials and ohmic resistances for the membranes, diluate, concentrate and rinse. The salt flux in Equation 1 depends on ion migration (first term) and ion diffusion (second term), while the water flux in Equation No. 2 depends on electro-osmosis (first term) and water diffusion (second term). In order to characterize the MSED Fujifilm membranes, we experimentally evaluate the following membrane parameters from these equations: ion transport numbers, membrane selectivity, membrane resistance, and limiting current density. These membrane parameters serve as inputs to an MSED model that we develop.

3.2. MSED Experimental Methods

The following parameters are experimentally determined in order to characterize MSED Neosepta and Fujifilm membranes in the brackish water salinity range: membrane resistance and limiting current density, membrane salt and water permeabilities, ion transport numbers, and membrane selectivity.

3.2.1. Experimental Set-up

The MSED experimental set-up (Figure 3-2) uses a PCCell ED200 stack that contains 10 cell pairs of Neosepta membranes (total active membrane area of 0.43 m^2), 20 spacers of 0.5 mm thickness and two end spacers in the electrode streams of 1 mm thickness. Diluate, concentrate, and electrode rinse circuits are in a batch configuration. Diluate, concentrate, and electrode rinse containers can hold up to 1 L, 4 L, and 4 L, respectively, of solution. Simulated groundwater containing sodium, calcium, magnesium, chloride, and sulfate serves as feedwater in the diluate and concentrate tanks. Sodium sulfate (0.2 M) is used as the electrode rinse to stabilize pH. Centrifugal pumps (Iwaki, model MD-55R (T)) circulate the three streams, and valved-rotameters regulate the constant flowrate of 95 liters per hour. The flow channel height is 0.5 mm. The power supply (GWINSTEK GPR-60600) applies a voltage to induce ion transport and separation across the stack. Feed and product water quality is measured using an inductively coupled plasma optical emission spectrometer. A heat exchanger regulates the concentrate temperature, with the stack effectively serving as a second heat exchanger that regulates the diluate temperature. All tests are conducted at 25° C.

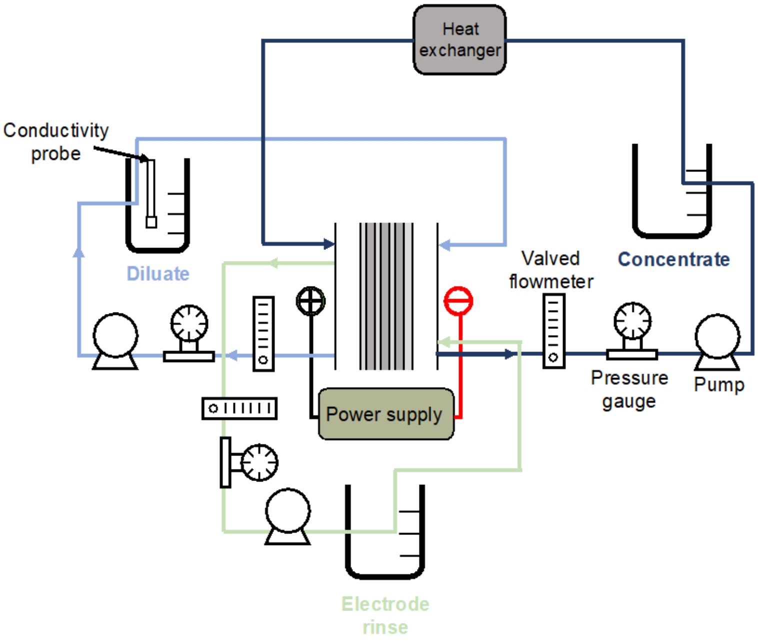

Figure 3-2. MSED set-up consisting of a diluate, concentrate, and rinse circuit feeding an ED200 stack.

3.2.2. Brackish Groundwaters Analyzed

In the present analysis, we define brackish groundwater (BGW) as containing 500 to 10,000 ppm TDS. To evaluate the impact of ionic composition on MSED membrane performance, we analyze multiple BGWs containing various cation and anion solute ratios, defined as:

$$r_{cation} = \frac{C_{Ca^{2+}}+C_{Mg^{2+}}}{C_{Na^{+}}+C_{Ca^{2+}}+C_{Mg^{2+}}} \tag{3}$$

$$r_{anion} = \frac{C_{SO_4{}^{2-}}}{C_{Cl^{-}}+C_{SO_4{}^{2-}}} \tag{4}$$

BGW compositions tested in the MSED experiments are selected based on BGW samples in the U.S. Geological Survey (USGS) major-ions dataset [15]. The dataset contains 28,000 U.S. BGW samples with complete composition data, not diverging from electroneutrality by more than 5 percent. Approximately 91 percent of the USGS samples contain between 500 and 3,000 ppm TDS. Table 3-1 contains 16 BGW solutions with different r_{cation}, r_{anion}, and TDS values analyzed in this study. The Cohen composition corresponds to the BGW composition used in the Cohen et al. study [6], the only prior work on upgrading BGW quality for agriculture using MSED. We define solute ratio in terms of C_j (mg/L), rather than w_j (milliequvalents per liter), in order to develop transport number fits as a function of measured ion concentrations C_j. For BGWs considered in this study, the correlation coefficient of solute ratio calculated using C_j and w_j is equal to 1 for cations and anions. Consequently, observed trends as a function of solute ratio will be the same using either concentration basis.

The sodium adsorption ratio (SAR) of the product waters is defined as:

$$SAR = \frac{W_{Na^{+}}}{\sqrt{0.5(W_{Ca^{+}}+W_{Mg^{+}})}} \tag{5}$$

where W is ion concentration in milliequivalents per liter. As a general rule, waters with low SAR (SAR ≤ 3) have no limitations on irrigation use; waters with a higher SAR (3 ≤ SAR ≤ 9) have slight to moderate limitations on irrigation use [18].

Table 3-1. BGW compositions analyzed in the MSED experiments. Compositions (Comp.) with TDS of 1,500 to 10,000 ppm were tested at approximately 1,500, 3,000, 5,000, and 10,000 ppm.

Label	r_{cation}	$r_{Ca^{2+}}$	$r_{Mg^{2+}}$	r_{anion}	TDS (ppm)
Comp. 1	0.40	0.32	0.08	0.40	1,500-10,000
Comp. 2	0.60	0.46	0.14	0.14	1,500-10,000
Comp. 3	0.21	0.13	0.09	0.64	1,500-10,000
Comp. 4	0.39	0.31	0.08	0.57	3,000
Comp. 5	0.40	0.33	0.07	0.21	3,000

Label	r_{cation}	$r_{Ca^{2+}}$	$r_{Mg^{2+}}$	r_{anion}	TDS (ppm)
Cohen	0.24	0.14	0.08	0.30	2,588

3.2.3. Membrane Resistance and Limiting Current Density

The MSED stack can be represented as the sum of ohmic terms $\bar{r}$, Donnan potentials E_{AEM} and E_{CEM}, and an electrode potential V_{el}:

$$V_{stack} = i\left[N_{cp}\left(2\bar{r}_m + \frac{\bar{r}_d}{\sigma} + \frac{\bar{r}_c}{\sigma}\right) + \bar{r}_m + 2\bar{r}_r\right] + N_{cp}(E_{AEM} + E_{CEM}) + V_{el} \tag{6}$$

where N_{cp} is number of cell pairs, r denotes the rinse solution, and σ denotes the spacer shadow effect. The circuit resistances can be written as the ratio of flow channel height h to electrical conductivity k:

$$\bar{r} = \frac{h}{k} \tag{7}$$

To determine membrane resistance and limiting current density, we conduct current-voltage tests at constant diluate and concentrate conductivity ($k_d = k_c = k$) for NaCl solutions containing a TDS of 800, 1,500, 3,000, 5,000, and 10,000 ppm and for Comp. 2 BGW solutions containing a TDS of 1,500, 3,000, and 5,000 ppm. The CEM and AEM resistance, which we assume to be equivalent, was evaluated at each conductivity using the slope of a linear fit of V_{stack} versus the applied current from Equation No. 6:

$$m = \left(2N_{cp} + 1\right)\bar{r}_m + \frac{2N_{cp}h}{\sigma k} + \frac{2h_r}{\sigma k_r} \tag{8}$$

The limiting current density was determined by employing the Cowan and Brown method [18]. The MSED stack electrical resistance ($\Delta V_{stack}/I$) was plotted as a function of the inverse of applied current ($1/I$) for each conductivity; the minimum point at which the electrical resistance begins to increase corresponds to the inverse of limiting current ($1/I_{lim}$).

3.2.4. Membrane Diffusion Permeability

To determine the diffusion permeabilities of the membranes to salt, we conducted tests at zero current ($i = 0$) with de-ionized water flowing in the diluate compartment at $t = 0$. Three tests for each of the four salinities were performed for Comp. 1, Comp. 2, and Comp. 3 to ensure repeatability. During these tests, an approximately constant concentrate conductivity was maintained by selecting an initial concentrate solution volume that was four times that of the diluate. The increase in concentration observed in the diluate compartment was attributed to osmosis. The change in concentration is halved to account for transport to both adjacent diluate streams, as observed in Equation No. 8. During this process, the effects of concentration polarization (CP) are neglected given the relatively short process run-time. The pumps were turned on and data for diluate conductivity and mass were recorded versus time for a total duration of 40 to 60 minutes. Based on Equation No. 1, in which the ion flux is defined, the ion permeability can be written as:

$$L_j = \frac{\Delta m_j / M_j}{\left(C_c - \frac{\Delta C_d}{2}\right)\Delta t A_m N_{cp}} \tag{9}$$

where Δm_j is the change in ion mass during a process run-time of Δt, and M_j is the ion molar mass.

3.2.5. Transport Number and Membrane Selectivity

Ion transport numbers were determined by running tests at constant current and measuring the mass of ions transported across the membranes in a fixed amount of time. Three tests were conducted at each set of conditions (16 BGW solutions: Comp. 1 through Comp. 5 and Cohen at specified salinities) to ensure repeatability. During these tests, simulated BGW served as the feedwater in the diluate and concentrate circuits. The pumps were turned on, and a constant current was applied across the stack, such that i/i_{lim} does not exceed 0.7, which is typical of brackish water operation in commercial ED systems [19]. Based on Equation No. 1, the ion transport number is defined as:

$$T_{s,j}^{cp} = \frac{\Delta w_j F}{i \Delta t A_m N_{cp}} \tag{10}$$

where Δw_j is the change in ion concentration in milliequivalents relative to the initial ion concentration at $t = 0$. Because we have used the Hittorf method, the ion diffusion term in Equation No. 1, which is nearly three orders of magnitude less than the ion migration term, is neglected. This has been validated even for high-salinity applications by McGovern et al. [17].

To quantify the MSED membranes' ability to selectively remove monovalent ions relative to divalent ions, we define a membrane permselectivity P as the ratio of the divalent to monovalent transport numbers, normalized by their initial ion concentrations at $t = 0$:

$$P_{mon}^{div} \equiv \frac{T_{div}/w_{div,o}}{T_{mon}/w_{mon,o}} \tag{11}$$

The closer P is to unity, the lower the membranes' monovalent selectivity. Smaller permselectivities denote better rejection of monovalent ions and allude to a more efficient MSED system.

3.3. MSED Process Model

A model for ion and water transport was developed using the experimentally determined parameters as inputs. The model discretizes the MSED stack into differential volumes and uses Equation Nos. 1 and 2 to quantify the overall ion and water transport. The model's purpose is to inform and direct the experimental approach while simultaneously validating results.

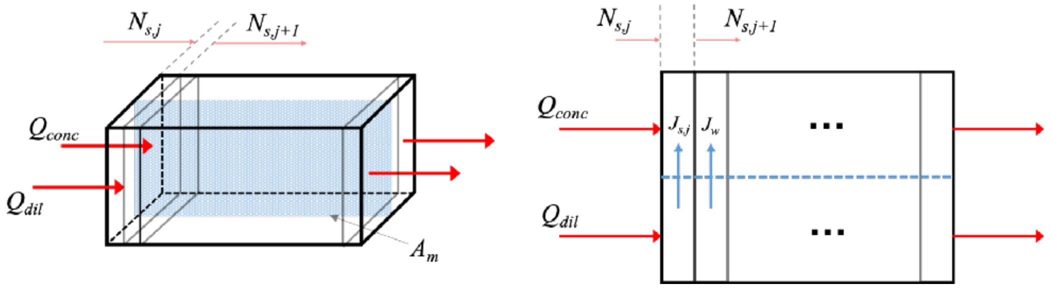

Figure 3-3. An MSED diagram illustrating conventions for the direction of salt and water flux across the membrane in each compartment of the stack.

The stagnant film model is used to quantify concentration polarization in the diluate and concentrate compartments. The stagnant film model has shown alignment with experiments even for high-salinity applications, justifying its usage in the brackish salinity range. Equation No. 12 represents the mathematical relation used to calculate the concentration boundary layer.

$$\Delta C_j = \left(\frac{T_{cu} - t_{cu,j}}{D_j}\right)\left(\frac{i}{zF}\right)\left(\frac{2h}{Sh}\right) \tag{12}$$

where ΔC_j is the difference in concentration between the bulk flow and membrane surface for species j. The concentration boundary layer is symmetric on both sides of the ion exchange membranes to conserve mass. T_{cu} is the counter ion transport number determined from experiments and $t_{cu,j}$ is the integral counter ion transport number. D_j is the diffusion coefficient of species j in water, h is the channel height in the MSED stack, and Sh is the Sherwood number. The empirical relation adopted by McGovern et al. for the MSED setup was used to determine the Sherwood number [20]:

$$Sh = 0.37 Re_D^{0.5} Sc^{0.33} \tag{13}$$

where Re_D is the Reynolds number based on the hydraulic diameter of the MSED stack and Sc is the Schmidt number. Re_D in the MSED set-up is approximately equal to 37, which falls in the Re_D range (25-50) required for Equation No. 13 to be valid.

The value for $t_{cu,j}$ commonly used in the literature is 0.5 for NaCl solutions [20]. Since this paper tests multi-ion solutions, the integral counter-ion transport number is calculated for each ion species using Equation No. 14.

$$t_{cu,j} = \frac{z_j D_j C_j}{\sum_{i=1}^{N_i} z_i D_i C_i} \tag{14}$$

where C_j is the equivalent concentration of ion species j, and i iterates through all cations or anions present within the solution.

3.4. Technology Comparison: Market Research and Cost Model

Primary market research on greenhouses and cost models for MSED, ED, RO, and CCRO are developed in order to perform a cost comparison of these technologies.

3.4.1. Market Research to Identify Greenhouse Industry Needs

To effectively compare desalination technologies for use in greenhouses, the metrics for comparison and the requirements for greenhouses need to be characterized. To identify the desalination needs and priorities of the greenhouse industries and evaluate the possible savings we carried out a detailed review of the literature, as well as phone and in-person interviews of greenhouse growers and operators.

We focused on greenhouses in North America that currently used desalination technologies. Within North America, we determined that desalination systems were currently being used in parts of California and Florida in the United States and in the state of Queretaro in Mexico. A total of 34 in-person interviews were conducted in these states: five in Florida, 10 in California, and 19 in Queretaro. The in-person interviews conducted in the United States covered 206 hectares, or 26 percent of the area under greenhouse cultivation in the United States [38]. The in-person interviews conducted in Mexico covered a cultivation area of 484 hectares, or approximately 14 percent of the area under cultivation in large greenhouses (larger than 5 hectares) that is reported in the literature [38]. Thus, the findings are representative of the industry's desalination needs.

3.4.1.1. Desalination System Configuration and Design Specifications

Figure 3-4 shows the typical water flow configuration in greenhouses that use groundwater. Groundwater is pumped from an aquifer to a desalination system that produces a brine stream and a treated water stream. Nutrients are added to the treated water to obtain a nutrient solution, which is sent to the greenhouse. Several greenhouses recirculate the water, leaving a greenhouse after disinfecting the water using ultraviolet radiation. In the greenhouses we interviewed, both the desalination brine and the discharge water from the greenhouse were used to irrigate field crops and trees such as avocados that were more salt-tolerant.

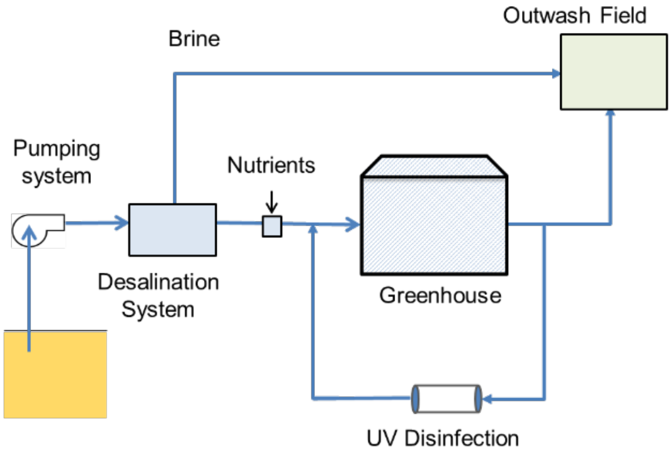

Figure 3-4. Diagram showing typical water flow in a greenhouse

Table 3-2 summarizes the desired desalination system specifications. For each parameter, both the range of values encountered in our interviews and the final design value chosen for our analysis is shown. The chosen values represented the most commonly found values at greenhouses that used desalination systems. For the calculations reported in this paper, each hectare under greenhouse cultivation needed a desalination system with a capacity of 60 m^3/day operated without supervision for 12 hours a day, year-round at a 90 percent capacity factor. The feed water was assumed to have 850 ppm of total dissolved solids. Greenhouses typically wanted a payback period of 2 years on their investments. Within our sample of greenhouses, the average cost of fertilization was \$3/m^2. The sodium level desired in nutrient water was 23 ppm (about 1 mM/L). The levels of calcium and magnesium varied with the type of vegetable cultivated. For our calculations, we assumed a representative desired value of 175 ppm of calcium ions (about 4.4 mM/L) and 40 ppm (about 1.7 mM/L) of magnesium ions.

Table 3-2. Desired desalination system specifications

Parameter	Units	Range	Value
System			
Capacity per hectare	m^3/day-ha	50-100	60
Feed water TDS	ppm	320-1,100	850
Operation time	hours	8-12	12
Type of operation	-	Auto.	Auto.
Desired payback	(yr.)	2-4	2
Fertilizer cost	\$/m^2	2.5-4.1	3
Desired nutrient water composition			
Na^+	ppm	23-115	23
Ca^{2+}	ppm	120-200	175
Mg^{2+}	ppm	40-80	40

3.4.1.2. Discussion on Greenhouse Priorities and Market Learnings

The key learnings related to the greenhouse industry and their desalination needs and priorities are discussed below.

3.4.1.2.1. Two Different Types of Greenhouse End Users with Different Priorities

From interviewing greenhouse growers, we realized that within the greenhouse industry, there were two very different types of end-users: greenhouses with areas less than 5 hectares under cultivation, and those with areas greater than 5 hectares. Greenhouses with less than 5 hectares under cultivation generally tended to be small family-owned operations with limited capital budgets and a strong preference to buy technology that has already been proven to be reliable. These greenhouses were less interested in obtaining fertilizer savings using partial desalination technologies. They were far more interested in achieving higher water recoveries from their desalination systems to reduce their groundwater usage and be prepared for potential future regulations on groundwater use.

Greenhouses with more than 5 hectares under cultivation had a more corporate ownership model with a greater focus on delivery return on investments to stockholders. These greenhouses were interested in cost savings wherever possible and were interested in new desalination technologies that could increase both water savings and fertilizer savings. We also observed significant economies of scale at work in the greenhouse industry, with profit margins generally increasing with acreage under cultivation. Larger greenhouses were interested in investing in new technologies but generally required payback periods less than 2 years.

3.4.1.2.2. Technologies Used in the Field

All the desalination systems used within the sample of greenhouses we interviewed in the United States used RO systems. In comparison, in the sample of greenhouses interviewed around Querétaro, Mexico, only one greenhouse used an RO system while the other greenhouses used ion-exchange resin-based systems. The technology choice was largely a reflection of the salinity of the groundwater in both regions.

The groundwater salinity in the greenhouse clusters around Querétaro, Mexico, was generally less than 400 ppm. In comparison, greenhouses that we sampled in the United States that used RO had groundwater salinities ranging from 575 to 1,300 ppm, with a salinity of 850 ppm being representative. Ion-exchange resin-based water treatment systems typically operate well only up to a salinity of 400 ppm. All the greenhouses we interviewed in the United States had groundwater salinities higher than the range of operation of ion-exchange resin-based systems. Furthermore, the budgets for equipment for greenhouses in Mexico was much lower than for greenhouses in the United States, and the Mexican operators overwhelmingly preferred the lower-cost ion-exchange resin-based systems (which were reportedly 70 percent the capital cost of RO and 40 percent the operating cost).

In view of their low salinity range of operation, ion-exchange resin-based systems are considered water softening systems and not desalination systems. For this paper, in order to make a fair comparison, we focused our analysis on desalination technologies for treating water with salinities greater than 500 ppm.

3.4.1.2.3. Low Desired Payback Periods

Greenhouse operators generally wanted the payback periods on capital to be 2 to 4 years, with the most common response in our interviews being 2 years. Despite the high revenues per m^3 of water enabled by desalination technologies, capital cost for RO equipment is only a fraction of the revenue enabled by RO. Due to widespread production of RO systems for industrial and municipal applications around the world and high competition between RO companies, RO systems are now a commodity product. Thus, newer desalination technologies, in order to compete with RO, must have capital costs comparable to RO, or at the maximum, a capital cost that can be paid off by the relative savings incurred over RO within a 2-year period:

$$CapEx_{max,desal} = CapEx_{RO} + 2 \times Sav_{desal,yr} \tag{15}$$

3.4.1.2.4. Price of Water

To estimate the value provided by increased water recovery from a desalination system, prices needs to be set on groundwater (feed water to the desalination system), product water, and brine discharge. During our interviews, we realized that there were several different water prices to consider and that there was a mismatch between the true value of the water and its current market price. Before selecting prices for groundwater, product water, and brine discharge for our analysis, a deeper discussion on water prices is needed.

Table 3-3 shows current water prices depending on the type of water. Water is typically heavily subsidized for agricultural use, with the average cost of water for a farm in the United States being \$0.027/m^3 [41]. Municipal water costs can be significantly higher, with agricultural users in Ventura County in southern California paying \$1.05/m^3 [43]. The high cost of municipal water has led several greenhouses to invest in wells to source groundwater at significantly lower costs.

Table 3-3. Range of Water Prices

Water source	Ref.	Water price	
		(\$/acre-foot)	(\$/m^3)
Groundwater tariff in Texas	[39]	1	0.0008
Cost of pumping per 100 feet	[40]	20.5	0.017
Average cost of farm water in the United States	[41]	33	0.027
Median cost of recharging groundwater in California	[42]	390	0.32
Cost of surface water for agricultural use in Ventura County, California	[43]	1294	1.05

True value of groundwater:

Historically, in the United States and other parts of the world, groundwater withdrawals were not heavily regulated, with withdrawal tariffs being non-existent or very low (e.g., groundwater tariffs are only \$0.0008/m^3 in Texas [39]). The current cost of groundwater for a greenhouse largely consists of capital cost for well construction and energy costs for lifting water. For every 100 feet of aquifer depth, the operating cost of pumping water is reported to be \$0.017/m^3 [40]. After amortization, the capital costs for a well are expected to add a few U.S. cents per m^3. However, these costs do not represent the true value of groundwater.

Due to increased withdrawals, greenhouses are increasingly concerned about regulatory tariffs being imposed on groundwater and about the long-term availability of groundwater for operations. Greenhouses are increasingly becoming more environmentally conscious, with some greenhouses we interviewed considering an accounting cost of water to make business decisions. They are increasingly recognizing that the current costs for groundwater may not be applicable in the future, especially given that greenhouses are often in operation for more than 20 years. We felt that a fair accounting cost of water should be representative of the true value of the water, and looking at the cost of recharging groundwater can be a good measure of the true value of groundwater. Several projects currently operate in California to recharge groundwater, with the median costs of recharging groundwater being \$0.32/m^3 [42]. For this paper, we assumed that a fair accounting cost for groundwater is the median cost of recharging groundwater (\$0.32/m^3.

True value of product water:

To calculate payback periods on desalination systems and compare desalination systems, we must also quantify the value of product water produced from a desalination system. One method of valuing desalination product water is by looking at the pricing of the alternative currently used by greenhouses: municipal groundwater. Thus, for this paper, we assumed that value of the product water is the market price of municipal water for agricultural users in Ventura County, California: \$1.05/m^3 [43]. More discussion around the value of product water can be found in Section 4.3.

Costs associated with brine discharge:

Most greenhouses we interviewed did not incur significant brine disposal costs. Desalination brine was typically mixed with nutrient-rich greenhouse discharge water and used to irrigate salt-resistant crops and trees, such as avocados grown outside the greenhouse. Only one greenhouse we interviewed used an evaporation pond. However, a few greenhouses incurred indirect brine disposal costs as a result of the need to buy land for growing salt-resistant crops outside the greenhouse. We could not accurately estimate what these indirect costs were.

Since these indirect costs were difficult to compute and even more difficult to generalize, for the general analysis presented here, we have assumed that brine disposal costs were \$0/m^3 (i.e., no costs associated with brine). However, results presented in later sections are presented in such a way that greenhouses can easily understand how brine disposal costs may affect desalination technology selection.

To summarize, for calculations presented in this paper, we used an accounting cost of groundwater of \$0.32/m^3, a price for the product water of \$1.05/m^3, and no costs for brine disposal.

3.4.2. Cost Model

3.4.2.1. Capital Costs

Specific capital costs (SpCapEx) for RO, CCRO, EDR and MS-EDR were calculated based on data in the literature, conversations with greenhouses who bought desalination systems and conversations with desalination system manufacturers. For RO, cost data were obtained from publicly available data from Forever Pure [44], from conversations with RO manufacturers [45-48], and from data provided by the greenhouses themselves. For CCRO, cost data were obtained from the manufacturer Desalitech [49], with CCRO systems typically costing twice that of RO for capacities of 54.5 to 272.5 m^3/day (10 to 50 gallons per minute [gpm]), 1.25 times that of RO for capacities of 272.5 to 817.6 m^3/day (50 to 150 gpm) and 1.1 times that of RO for capacities larger than 817.6 m^3/day (150 gpm). For EDR, costs were obtained from the literature [17, 25, 35, 50, 51] and from conversations with a manufacturer [34]. MS-EDR for brackish desalination has not yet been widely deployed, to the best of our knowledge. Since greenhouse water treatment only requires selective removal of sodium, we assumed that for MS-EDR stacks in greenhouses, only the cation exchange membranes need to be monovalent selective (i.e., anion exchange membranes in these stacks are conventional EDR membranes that are not monovalent selective). From manufacturer conversations, we assumed that using cation selective MS-EDR membranes will lead to a 10 percent premium in costs for an MS-EDR stack over an EDR stack.

3.4.2.2. Energy Consumption and Costs

The specific energy consumption (SEC) for RO, CCRO, EDR and MS-EDR were obtained using process models in the literature that were adapted for the conditions relevant to greenhouse use. RO SEC was estimated using a model reported by Nayar et al. [12] and Warsinger et al. [13]. The RO systems were assumed to operate at a recovery of 70 percent, like systems currently used in the field, with the pumps assumed to be 70 percent efficient. CCRO SEC was estimated using a model reported previously by Warsinger et al. [13]. For the paper, CCRO systems were assumed to operate at a recovery of 90 percent. EDR and MS-EDR SEC was calculated using an adaptation of process models previously developed and validated by Nayar et al. [20, 52] for treating seawater and concentrated seawater. The membrane transport model for the EDR process model was previously used by McGovern et al. to simulate the performance of brackish ED systems [35]. The energy consumption predicted from these models was verified against data from the literature [25], with our values matching the reported values in the literature to within 4 percent.

For the MS-EDR process model, sodium chloride transport properties for the MS-EDR membranes Neosepta CMS and ACS were used [53]. Brackish MS-EDR systems in the field are expected to be using newer membranes from FujiFilm designed for brackish water desalination. These membranes are expected to be more selective at brackish salinities than the Neosepta membranes; however, we have assumed that the resistance characteristics and sodium transport will be similar to Neosepta CMS and ACS membranes. The EDR and MS-EDR systems were assumed to be operating at a recovery of 80 percent. It must be noted that all the energy consumption process models assumed groundwater to be an aqueous solution of sodium chloride—an assumption shown to be accurate for predicting energy consumption [17, 25].

To calculate energy costs, we assumed an electricity price ($Cost_{elec}$) of \$0.10/kWh_e, a daily system operation time of 12 hours, and a capacity factor (Cap_{fac}) of 90 percent:

$$OpEx_{energy,yr} = SEC \times Cost_{elec} \times Cap_{\frac{m^3}{day}} \times \left(\frac{12}{24}\right) \times 365 \times Cap_{fac} \qquad (16)$$

3.4.2.3. Membrane Replacement Costs

Membrane replacement costs ($Cost_{memb}$) were calculated for a 600 m^3/day system, corresponding to the desalination needs of a 10-hectare greenhouse. RO membrane replacement costs were estimated using an online calculator from Suez Water [54]. CCRO systems were assumed to have the same membrane replacement cost as an RO system. EDR and MS-EDR membrane areas were estimated using the process model developed by Nayar et al. described in Section 3.4.2.2. The process models were previously validated [20, 52] for accurately calculating membrane area for seawater brine concentration applications. For this study, we further validated the model against data reported by Wright et al. [25] for a commercial EDR stack, with our model predicting membrane area within 18 percent of experimental values.

Brackish RO membrane elements were assumed to cost \$550 per element [54]. EDR membranes were assumed to have a cost of \$160/m^2 [17]. MS-EDR membranes for high-salinity applications cost \$222/m^2 [20]. For brackish applications, newer MS-EDR membranes can cost between \$150 and \$250/m^2 [34]. For the purpose of this study, we assumed an average MS-EDR membrane cost of \$200/m^2.

From our interviews, RO membranes are replaced on average every 4 years. CCRO membranes in the field were reported to last longer than RO membranes because the recirculation of water in CCRO generally led to lower scaling and fouling risks and reduced cleaning requirements compared to RO [49]. From manufacturer conversations [49], we conservatively assumed that CCRO membranes need replacement every 5 years. From the literature, EDR membranes are expected to be replaced every 10 years [17, 50]. MS-EDR membranes developed for high-salinity applications have a membrane life of 7 years [20, 52]. We assumed conservatively that MS-EDR membranes designed for brackish desalination will also have a membrane life of 7 years.

For this paper, membrane replacement costs were annualized over the membrane lifetime (t_{memb}) without assuming an interest rate to obtain a simple annualized membrane replacement cost:

$$OpEx_{memb,yr} = \frac{Cost_{memb}}{t_{memb}} \tag{17}$$

3.4.2.4. Other Operating Costs

Greenhouses have annual maintenance contracts related to their desalination equipment. These costs cover the cost of annual inspection by an experienced technician and the cost of using chemicals and anti-scalants. Due to the variability in pricing of maintenance contracts with location, we could not accurately estimate the operating costs. Since these costs are not expected to vary much between technologies, RO, CCRO, EDR, and MS-EDR systems can be effectively compared without including these operating costs.

3.4.2.5. Value Provided

To effectively compare desalination systems, the value provided by systems in terms of water savings from increased recovery and fertilizer savings from partial desalination need to be quantified. Since both water and fertilizer savings vary between greenhouses, we characterized these savings to help greenhouse industry end-users make their purchasing decisions.

3.4.2.5.1. Water Savings from Increased Desalination System Recovery

Conventional brackish RO systems operated at a recovery ratio (RR) of 70 percent, with EDR, MS-EDR and CCRO systems capable of operating at higher recoveries. Operating at higher recoveries can lead to savings in both feedwater costs and brine disposal costs.

The annual feedwater savings per hectare from operating at a higher recovery than 70 percent was captured using the following equation:

$$Sav_{RR,feed,ha} = Cap_{ha} \times (\frac{Op.hr.}{24}) \times (\frac{1}{0.7} - \frac{1}{RR}) \times 365 \times Cap_{fac} \times Cost_{feed,w} \tag{18}$$

where the values for product water capacity per hectare (Cap_{ha}) and daily hours of operation (Op.hr.) were sourced from Table 3-2 as 60 m^3/ha and 12 hours per day respectively. The capacity factor (Cap_{fac}) for the greenhouse was assumed to be 0.9.

3.4.2.5.2. Fertilizer savings from MS-EDR

The ability of MS-EDR systems to preferentially remove sodium over calcium and magnesium ions can lead to fertilizer savings for greenhouses. Currently, greenhouses using RO need to add significant amounts of calcium and magnesium to the obtain the desired composition of nutrient water. Calcium and magnesium salts contribute approximately to 1/3 of annual fertilizer costs:

$$Cost_{Ca,Mg,ha} = {Cost_{fert,ha}}/{3} \tag{19}$$

Where $Cost_{fert,ha}$ from Table 3-2 varied from \$2.5 to \$4.1/m^2 within the sample of greenhouses we interviewed. Greenhouses growing flowers incurred much lower fertilization costs than those growing vegetables. Furthermore, the degree to which greenhouses recirculated their nutrient solutions affected their overall fertilization costs.

The ratio of calcium and magnesium salts saved using MS-EDR systems ($r_{Ca,Mg,saved}$) depends on both the amount of calcium and magnesium within groundwater and the amount of selectivity of the MS-EDR membranes towards calcium and magnesium ions:

$$r_{Ca,Mg,saved} = r_{Ca,Mg,gw} \times r_{Ca,Mg,selec} \tag{20}$$

Where $r_{Ca,Mg,gw}$ is the ratio of the concentration of calcium and magnesium ions in ground water to that in the nutrient solution (from Table 3-2):

$$r_{Ca,Mg,gw} = \frac{[Ca^{2+}]_{gw}+[Mg^{2+}]_{gw}}{[Ca^{2+}]ns+[Mg^{2+}]ns} \tag{21}$$

And $r_{Ca,Mg,selec}$ is the ratio of the concentration of calcium and magnesium ions in the product water of an MS-EDR system to that in the feed.

$$r_{Ca,Mg,selec} = \frac{[Ca^{2+}]_{p,MS-EDR}+[Mg^{2+}]_{p,MS-EDR}}{[Ca^{2+}]_{f,MS-EDR}+[Mg^{2+}]_{f,MS-EDR}} \tag{22}$$

Since MS-EDR systems have yet to be piloted in greenhouses, the exact selectivity is uncertain. Furthermore, the amount of calcium and magnesium in groundwater varies significantly by location. Thus, we felt it best to estimate the potential cost savings across a wide range of calcium and magnesium savings:

$$Sav_{Ca,Mg,ha} = Cost_{Ca,Mg,ha} \times r_{Ca,Mg,saved} \tag{23}$$

3.4.2.6. Overall Technology Comparison

The desalination technologies RO, CCRO, EDR, and MS-EDR can be effectively compared in terms of the payback periods on the technologies. The capital costs, energy costs, and membrane replacement costs and the savings from increased desalination system recoveries and fertilizer savings are combined together to calculate a simple payback period (SPP):

$$SPP = \frac{CapEx}{Value_{pw} + Sav - OpEx} \tag{24}$$

To effectively compare against RO, we also calculated a relative payback period (RPP_{tech}) for CCRO, EDR, and MS-EDR:

$$RPP_{tech} = \frac{CapEx_{tech} - CapEx_{Ro}}{Sav_{tech} - (OpEx_{tech} - OpEx_{RO})} \tag{25}$$

The RPP removed the value of the product water from the calculation, and estimated whether the additional capital cost in a technology alternative to RO was justified by the savings the technology produced over RO.

4. Results and Discussion

First, we evaluate the techno-economic feasibility of MSED compared to other brackish desalination technologies for agricultural applications, based on primary market research we conducted with more than 70 greenhouses. These include conventional technologies, such as reverse osmosis (RO) and electrodialysis (ED), and advanced technologies, such as closed-circuit reverse osmosis (CCRO). The analysis determines the levelized costs of water, the capital costs and energy requirements of these technologies, and how these vary with feed salinity, system capacity, and recovery ratio. The results indicate that MSED would pay back greenhouses within the desired 2-year period.

Second, we build a bench-scale setup to experientially characterize MSED membrane properties, including monovalent selectivity, ion transport, limiting current, and resistance, for multiple brackish feedwaters and for two sets of MSED membranes: the widely used Neosepta ACS/CMS membranes and the new Fujifilm Type 16 membranes. Both MSED membranes show notable monovalent selectivity for all tested brackish water compositions, reflecting the potential of the technology for selective desalination in greenhouses. Finally, we show that a multi-ion transport model can predict the Neosepta and Fujifilm MSED systems within 6 percent and 8 percent, respectively.

4.1. Techno-economic Comparison of RO, CCRO, EDR, and Monovalent-selective EDR

4.1.1. Energy Consumption

Figure 4-1 shows a comparison of the specific energy consumption of RO, CCRO, EDR, and MS-EDR for treating feed water with a salinity of 850 ppm. While the RO and CCRO systems were assumed to produce a product salinity of 25 ppm, the ED and MS-EDR systems were assumed to deliver a product salinity of 250 ppm. CCRO consumed the lowest specific energy at 0.49 kWh_e/m^3 followed by EDR at 0.51 kWh_e/m^3. MS-EDR consumed slightly more energy due to the higher resistance of MS-EDR membranes over conventional EDR membranes. RO consumed the most specific energy at 0.60 kWh_e/m^3, as they had the lowest recovery ratio among the four systems of only 70 percent.

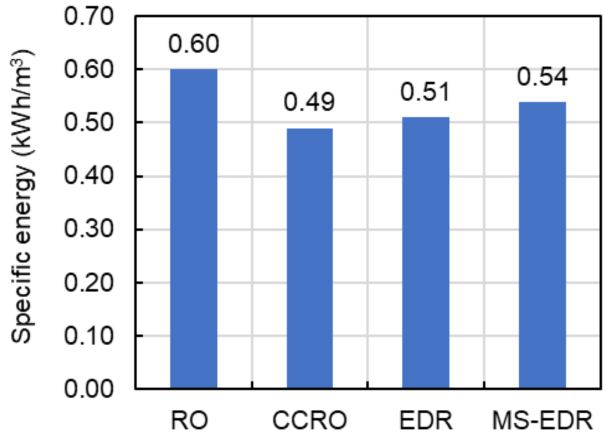

Figure 4-1. Specific energy consumption for RO, CCRO, EDR ,and MS-EDR for treating 850 ppm feed water

4.1.2. Operating Costs: Membrane Replacement and Energy

Figure 4-2 shows a comparison of annual energy and membrane replacement costs for RO, CCRO, EDR, and MS-EDR systems treating feed water of salinity 850 ppm at a capacity of 600 m^3/day of product water (i.e., for a 10-hectare greenhouse). The sum of the annual energy and membrane replacement costs for RO, CCRO, EDR, and MS-EDR systems were $10,863, $8789, $11,992 and $17,799 respectively.

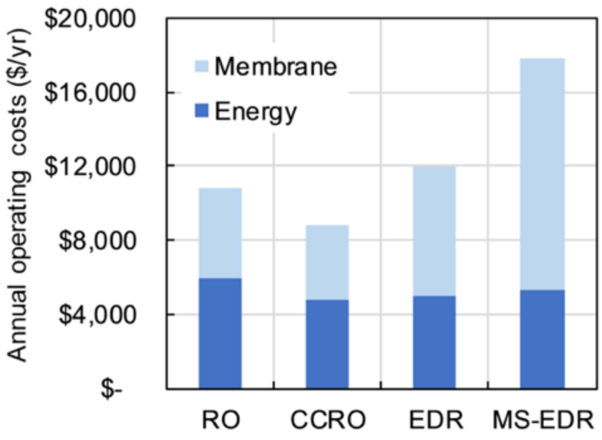

Figure 4-2. Annual costs for energy and membrane replacement for RO, CCRO, EDR, and MS-EDR for treating 850 ppm feed water

For RO systems, on average, to achieve 70 percent recovery at a flow rate of 600 m^3/day, 36 brackish RO elements were needed [54], with the total RO membrane replacement cost being $19,800 (17 percent of the capital cost of an RO system). The RO membrane replacement cost as a proportion of total capital costs was corroborated in our interviews. CCRO systems were assumed to have the same membrane replacement costs but with the membranes assumed to last 5 years instead of 4 years, based on manufacturer conversations [49]. EDR membrane replacement cost is significantly more at $69,650, with MS-EDR membrane replacement costing even more at $87,400. EDR and MS-EDR membranes amounted to 53 percent and 58 percent of their respective capital costs.

Currently, the active brackish RO plants in the world outnumber brackish ED/EDR plants at least 10-fold [55], with EDR seen more as a niche technology [23]. Consequently, RO membranes are currently produced in much higher volumes than EDR and MS-EDR membranes, leading to much lower costs for the RO membranes. While EDR and MS-EDR systems consumed less energy than a conventional RO system, the energy savings were superseded by the higher membrane replacement costs. However, the savings from operating at a higher desalination system recovery and potential fertilizer savings must be considered to determine if the higher operating and capital costs are justified.

4.1.3. Value Provided

To effectively compare desalination systems, the value provided by systems in terms of water savings from increased recovery and fertilizer savings from partial desalination need to be quantified. Since both water and fertilizer savings vary between greenhouses, we characterized these savings to help greenhouse industry end-users make their purchasing decisions.

4.1.3.1. Water Savings from Increased Desalination System Recovery

Figure 4-3 shows the annual savings in feedwater costs, calculated from Equation No. 8, varying with recovery ratio and feedwater costs. Figure 4-3 can also be used to separately calculate the annual savings in brine disposal costs from operating desalination systems at higher recoveries. Since the product water required is fixed, the mass flow rate of feedwater reduced at higher recovery is numerically equal to the mass flow rate of brine reduced. Thus, the labels shown for feedwater costs can also be read as the sum of feedwater costs and brine disposal costs. Greenhouses that incur brine disposal costs can use Figure 4-3 to calculate the savings in brine disposal costs, which must be added to the savings in feedwater costs. As an example, if we assume zero brine disposal costs and a feedwater cost of $0.32/m^2 equivalent to the median cost of recharging groundwater in California, the annual savings per hectare at recoveries of 80 percent and 90 percent was $563 and $1,001, respectively. If the brine disposal costs were instead $0.18/m^3, bringing the sum of feedwater and brine disposal costs to $0.50/m^3, from Figure 4-3, the annual savings per hectare at recoveries of 80 percent and 90 percent will be $880 and $1,564, respectively.

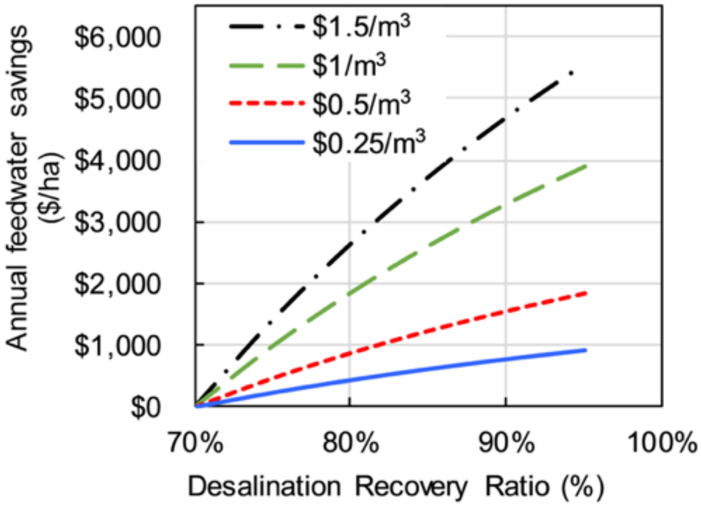

Figure 4-3. Annual water savings for desalination recovery ratios greater than 70 percent for various effective feedwater prices

4.1.3.2. Fertilizer Savings from MS-EDR

Figure 4-4 shows the annual fertilizer savings per hectare of greenhouse cultivation, calculated using Equation 13, varying with the percentage of calcium and magnesium salts saved and the annual fertilization costs for a greenhouse. From our interviews, the average annual cost of fertilization was $3/m^2. Thus, on average, the annual cost of calcium and magnesium salts per hectare ($Cost_{Ca,Mg}$) was approximately $1/m^2. Within the available sample of greenhouses where the groundwater salinity was greater than 500 ppm, the value for $r_{Ca,Mg,gw}$ varied from 21 to 86 percent, with an average value of 53 percent. If we assume that $r_{Ca,Mg,selec}$ for MS-EDR systems was 33 percent, we get a range of potential savings in calcium and magnesium salts of 7 to 29 percent. From Figure 4-4, for an annual fertilizer cost of $3/m^2, the fertilizer savings would thus be in the range of $700 to $5,800/m^2.

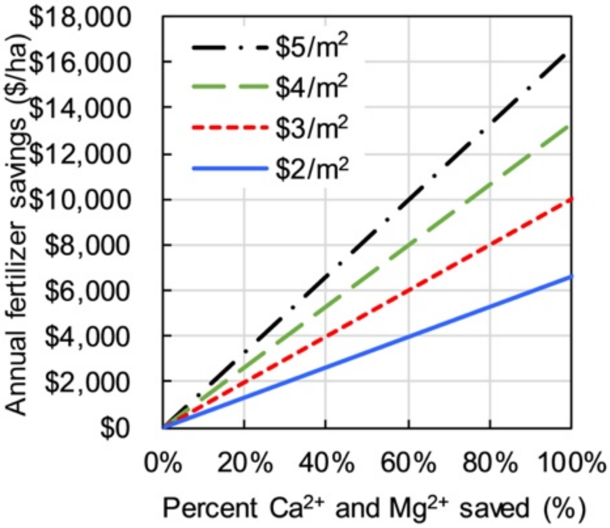

Figure 4-4. Variation of annual savings in fertilizer from reduced addition of calcium and magnesium expressed as a function of percent of calcium and magnesium saved at different rates of fertilizer use

4.1.3.3. Value of Product Water

Greenhouse operators we interviewed were interested in short payback periods, preferably less than 2 years. However, to calculate a payback period, a value must also be assigned to the product water. The value of product water is different from that of groundwater. Greenhouses currently drill wells and use groundwater largely because municipal water is either not available or is too expensive. For quantifying the value of product water, we chose the cost of the alternative to desalinated groundwater which is, commercially available municipal water.

From Section 3.4.1, the price of municipal water for agricultural use in Ventura County, California, was $\$1.05/m^3$ [43]. The annual value of the product water as a function of capacity, daily hours of operation, and capacity factor was thus:

$$Value_{pw} = Cap_{m^3/day} \times \left(\frac{Op.hr}{24}\right) \times 365 \times Cap_{fac} \times 1.05[\$/m^3] \tag{26}$$

For a 10-hectare greenhouse operating a 600 m^3/day desalination system for 12 hours a day at a 90 percent capacity factor, the annual value of the product water was $206,955.

4.1.4. Overall Technology Comparison

Table 4-1 shows the capital costs, energy costs, membrane replacement costs, the value from water savings and fertilizer savings, and the simple and relative payback periods for RO, CCRO, EDR, and MS-EDR systems for a 10-hectare greenhouse. The systems had a capacity of 600 m^3/day, assuming 12 hours a day of operation with a 90 percent capacity factor, treating 850 ppm of feedwater. The recovery ratios of the RO, CCRO, EDR, and MS-EDR systems were 70 percent, 90 percent, 80 percent, and 80 percent, respectively. Feedwater savings were calculated assuming a feedwater cost of $\$0.32/m^3$, while product water was valued at $\$1.05/m^3$. It was assumed conservatively that 15 percent of the calcium and magnesium needed in the nutrient solution could be saved by using the MS-EDR system. The results on simple and relative payback periods can be extended to greenhouses larger than 10 hectares.

Table 4-1. Capital costs, operating costs, savings created, simple payback period and relative payback period for RO, CCRO, EDR, and MS-EDR systems for a 10-hectare greenhouse with treatment capacity of 600 m^3/day.

Parameters	Units	RO	CCRO	EDR	MS-EDR
CapEx	$	115,898	144,873	131,000	144,100
OpEx$_{energy,yr}$	$	5,913	4,829	5,028	5,312
OpEx$_{memb,yr}$	$	4,950	3,960	6,964	12,487
Savings$_{Ca,Mg}$ at 15% Ca^{2+} and Mg^{2+} ions saved	$	-	-	-	15,000
Savings$_{RR,feed}$ at 0.32 $/m^3	$	-	10,011	5,631	5,631
Net annual operating costs	$	10,863	-1,222	6,361	-2,833
Value$_{Pw}$	$	206,955	206,955	206,955	206,955
SPP	months	7.1	8.4	7.8	8.2
RPP	years		2.4	3.4	2.1

4.1.4.1. Simple Payback Periods Can Be Less Than 9 Months

Figure 4-5 shows the simple payback periods for the RO, CCRO, EDR and MS-EDR systems. When compared against municipal water priced at $1.05/m^3, the payback periods for all the systems were less than 12 months. Considering that these systems are expected to have a life of 15 years, greenhouses obtain significant value from desalination. Conventional RO had the shortest simple payback period at 7.1 months. CCRO, EDR, and MS-EDR systems were estimated to have a payback period of 8.4, 7.8, and 8.2 months respectively.

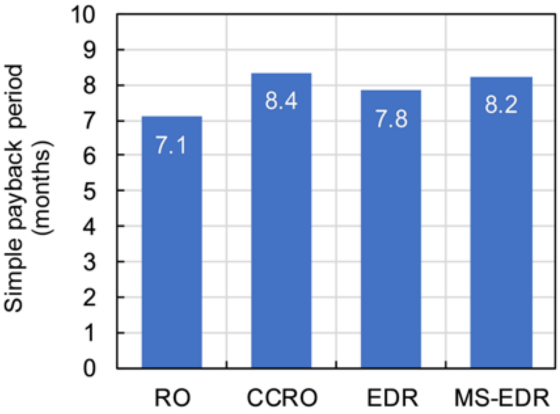

Figure 4-5. Simple payback period for RO, CCRO, EDR, and MS-EDR for a 10-hectare greenhouse treating feedwater of salinity 850 ppm, assuming product water value of $\$1.05/m^3$, feedwater cost of $\$0.32/m^3$, and 15 percent savings in calcium and magnesium ions.

4.1.4.2. Variation of Relative Payback Periods with Feedwater Costs and Degree of Calcium and Magnesium Saved

Table 4-1 also showed the relative payback periods of CCRO, EDR, and MS-EDR systems when compared against RO without accounting for the value of product water. When the sum of feedwater and brine disposal costs was $\$0.32/m^3$, the relative payback periods for CCRO was 2.4 years, while that of EDR was 3.4 years. If MS-EDR systems can save at least 15 percent of the calcium and magnesium needed for nutrient solutions, the relative payback period of MS-EDR will be less than 2.1 years, justifying the higher membrane costs.

However, in practice, the cost of feedwater and brine disposal, the value of product water, the amount of calcium and magnesium in groundwater, and the practical selectivity of newer MS-EDR membranes may be different from our assumptions. To reduce the uncertainty on the relative payback period, we varied feedwater costs and the percentage of calcium and magnesium needed for nutrient solutions that was saved and calculated the relative payback periods for each system.

Figure 4-6 shows the variation of the relative payback period of MS-EDR with the percent of calcium and magnesium saved and the sum of the feedwater and brine disposal costs. The relative payback period was very sensitive to the percent of calcium and magnesium saved, especially for values lower than 30 percent. Regardless of feedwater costs, if MS-EDR systems can save 20 percent of the calcium and magnesium needed for nutrient solutions, the relative payback period will be less than 2.5 years, enough for the technology to be adopted. This number can be used to inform MS-EDR membrane designers of the target values for $r_{Ca,Mg,selec}$ for the MS-EDR membranes.

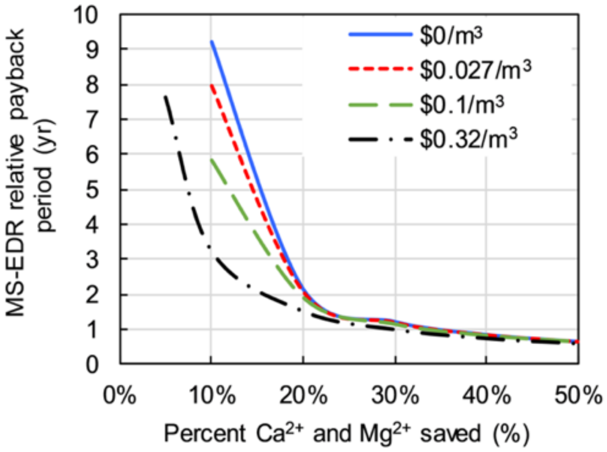

Figure 4-6. Variation of relative payback period for an MS-EDR system with percent of calcium and magnesium saved at different feedwater costs for a 10-hectare greenhouse assuming \$3/m^2 fertilization costs.

We reported that the greenhouses we sampled where the TDS was greater than 500 ppm on average had groundwater that already contained 53 percent of the calcium and magnesium needed for typical nutrient solutions. Thus, if MS-EDR membranes could retain at least 38 percent of the calcium and magnesium in the feedwater in the product water (i.e., $r_{Ca,Mg,selec}$ = 38 percent), MS-EDR can be adopted by several greenhouses. For comparison, Cohen et al. [19] had reported experiments on Selemion CSO MS-EDR membranes that showed the membranes saving 42 percent of the calcium and 57 percent of the magnesium in feedwater. Thus, MS-EDR systems show considerable promise for application in greenhouses with sizes greater than 10 hectares, justifying further research and development on the technology.

Figure 4-7 shows the variation of the relative payback period of CCRO and EDR systems with the sum of the feedwater and brine disposal costs for a 10-hectare greenhouse. Shifting to CCRO from conventional RO is economical when the sum of the feedwater and brine disposal cost is greater than \$0.24/m^3 when the relative payback period becomes 3 years. Similarly, shifting to EDR from conventional RO is economical when the sum of feedwater and brine disposal cost is greater than \$0.35/m^3. At the capacity we considered, CCRO systems were slightly more expensive than EDR systems. However, CCRO had a lower operating cost than EDR and also operated at a higher recovery ratio of 90 percent, compared to 80 percent for the EDR system, creating significant water savings and allowing CCRO to quickly make up for the higher capital costs. Thus, CCRO relative payback periods were lower than that for EDR for the same sum of feedwater and brine disposal costs. CCRO relative payback periods are expected to be even better at higher capacities since specific capital cost of CCRO decreases significantly.

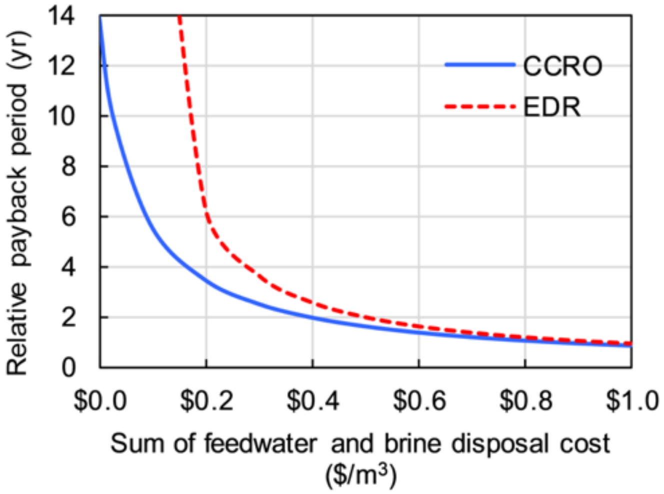

Figure 4-7. Variation of relative payback period for CCRO and EDR systems with the sum of feedwater and brine disposal costs for a 10-hectare greenhouse.

EDR may not be viable in several greenhouses, and the results for EDR shown in Figure 4-7 are applicable only for some greenhouses. While CCRO product water is very similar to RO product water, EDR product water in our simulations was more saline at 250 ppm. EDR system costs increase significantly if the product salinity is reduced further. These systems can be used in greenhouses only if the amount of sodium in EDR product water is less than or equal to the 23 ppm greenhouses need. Since EDR is not selective to sodium, the proportion of sodium relative to total salinity will not change between the feed and product streams, even as the total salinity is reduced. Thus, for an 850 ppm EDR feed stream, the sodium concentration in the feed must be less than 78 ppm to result in a 250 ppm EDR product stream with a sodium concentrations less than 23 ppm. Furthermore, pilot tests need to be conducted in greenhouses with EDR systems to confirm their applicability in greenhouses. Since CCRO systems have been commercially deployed widely and have product water qualities similar to that of RO, CCRO can be deployed in greenhouses without the need for pilot testing. Thus, from an adoption point of view, CCRO systems can be more easily adopted by greenhouses compared to EDR and MS-EDR systems.

4.1.5. Limitations and Areas for Future Research

- Simulations and results shown for desalination systems assumed a feedwater salinity of 850 ppm. Our general findings on the economic performance of RO, CCRO, EDR, and MS-EDR systems may be valid for feedwaters with salinities up to 1,000 ppm. However, beyond 1,000 ppm, the results may vary significantly. Future work can compare these technologies at higher salinities.
- We assumed a range of selectivity for MS-EDR membranes while carrying out an analysis on the potential of MS-EDR. Our analysis shows that future research and development efforts on the MS-EDR technology are commercially justified. However, significant uncertainties remain on the MS-EDR technology when applied to brackish water conditions, especially on the selectivity of these membranes toward sodium and

the membrane life. Lab-scale tests and pilot tests at greenhouses are needed to fully validate the potential of MS-EDR systems.

- Future work can include more performance comparisons with ion-exchange resin systems for feedwater salinities lower than 500 ppm, and with nanofiltration. Comparing these additional technologies in a detailed manner was beyond the scope of this work.
- A framework and approach for comparing RO, CCRO, EDR, and MS-EDR was presented. While the overall approach and broad trends may be valid across geographies, specific values of payback periods and relative payback periods are sensitive to the cost of groundwater and the value of product water. For several calculations presented in this paper, the payback periods were calculated using an accounting cost of groundwater of \$0.32/m^3 and a value of the product water of \$1.05/m^3. These numbers were sourced from southern California and are what we believe are the best representative numbers on the real costs and value of groundwater and product water. To make decisions on technology investments in other geographies, the same framework can be used but the groundwater costs and the value of product water must be selected appropriately, with the evaluation done on a case-by-case basis.

4.2. Characterization of Neosepta CMS/ACS Membranes

This section investigates the selectivity of Neosepta CMS/ACS membranes for monovalent ions in the brackish salinity range and estimates the achievable savings in fertilizer costs. First, we run experiments on 16 brackish groundwater compositions to determine membrane selectivity, membrane resistance, membrane permeability, and limiting current density. Then, we explore trends in membrane selectivity as a function of brackish groundwater composition, both total dissolved solids (TDS) and ionic composition. Lastly, the experimentally determined membrane selectivities are used to evaluate the nutrient and fertilizer cost savings of MSED relative to RO for 6,000 nutrient-rich BGWs across the United States. We show the geographic distribution of these BGWs in order to identify regions with MSED potential. These results are representative of a bench-scale setup. Because system parameters may vary with scale, pilot studies in greenhouses are necessary to fully characterize MSED systems for real-world applications.

4.2.1. Membrane Resistance and Limiting Current Density

Because BGW composition varies greatly with location, the membrane resistance and limiting current density will not, in practice, be characterized for every BGW feedwater to an MSED system. Therefore, we determine these parameters for NaCl solutions with BGW salinities. These NaCl results are equivalent to a lower bound on membrane resistance and limiting current density of any BGW solution. Consequently, they serve as a useful benchmark for multi-ionic solution behavior.

4.2.1.1. Membrane Resistance

Membrane resistance is typically evaluated at standard conditions (i.e., in 0.5 M (29 g/kg) NaCl solution [55]). However, this resistance value is insufficient for agricultural applications in which source water contains less than 10 g/kg [14]. Therefore, we determine Neosepta membrane resistance for 0.8 to 35 g/kg NaCl solutions. Consistent with the literature [55, 56], we find that membrane resistance increases significantly as salinity decreases (see Figure 4-8); a possible drawback of using MSED in the BGW range is resistive losses in the stack [57].

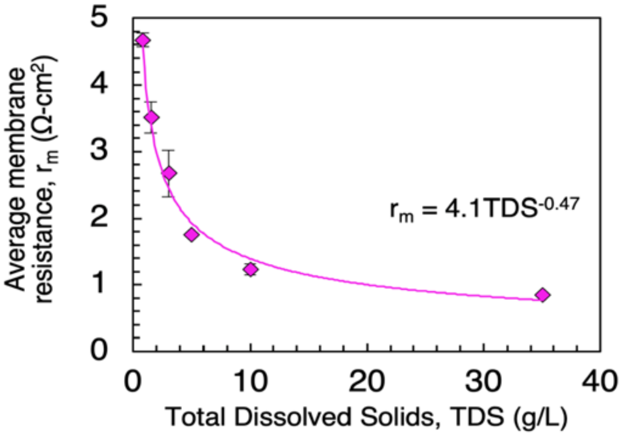

Figure 4-8. CEM and AEM resistance of Neosepta membranes for NaCl solutions containing different TDS. Values obtained match those in the literature (rm = 1.8–3.8 Ω-cm^2) [6].

4.2.1.2. Limiting Current Density

Operating at an applied current near or above the limiting current can impede the performance of MSED membranes. Consequently, it is important to quantify the limiting current in order to optimize MSED system performance. Figure 4-9 shows the linear dependence of limiting current density on sodium concentration for NaCl and Comp. 2 solutions. Groundwater has a higher current density than NaCl solutions due to the presence of other cations, in addition to sodium, that carry the current. In multi-ionic groundwater solutions, monovalent selective CEMs first deplete sodium from the boundary layer adjacent to the membrane before depleting divalent ions. Therefore, the limiting current is no longer a function of only sodium concentration. Figure 4-10 reflects the trade-off between monovalent selectivity and applied current density. Monovalent selectivity decreases (i.e., permselectivity increases) when the system operates at a current above the limiting current density.

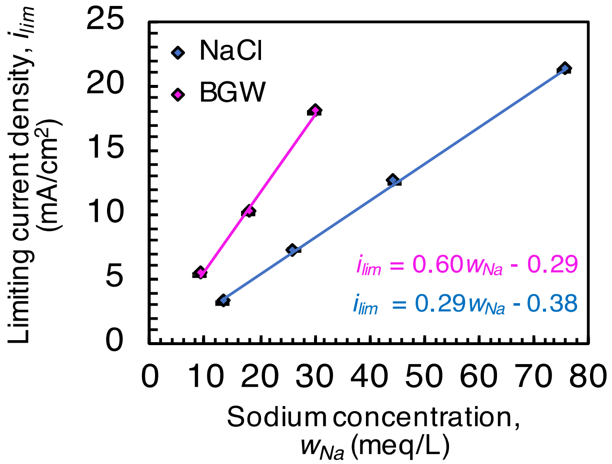

Figure 4-9. Limiting current density as a function of sodium concentration in the diluate for various dilutions of sodium chloride solution and Comp. 2

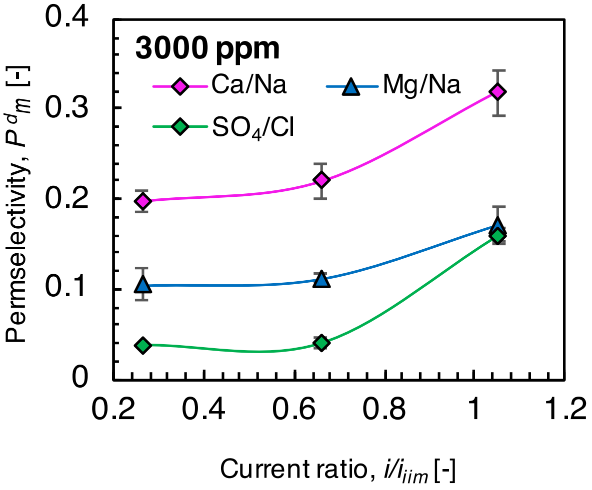

Figure 4-10. Membrane permselectivity as a function of the ratio of applied current to limiting current for a 3,000 ppm BGW solution (Comp. 2). Once the limiting current density is surpassed (i/i_{lim} > 1), the permselectivity no longer linearly increases with current, reflecting decreased membrane performance.

4.2.2. Membrane Diffusion Permeability

The ion permeabilities for Ca^{2+}, Mg^{2+}, Na^+, Cl^-, and SO_4^{2-} were experimentally determined for various dilutions of Comp. 1, Comp. 2, and Comp. 3. They were the same order of magnitude across all compositions and salinities. Table 4-2 includes these average values and standard deviations; the standard deviations are large because the permeability measurements are based on small changes in diluate concentration. Permeability values of the monovalent ions are the same order of magnitude as those of regular ED Neosepta membranes [17]. As expected, the divalent ions are less permeable than the monovalent ions as a result of the monovalent selectivity of the membranes.

Table 4-2. Ion permeabilities L_j average and standard deviation for various BGW dilutions

Ion	$L_{j,average}$ (m/s)	$L_{j,st\ dev.}$ (m/s)
Na^+	3.1×10^{-8}	1.4×10^{-8}
Ca^{2+}	4.7×10^{-9}	1.0×10^{-9}
Mg^{2+}	3.5×10^{-9}	1.8×10^{-9}
Cl^-	3.1×10^{-8}	1.4×10^{-8}
SO_4^{2-}	6.7×10^{-9}	1.5×10^{-9}

4.2.3. Membrane Selectivity

We consider 16 BGW compositions in our selectivity analysis due to significant variations in BGW ionic composition with location. In contrast to the Cohen et al. study, Neosepta CEMs and AEMs show selectivity toward monovalent ions in the brackish salinity range. A key finding is that small divalent transport alone does not correspond to increased monovalent selectivity, for it is the relative divalent-to-monovalent transport that determines overall selectivity. We explore trends in ion transport and selectivity as a function of time in a given experiment, with a comparison to our multi-ion transport model. We also investigate the relationship between selectivity and composition (BGW salinity, solute ratio) across experiments. Counter-ion (i.e., an ion with an electric charge opposite to the membrane) and co-ion (i.e., an ion with the same electric charge as the membrane) solute ratio effects on counter-ion permselectivity are considered. Selectivity appears to be insensitive to BGW salinity and may be sensitive to counter-ion solute ratio.

4.2.3.1. Permselectivity for 16 BGW Compositions

The Neosepta CEMs and AEMs demonstrate promising monovalent permselectivity for 16 BGW compositions, with a maximum standard deviation of 20 percent. Calcium permselectivity across all compositions is 0.26±0.03. This corresponds to an overall removal of 3.6 to 4.6 times more sodium than calcium across the CEMs. Magnesium permselectivity across all compositions is 0.15±0.03, corresponding to 5.7 to 8.7 times reduction of sodium relative to magnesium. Magnesium selectivity is greater than that of calcium, due to differences in their hydration energies. In order to cross the membranes, the ions must partially or completely shed their hydration shell. Magnesium has a larger hydration energy (1,904 kJ/mol) and thus lower removal rate than calcium (1,592 kJ/mol) [58]. Sulfate permselectivity across all compositions is 0.17±0.03, representing a removal of 4.8 to 7.7 times more chloride ions than sulfate ions. Table 4-3 shows permselectivities for each BGW composition.

Table 4-3. Calcium, magnesium, and sodium permselectivity for 16 BGW compositions. The first two columns indicate BGW composition

Solute Ratio	TDS (ppm)	P_{Na}^{Ca}	P_{Na}^{Mg}	$P_{Cl}^{SO_4}$
Comp. 1	1,542	0.27±0.02	0.15±0.01	0.22±0.01
	2,687	0.23±0.01	0.13±0.02	0.15±0.01
	4,190	0.28±0.02	0.14±0.01	0.10±0.01
	10,810	0.26±0.02	0.13±0.01	0.14±0.01
Comp. 2	1,380	0.25±0.02	0.10±0.02	0.13±0.01
	2,014	0.23±0.01	0.14±0.02	0.17±0.02
	3,013	0.22±0.02	0.11±0.01	0.11±0.01
	4,643	0.20±0.02	0.11±0.02	0.14±0.008
	10,660	0.27±0.02	0.18±0.01	0.20±0.01
Comp. 3	1,391	0.29±0.03	0.20±0.01	0.24±0.005
	2,813	0.27±0.01	0.16±0.01	0.23±0.009
	4,668	0.29±0.03	0.14±0.006	0.19±0.01
	10,771	0.24±0.01	0.17±0.02	0.12±0.01
Comp. 4	2,819	0.27±0.02	0.17±0.01	0.23±0.004
Comp. 5	3,177	0.25±0.02	0.14±0.03	0.13±0.01
Cohen	2,588	0.27±0.01	0.16±0.02	0.16±0.02

4.2.3.2. Comparison to Prior Literature

To our knowledge, Cohen et al. has conducted the only previous measurements on upgrading groundwater quality for irrigation using MSED Neosepta membranes [6]. They tested these membranes on Mashabei BGW (see Table 4-4) to determine monovalent permselectivity. Their results do not report experimental error, so it is unclear whether one or multiple trials were run. The study found that Neosepta CEMs are divalent selective, removing more calcium and magnesium than sodium during the desalination process. We conducted five trials using the same MSED stack (PCCell ED200), membranes (Neosepta), and feedwater as in the Cohen study. Our results indicate that the Neosepta CEMs are monovalent selective, showing "notable separation," according to the benchmark provided by Cohen et al. According to Cohen, notable separation corresponds to a removal ratio for Na^+, Ca^{2+}, and Mg^{2+} of 52 percent, 44 percent, and 24 percent, respectively. According to our permselectivity definition, these values correspond to a calcium selectivity of 0.85 and a magnesium selectivity of 0.46. We find a calcium permselectivity of 0.28±0.03, compared to Cohen's 1.7, and magnesium permselectivity of 0.18±0.02, compared to Cohen's 1.5. Table 4-4 shows a more detailed comparison of results. Exchanges with the membrane manufacturer also suggest that undamaged Neosepta membranes will always be monovalent selective [58]. Our findings for other compositions further corroborate the monovalent selectivity of Neosepta CEMs.

Table 4-4. Comparison of our MSED ion reductions to those of Cohen, with Mashabei BGW composition as feedwater.

Ion	Cohen Feedwater (ppm)	Our Feedwater (ppm)	Cohen Ion Reductions (%)	Our Ion Reductions (%)
Na^+	730	725±60	48	65±3.6
Ca^{2+}	135	134±6.2	80	19±2.8
Mg^{2+}	80	81±4.9	70	11±1.3
Cl^-	1,150	1,158±81	73	64±3.4
SO_4^{2-}	500	490±18	3	11±1.2

4.2.3.3. Trends in Desalination Process Time: Experiments and Model

Throughout the course of an experiment, we observe consistent trends in normalized concentration drop and membrane selectivity across BGW compositions. Figure 4-11 shows a representative experiment of Comp. 1 containing a TDS of 3,000 ppm. The normalized concentrations of Ca2+, Mg2+, and Na+ and membrane selectivity for monovalent ions linearly decrease with process time. In other words, the membrane selectivity worsens with decreasing diluate salinity, matching trends in the literature [6]. Because the initial concentration ratio is the same for a given experiment, the trend in membrane selectivity with time also represents that of transport number ratio (i.e., divalent relative to monovalent transport number). The transport number ratio depends solely on the change in ion concentration over process time because the other parameters in the equation for transport number (Equation No. 9) are the same in a given experiment. Consequently, the transport number ratio, and thus membrane selectivity, should linearly vary with time. The MSED model matches the experimental trends in normalized concentration drop within 8 percent error, as shown in Figure 4-12.

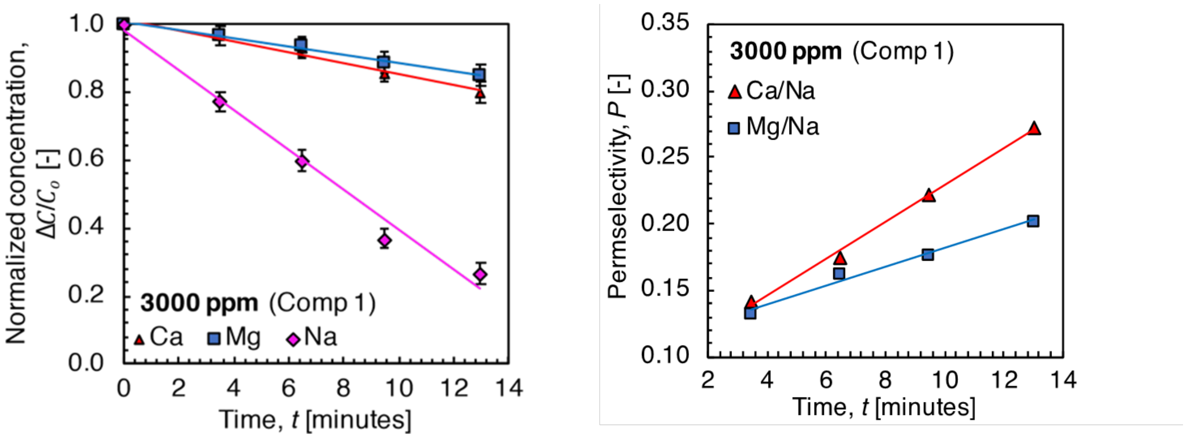

(a) (b)

Figure 4-11. (a) Normalized cation concentration and (b) membrane permselectivity as a function of desalination process time for a 3,000 ppm BGW solution.

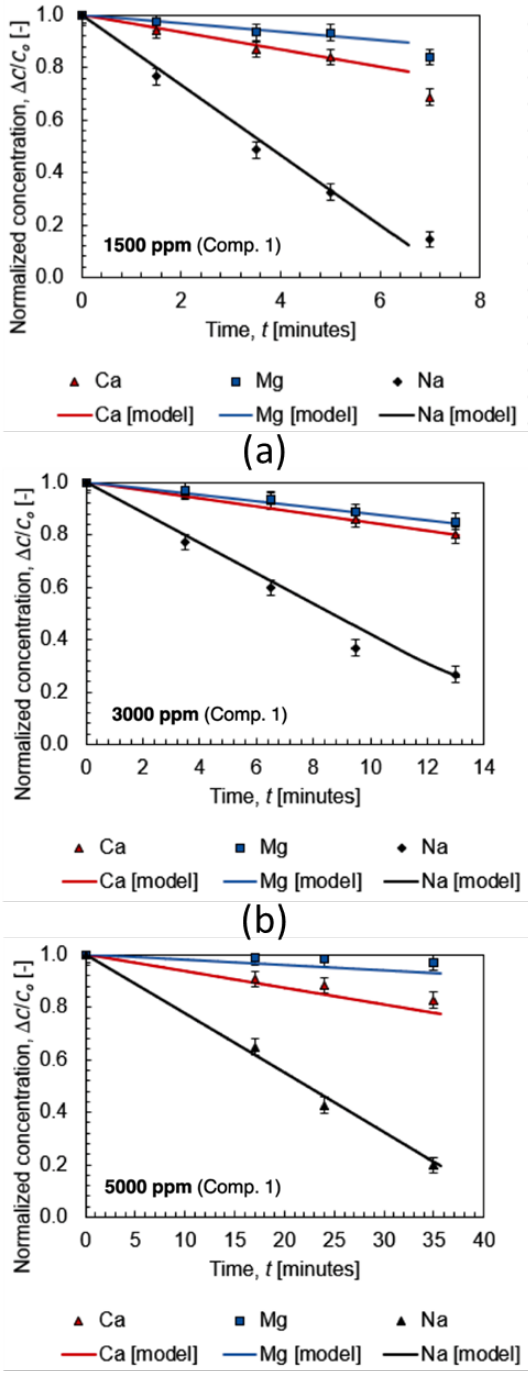

(a)

(b)

(c)

Figure 4-12. Normalized cation concentration as a function of desalination process time for BGW containing (a) 1,500 ppm, (b) 3,000 ppm, and (c) 5,000 ppm, with a comparison to the MSED model.

4.2.3.4. Trends in Counter-ion Solute Ratio at Fixed TDS

This section investigates trends in transport number and monovalent selectivity as a function of counter-ion solute ratio for six different compositions at a fixed TDS of 2,861 ± 199 ppm. All cation plots contain four data points representing composition. An average value is taken for Comp. 1, Comp. 4, and Comp. 5, which have the same cation, but different anion solute ratios ($r_{cation} = 0.39 \pm 0.0036$).

Figure 4-13 illustrates the linear relationship ($r^2 > 0.85$ for all plots) between ion transport number and solute ratio. The divalent transport number increases with solute ratio, while the monovalent transport number decreases with solute ratio, for both cations and anions. A higher solute ratio corresponds to a higher concentration of divalent ions relative to monovalent ions. Therefore, a given monovalent ion must compete with more divalent ions to be transported across the membranes. This competition reduces the amount of monovalent transport and increases the amount of divalent transport.

Cation and anion permselectivities *P*, based on ion transport numbers, show a linear relationship with cation and anion solute ratio, respectively (see Figure 4-14(a) and (b)). However, cation permselectivity decreases with cation solute ratio, while anion permselectivity increases with anion solute ratio. The difference in trends appears to result from differences in the rate of change in transport number ratio with solute ratio of cations compared to anions. Figure 4-14 (c) shows that the cation transport number ratio varies with r, while the anion transport number ratio varies with r^2. Because the initial concentration ratio is proportional to r, trends in transport number ratio match those in membrane selectivity. Consequently, the cation permselectivity is proportional to $A-\frac{B}{r}$, where A and B are constants and $B < A < 1$. As r_{cation} increases, permselectivity decreases. The anion permselectivity is proportional to Dr, where $D < 1$. Consequently, as r_{anion} increases, anion permselectivity increases. The errors in membrane selectivity as a function of solute ratio overlap, indicating that membrane selectivity may be sensitive to solute ratio.

4.2.3.5. Trends in Co-ion Solute Ratio at Fixed TDS

This section discusses the impact of co-ions on counter-ion permselectivity, based on the data in Table 4-3. Comp. 1 ($r_{anion} = 0.40$), Comp. 4 ($r_{anion} = 0.61$) and Comp. 5 ($r_{anion} = 0.21$) have different anion solute ratios and the same cation solute ratio. At a fixed TDS (2,894±254), there appear to be no trends in anion solute ratio with calcium or magnesium permselectivity. The correlation coefficient between anion solute ratio and calcium permselectivity is 0.52. The average calcium permselectivity is 0.25±0.02 (8 percent standard deviation), reflecting the lack of variation in permselectivity despite differences in sulfate concentration. Comp. 3 ($r_{cation} = 0.21$) and Comp. 4 ($r_{cation} = 0.39$) have different cation solute ratios and anion solute ratios that differ by 5 percent. At a fixed TDS (2,913±141), their anion permselectivities are equivalent, suggesting that cation concentration differences do not notably influence these values. Additional BGWs with the same counter-ion and different co-ion solute ratios should be investigated to conclusively determine the effect of co-ions on counter-ion permselectivity.

4.2.3.6. Trends in TDS at Fixed Solute Ratio

We investigate trends in transport number and monovalent selectivity as a function of initial BGW salinity at fixed solute ratio. Four salinities in the 1,000 to 10,000 ppm range are analyzed, though the majority of BGW samples from the U.S. Geological Survey (USGS) dataset contain a TDS of 500 to 3,000 ppm [14]. Figure 4-15 illustrates the cation and anion transport numbers as a function of initial BGW salinity for three compositions (Comp. 1, Comp. 2, and Comp. 3). There appear to be no trends in transport number as a function of salinity. The error bars for a given ion overlap with one another, further reflecting the little variation in transport number across salinities. Consequently, no trends in permselectivity, which depend solely on transport numbers at a fixed solute ratio, are observed with initial salinity (see Figure 4-16). The brackish salinity range is relatively small compared to ED transport number fits in the literature, which often range from BGW salinities to 200,000 ppm [17]. As a result, the absence of trends in transport number across this narrow salinity range is expected.

4.2.4. Implications of Work

Our conducted experiments have proven that the Neosepta membranes are monovalent selective. Consequently, MSED is able to preserve divalent ions already present in the source water, which are typically added as fertilizer after using RO. This section aims to provide a first-order approximation of MSED fertilizer savings relative to RO for U.S. groundwaters containing sufficient nutrient concentrations. Groundwater data are acquired from the 2017 USGS major-ions groundwater dataset [15]. It contains 28,000 brackish groundwater samples with complete composition data, not diverging from electroneutrality by more than 5 percent. These samples are not uniformly distributed by location and tend to be biased in favor of freshwater and shallow resources. Particularly high densities of groundwater samples occur in the Dakotas, Texas, the Central Valley in California, and southeastern Kansas.

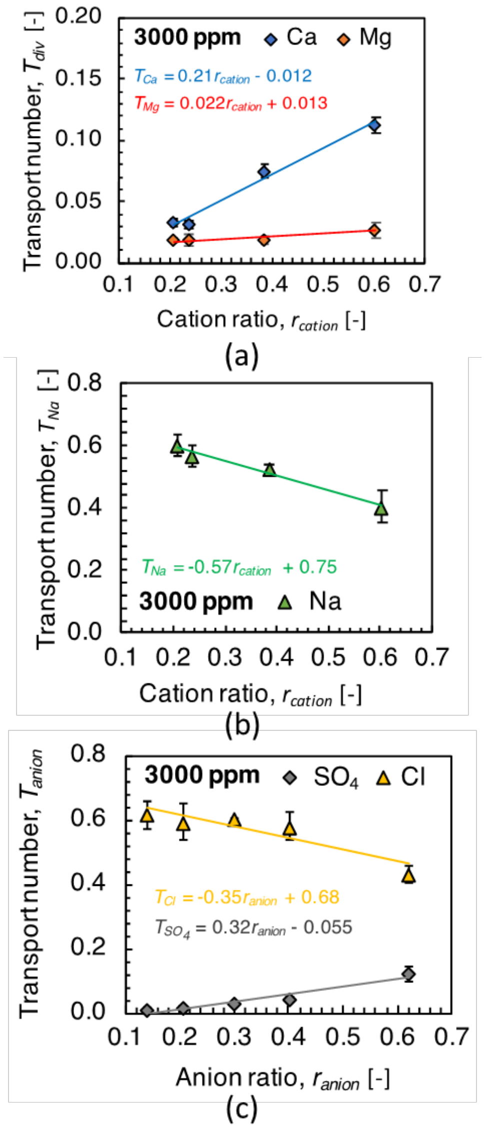

Figure 4-13. (a) Divalent cation and (b) sodium transport numbers as a function of cation solute ratio for BGWs containing a TDS of 3,000 ppm. (c) Anion transport numbers as a function of anion solute ratio for BGWs containing a TDS of 3,000 ppm.

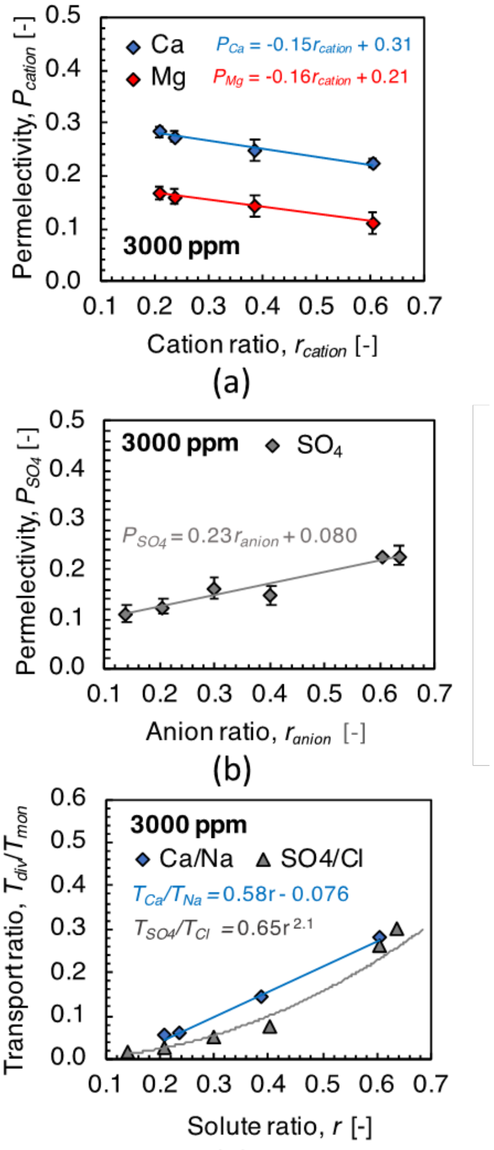

(a)

(b)

(c)

Figure 4-14. (a) CEM selectivity, (b) AEM selectivity, and (c) ratio of divalent to monovalent transport number for CEMs and AEMs, as a function of cation and anion solute ratio, respectively, for BGWs containing a TDS of 3,000 ppm.

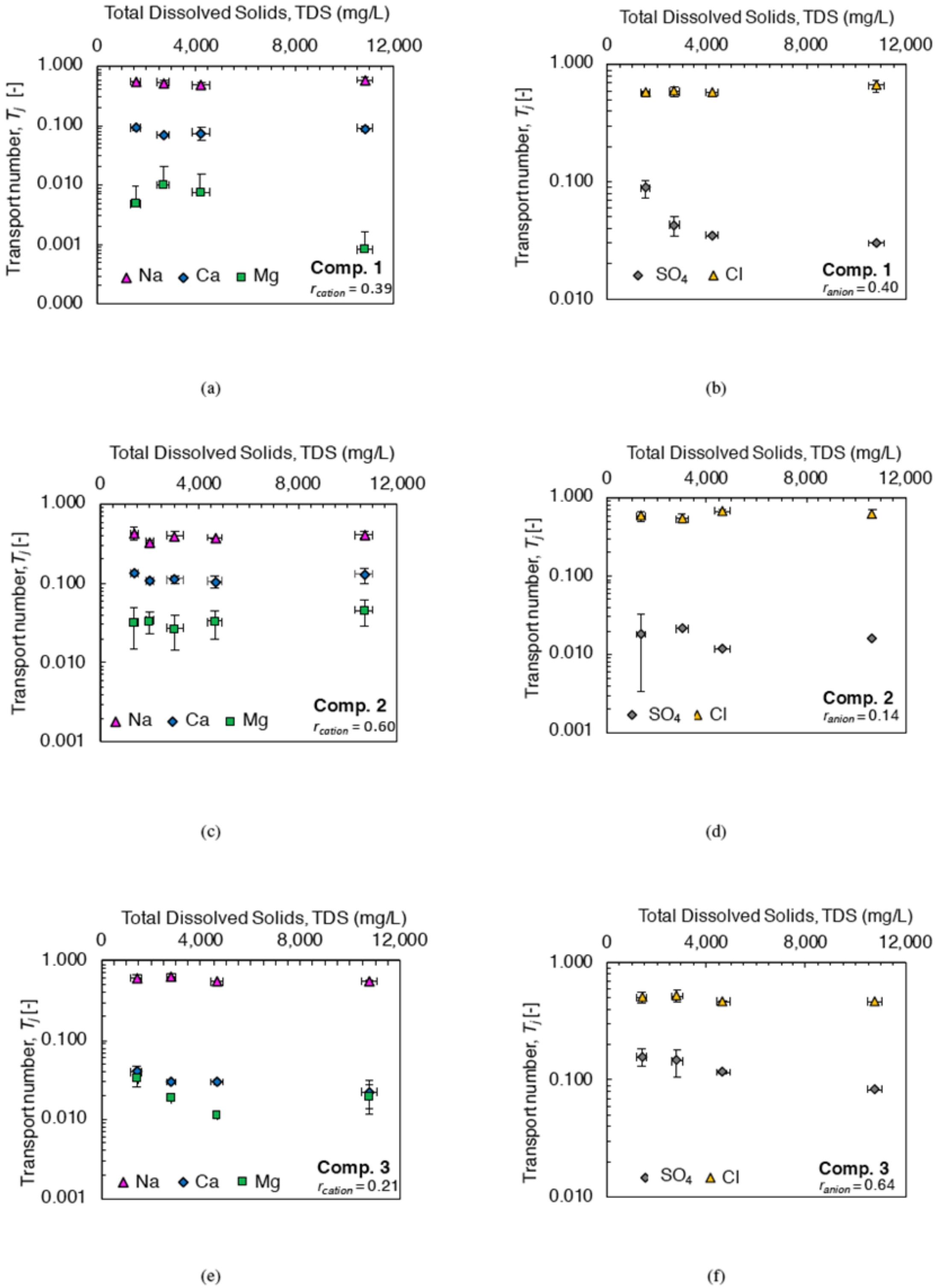

(a)

(b)

(c)

(d)

(e)

(f)

Figure 4-15. Cation transport numbers on a logarithmic scale as a function of TDS for (a) Comp. 1, (c) Comp. 2, and (e) Comp. 3. Anion transport numbers on a logarithmic scale as a function of TDS for (b) Comp. 1, (d) Comp. 2, and (f) Comp. 3.

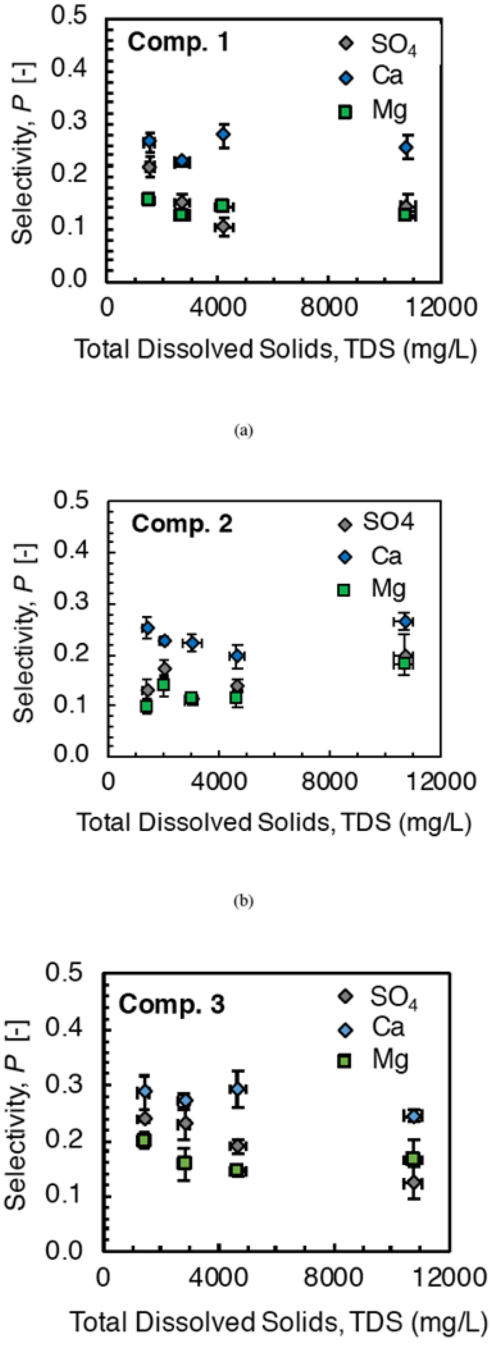

(a)

(b)

(c)

Figure 4-16. Membrane selectivity as a function of TDS for (a) Comp. 1, (b) Comp. 2, and (c) Comp. 3.

Fertilizer is composed of the most essential macronutrients for crop growth: phosphate, nitrate, potassium, calcium, magnesium, and sulfate. Water-soluble salts used to achieve desired ion concentrations in fertilizer can vary in amount and composition, depending on soil composition, crop, and other factors. Common salts in fertilizer are gypsum, Epsom, potassium chloride and/or sulfate, ammonium nitrate and/or sodium nitrate, and ammonium phosphate. Gypsum and Epsom, which add calcium and magnesium, respectively, are cost-efficient and maintain pH without varying the composition of other nutrients. The addition of 3.06×10^{-4} kg of gypsum to 1 m^2 of soil results in a 110-ppm increase in calcium [29]. The addition of 4.09×10^{-4} kg of Epsom to 1 m^2 of soil results in a 50-ppm increase in magnesium [59]. Based on gypsum and Epsom prices on Amazon [62, 63], the costs of adding calcium and magnesium to soil in greenhouses are calculated (see Table 4-5). Unlike calcium and magnesium, sulfate is added by multiple salts (e.g., gypsum, Epsom, potassium sulfate). Consequently, this analysis only considers calcium and magnesium in fertilizer savings; the MSED cation savings represent a lower bound on total possible nutrient savings from cations and sulfate.

Table 4-5. Fertilizer cost $F_{cost,div}$ to add 1 ppm of divalent ions to 1 m^2 of a greenhouse

Ion	$F_{cost,div}$ (\$ m^{-2} ppm^{-1})
Ca^{2+}	2.69×10^{-3}
Mg^{2+}	1.71×10^{-3}

Although the desired product water for irrigation is crop-specific, our goal is to determine a first-order approximation of MSED savings independent of crop. Consequently, we define samples with potential for MSED treatment as containing calcium (Ca > 150 ppm), magnesium (Mg > 50 ppm), and/or sulfate (SO_4 > 50ppm) concentrations greater than the target levels for irrigation water at large (see Table 4-6). Of the 28,000 brackish groundwater samples, 5,069 samples contain sufficient calcium, magnesium, and sulfate; 5,161 samples contain sufficient calcium and magnesium; 6,726 samples contain sufficient calcium; and 8,453 samples contain sufficient magnesium.

Figure 4-17 shows groundwaters that contain enough calcium and magnesium, in addition to sulfate, that MSED can preserve in the water. These groundwaters exist in all areas for which groundwater data is available, including in agriculture regions such as the Central Valley in California and parts of the Dakotas, Texas, Iowa, and Oklahoma.

Table 4-6. Water quality recommendations for agriculture [30, 31].

Ion	Concentration (ppm)
Ca^{2+}	80-150
Mg^{2+}	30-50
Na^{+}	Low as possible
SO_4^{2-}	>50
Cl^{-}	>20

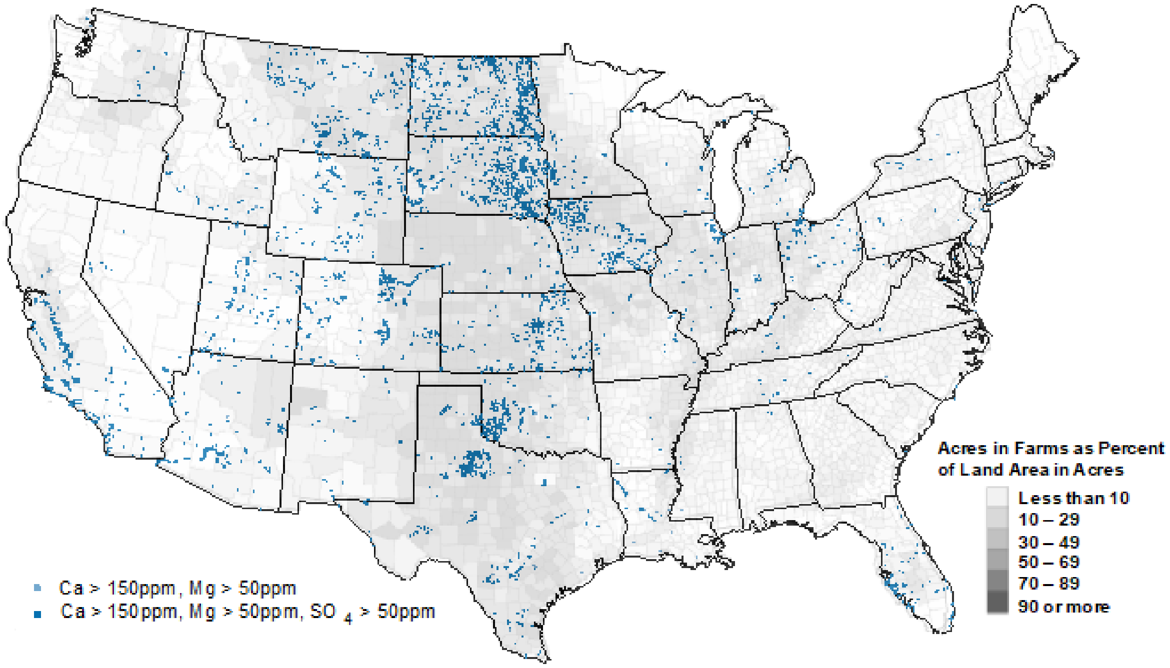

Figure 4-17. Map of BGW samples containing specified concentrations of Ca^{2+}, Mg^{2+}, and/or SO_4^{2-} from USGS dataset, overlaid on map of percent of acres farmed in a given county (modified from [66]). Each dot corresponds to a BGW sample. The grayer a county, the more farmland is present.

The groundwater samples containing sufficient levels of calcium and magnesium serve as the feedwater to the MSED system for which savings are determined. The calcium permselectivity (error of 11.5 percent) and magnesium permselectivity (error of 20 percent) are used to characterize the MSED membranes. The final concentration of calcium, the dominant ion in fertilizer cost savings, is set to 150 ppm for all groundwaters. Equation No. 8 is then used to calculate the unknown final sodium and magnesium concentrations. RO final concentrations, which serve as the baseline of comparison to MSED, are determined from the feedwater composition and ion percent reductions in Table 4-7. We ensure that the final sodium concentration remains below 100 ppm [67]. Based on these values, MSED savings in ion percent reductions $S_{\%,\text{div}}$ (%), final ion concentrations $S_{\text{ppm,div}}$ (ppm), and fertilizer cost $S_{\$,\text{div}}$ ($\$\cdot\text{ha}^{-1}\cdot\text{yr}^{-1}$), assuming on growing season per year, relative to RO are determined (see Table 4-8):

$$S_{\%,div} = 100\frac{(C_{div,i}-C_{div,f|RO})-(C_{div,i}-C_{div,f|MSED-R})}{C_{div,i}} \tag{27}$$

$$S_{ppm,div} = \frac{S_{\%,div}}{100}C_{div,i} \tag{28}$$

$$S_{\$,div} = \left(S_{ppm,div}\right)\left(F_{cost,div}\right) \tag{29}$$

Figure 4-18 shows the geographic distribution of fertilizer cost savings $S_{\$,\text{Ca+Mg}}$ for a representative case from Table 4-8 $\left(P_{Na,avg.}^{Ca}, P_{Na,avg.}^{Mg}\right)$. Similar to Figure 4-17, these savings exist in groundwater samples across the United States that overlap with agriculture regions, highlighting the potential for MS-EDR adoption. If MSED is to replace RO, a commodity product with lower capital and annual operating costs, its savings must offset differences in these technologies' costs within a specified payback period. Interviews we conducted with greenhouses indicate a desired payback period of 2 years on their investments. Farm size is a key indicator in determining the payback period. MSED savings linearly increase with farm size; capital and operating costs also increase with farm size, although changes in these costs decrease with farm size. These two trends suggest that larger farms would benefit more from MSED and are better initial adopters of this technology.

We consider the RO and MSED capital and operating costs for a 10-hectare farm treating groundwater containing 850 ppm of TDS [67]. Each hectare under greenhouse cultivation is assumed to require a desalination system with a capacity of 60 m^3/day operated without supervision for 12 hr/day annually at a 90 percent capacity factor. We consider the average annual fertilizer savings as $4,920/hectare and water savings for the recovery values of 90 percent for MSED and 80 percent for RO. The total cost of each desalination technology after 1 year of operation is then calculated as:

$$Net\ Cost\ (year\ one) = CapEx\frac{r(1+r)^n}{(1+r)^n-1} + OpEx - savings \tag{30}$$

where r corresponds to an annual interest rate of 8 percent [34] and n corresponds to a time period of 15 years, the expected life of RO and MSED systems [67]. The savings are equal to zero for RO. Table 4-9 shows that MSED will pay back greenhouses in less than 1 year. The total cost of MSED is less than that of RO after 1 year of operation, when considering fertilizer savings and the combined savings from fertilizer and water recovery. MSED saves $43,569 annually compared to RO, when considering MSED fertilizer and water savings.

Table 4-7. Typical RO ion percent reductions for BGW [6].

Ion	Ion Reduction (%)
Ca^{2+}	90
Mg^{2+}	99
Na^{+}	97
SO_4^{2-}	99
Cl^{-}	98

Note: Percent reduction was determined using the formula: $100\frac{C_{div,i}-C_{div,f|RO}}{C_{div,i}}$

Table 4-8. MSED savings in ion percent reductions, final ion concentrations, and fertilizer cost relative to RO for $C_{Ca,f}$ =150 ppm and nine different cases of P_{Na}^{Ca} and P_{Na}^{Mg} (avg., +stdev., −stdev.).

$P_{Na,avg.}^{Ca}$	$P_{Na,avg.}^{Mg}$	$S_{\%,Ca}$	$S_{\%,Mg}$	$S_{ppm,Ca}$	$S_{ppm,Mg}$	$S_{\$,Ca}$	$S_{\$,Mg}$	$S_{\$,Ca+Mg}$
Avg.	Avg.	75	90	132	81	$3,563	$1,379	$4,942
Avg.	+stdev.	75	89	132	79	$3,563	$1,352	$4,915
Avg.	-stdev.	75	92	132	82	$3,563	$1,406	$4,969
+stdev.	Avg.	73	90	132	81	$3,553	$1,390	$4,944
+stdev.	+stdev.	73	89	132	80	$3,553	$1,364	$4,917
+stdev.	-stdev.	73	92	132	83	$3,553	$1,417	$4,970
-stdev.	Avg.	77	91	133	80	$3,575	$1,373	$4,948
-stdev.	+stdev.	77	89	133	79	$3,575	$1,347	$4,922
-stdev.	-stdev.	77	92	133	82	$3,575	$1,400	$4,975

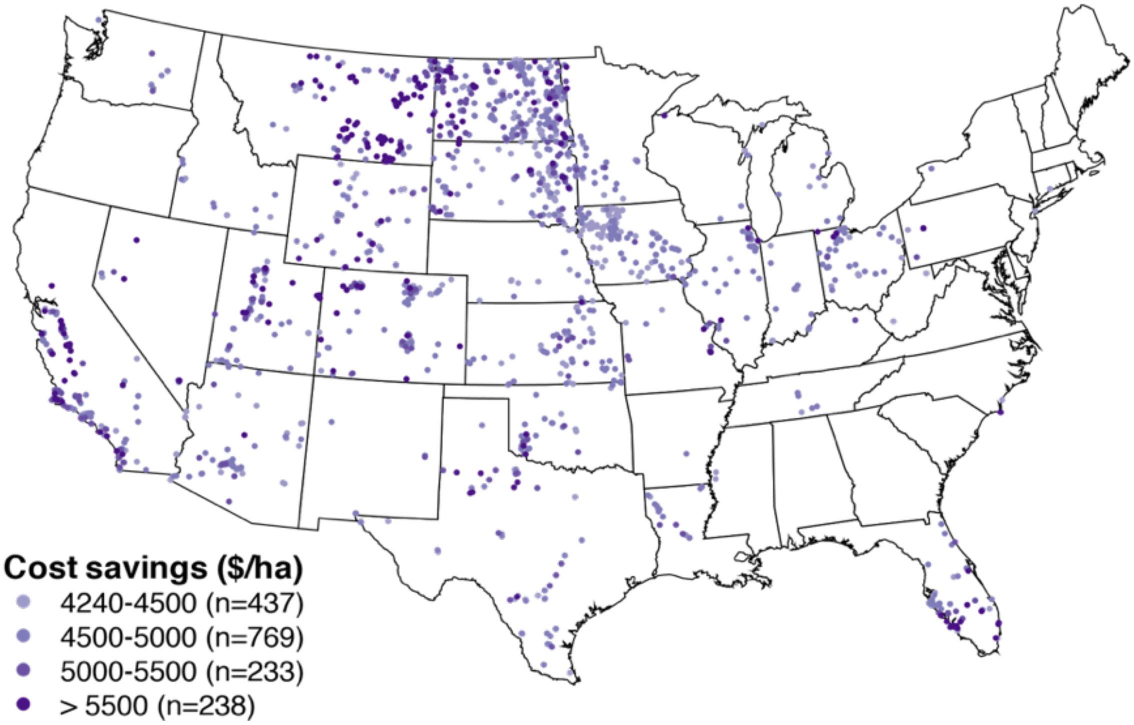

Figure 4-18. Map of total fertilizer cost savings for cations in BGW samples from the USGS dataset. Each dot corresponds to a BGW sample.

Table 4-9. MSED and RO net costs after 1 year of operation for a 10-hectare farm, based on annual capital and operating costs, as well as fertilizer and/or water savings. The MSED net costs are negative due to the fact that the annual savings exceed the total costs. MSED savings relative to RO are equivalent to the difference in their net costs.

	MSED-R	RO
Annual CapEx	$16,835	$13,540
OpEx	$17,799	$10,863
Fertilizer Savings	$49,420	-
Net Cost (Year 1)	-$14,786	$24,403
Water Savings	$4,380	-
Net Cost (Year 1)	-$19,166	$28,135

4.3. Characterization of Fujifilm Type 16 MSED Membranes

This section presents experimental results of membrane monovalent selectivity for a bench-scale MSED system containing Fujifilm membranes. Because BGW composition varies significantly with location, we analyze 13 diverse BGWs to characterize Fujifilm membrane selectivity. Trends in selectivity and BGW composition, both TDS and solute ratio, are explored. Our results suggest that membrane selectivity may be sensitive to solute ratio and is independent of BGW salinity. In order to benchmark Fujifilm membrane behavior, we compare these outcomes to those of the widely used Neosepta membranes.

All results represent a bench-scale setup. System parameters may vary with scale for a variety of reasons, including differences in transport characteristics, operating conditions, and system configurations. Consequently, pilot studies in greenhouses are required to fully characterize MSED systems for real-world applications.

4.3.1. Trends in Desalination Process Time: Experiments and Model

Across the considered BGWs, normalized ion concentration drop and membrane permselectivity linearly vary with desalination process time in a given experiment. Consistent with the literature [77, 82] this trend indicates that membrane selectivity declines as diluate salinity decreases. The relationship of process time with membrane permselectivity is equivalent to that with transport number ratio $T_{div}=T_{Na}$, because the initial ion concentration is fixed in a given experiment. The only parameters in transport number ratio that vary in a trial are the changes in ion concentration and process time. Therefore, transport number ratio and membrane selectivity trends must match the linear trend in normalized ion concentration drop with time. Figure 4-19 shows that the developed MSED model matches the experimental trends in normalized concentration drop with a maximum difference of 6 percent.

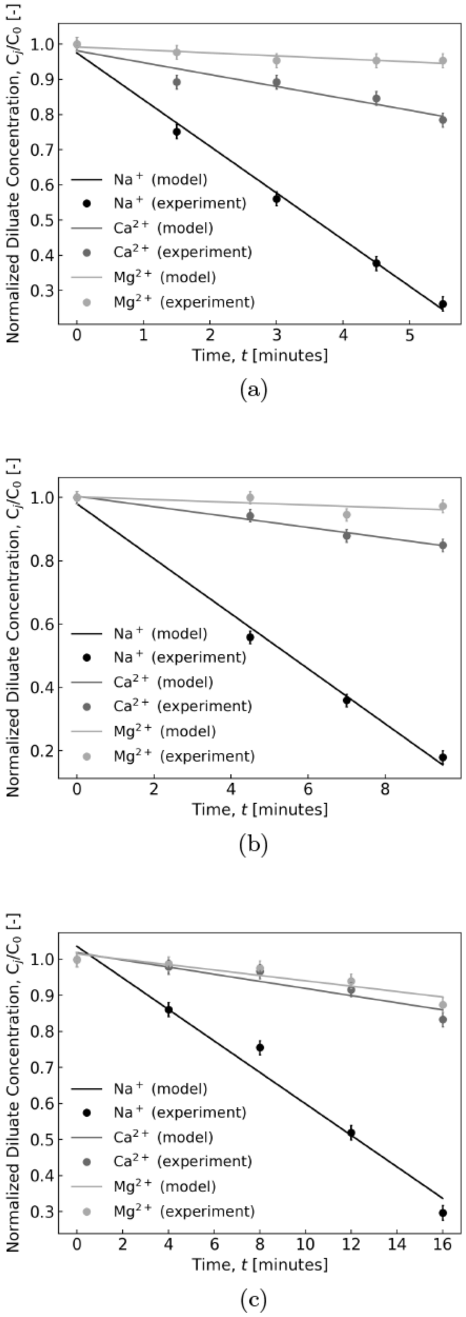

(a)

(b)

(c)

Figure 4-19. Normalized cation concentration as a function of desalination process time for BGW containing (a) 1,500 ppm, (b) 3,000 ppm, and (c) 5,000 ppm, with a comparison to the MSED model.

4.3.2. Permselectivity for 13 BGW Compositions

The Fujifilm CEMs and AEMs show notable selectivity toward monovalent ions across the 13 BGW compositions. The average magnesium selectivity is 0.08±0.04, representing a factor of

8.3 to 26 removal of sodium relative to magnesium. The average calcium permselectivity is 0.18±0.08, corresponding to a factor of 3.7 to 10 reduction of sodium relative to calcium. The lower hydration energy of calcium (1,592 kJ/mol) compared to magnesium (1,904 kJ/mol) accounts for calcium's higher permselectivity (i.e., lower removal rate), because ions must partly or entirely shed their hydration shell to traverse the membranes [91]. Average sulfate permselectivity across all compositions is 0.18±0.12, corresponding to a factor of 3.3 to 20 removal of chloride relative to sulfate. The maximum standard deviation σ from the average values is 25 percent for cations and 33 percent for anions. The permselectivities for each BGW solution are shown in Table 4-10. The SARs of Comp. 1, Comp. 2, Comp. 3, and Cohen product waters are 1.8 ± 0.7, 1.6 ± 0.4, 3.6 ± 0.3, and 2.2 ± 0.4, respectively.

4.3.2.1. Observed Trends in Solute Ratio at Fixed TDS

We explore trends in solute ratio with transport number and monovalent selectivity for Comp. 1, Comp. 2, Comp. 3, and Cohen solutions at a fixed TDS of 2,750 ± 154 mg/L. Transport number linearly depends on solute ratio, with monovalent transport numbers decreasing and divalent transport numbers increasing with cation and anion solute ratio. At lower solute ratios, fewer divalent ions will compete with monovalent ions to cross the membranes, resulting in increased monovalent transport and decreased divalent transport. Conversely, at higher solute ratios, monovalent ions will compete with more divalent ions to cross the membranes, leading to reduced monovalent transport and greater divalent transport.

Figure 4-20 illustrates the linear relationship between permselectivity and solute ratio. Anion permselectivity increases with anion solute ratio, while cation permselectivity decreases with cation solute ratio. Differences in the rate of change in transport number ratio with solute ratio for anions and cations seem to account for the discrepancy in the permselectivity trends. Trends in permselectivity mirror those in transport number ratio, because solute ratio is proportional to the initial concentration ratio (i.e., $P_{mon}^{div} \propto \frac{T_{div}/T_{mon}}{r}$). If we divide the transport number ratio equations in Figure 4-20(c) by r, anion permselectivity varies with $A(r_{\text{anion}})$ [70, 77] and cation permselectivity varies with $B+D/r_{\text{cation}}$, where A, B, and D are constants greater than 0. Consequently, anion permselectivity increases as r_{anion} increases, while cation permselectivity decreases as r_{cation} increases. The overlapping error bars in membrane selectivity suggest that the parameter may be sensitive to solute ratio.

Counter-ion (i.e., an ion with an electric charge opposite to the membrane) permselectivity may be influenced by coion (i.e., an ion with the same electric charge as the membrane) concentrations. For example, Comp. 3 ($r_{\text{anion}} = 0.64$) and Cohen ($r_{\text{anion}} = 0.30$) have substantially different anion solute ratios and relatively similar cation solute ratios (13 percent difference). At a fixed TDS of 2,624 ± 83.6, the average calcium permselectivity is 0.21 ± 0.02 (σ of 6 percent), suggesting little variation in calcium permselectivity despite differences in sulfate concentration. In comparison, the average magnesium permselectivity is 0.09±0.04 (σ of 18 percent), reflecting a larger variation in permselectivity with differences in sulfate levels. More BGWs with similar counter-ion and different co-ion solute ratios would need to be analyzed to establish the effect of co-ions on counter-ion permselectivity.

Table 4-10. Calcium, magnesium and sulfate permselectivity for 13 BGW compositions. The first two columns correspond to BGW composition.

Solute Ratio	TDS (mg/L)	P_{Na}^{Ca}	P_{Na}^{Mg}	$P_{Cl}^{SO_4}$
Comp. 1	1,295	0.21±0.03	0.09±0.02	0.21±0.02
	2,858	0.14±0.03	0.06±0.02	0.18±0.10
	4,408	0.19±0.03	0.09±0.02	0.16±0.02
	10,396	0.16±0.04	0.09±0.03	0.27±0.02
Comp. 2	1,483	0.18±0.02	0.05±0.002	0.10±0.01
	2,895	0.10±0.05	0.06±0.004	0.12±0.01
	4,756	0.19±0.02	0.10±0.002	0.15±0.008
	7,814	0.22±0.02	0.09±0.003	0.10±0.01
Comp. 3	1,450	0.13±0.03	0.07±0.02	0.22±0.04
	2,683	0.22±0.03	0.10±0.01	0.28±0.01
	4,276	0.22±0.02	0.05±0.007	0.23±0.01
	8,491	0.21±0.01	0.09±0.002	0.18±0.02
Cohen	2,564	0.20±0.02	0.08±0.02	0.11±0.02

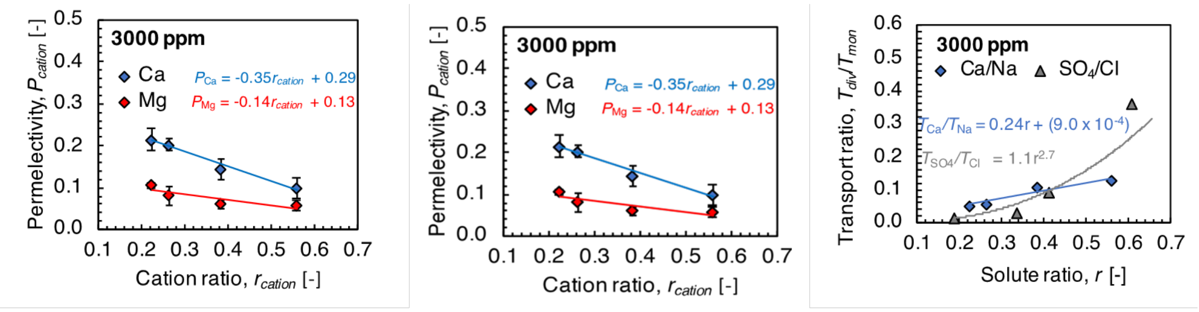

(a) (b) (c)

Figure 4-20. (a) CEM selectivity, (b) AEM selectivity, and (c) ratio of divalent to monovalent transport number for CEMs and AEMs, as a function of cation and anion solute ratio, respectively, for BGWs containing a TDS of 3,000 mg/L.

4.3.2.2. Observed Trends in TDS at Fixed Solute Ratio

This section investigates trends in transport number and monovalent selectivity with initial diluate salinity, when the initial solute ratio is held constant. Although the TDS of most BGW samples in the USGS dataset range from 500 mg/L to 3,000 mg/L [85] we consider four salinities in the 1,000 mg/L to 10,000 mg/L BGW range per ionic composition for completeness. We observe no trends in transport number as a function of initial diluate salinity for Comp. 1, Comp. 2, and Comp. 3. Moreover, the overlapping error bars illustrate the insignificant variation in a given ion transport number across the BGW salinity range. Because permselectivity is only a function of transport numbers at a constant solute ratio, there similarly appear to be no trends in permselectivity with initial salinity (Figure 4-21). The lack of observed trends may stem from the narrowness of the BGW salinity range compared to the broad salinity range typically considered in ED transport number fits in the literature (e.g., BGW salinities up to 200,000 mg/L) [90].

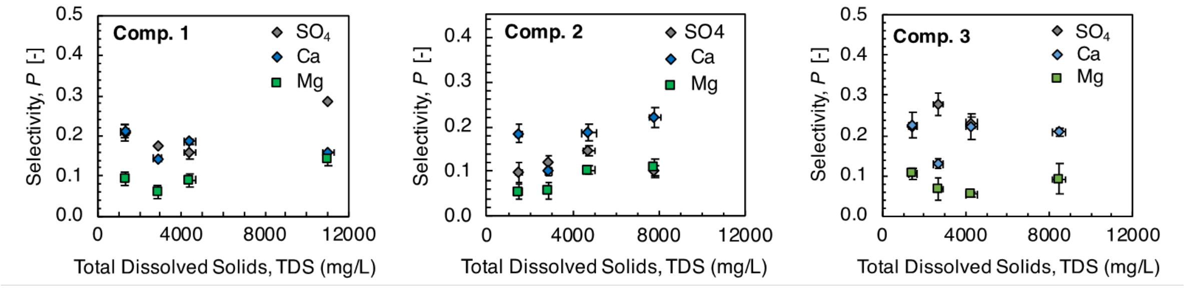

(a) (b) (c)

Figure 4-21. Membrane permselectivity as a function of TDS for (a) Comp. 1, (b) Comp. 2, and (c) Comp. 3.

4.3.3. Comparison to Neosepta MSED Membranes

This section compares the performance in the BGW salinity range of the recently developed Fujifilm membranes to the widely used Neosepta MSED membranes. The Neosepta membranes are characterized for the same 13 BGW compositions as the Fujifilm membranes [83]. Across these compositions, Fujifilm CEMs show notably better monovalent selectivity, while the Fujifilm AEMs show moderately worse monovalent selectivity than the Neosepta membranes (Table 4-12). The average Fujifilm calcium and magnesium permselectivities are 28 percent and 47 percent, respectively, less than those of Neosepta. If we account for standard deviation (Pavg. $\pm 2\sigma$), the Neosepta CEMs remove a factor of 3.1 to 5.2 more sodium than calcium, in comparison to Fujifilm's 3.7 to 10, and a factor of 4.8 to 11 more sodium than magnesium, in comparison to Fujifilm's 8.3 to 26. The average Fujifilm sulfate permselectivity is 4.1 percent less than that of Neosepta. If we account for standard deviation (Pavg. $\pm 2\sigma$), the Neosepta AEMs remove a factor of 4.3 to 9.4 more chloride than sulfate, in comparison to Fujifilm's 3.3 to 20. Considering CEM and AEM performance, Fujifilm membrane performance overall is superior to that of Neosepta for BGWs. In addition, the Fujifilm and Neosepta membranes show similar trends in permselectivity with BGW composition. There appears to be no relationship between permselectivity and TDS and a linear relationship between permselectivity and solute ratio.

Cation and anion permselectivity increases with decreasing cation and increasing anion solute ratio, respectively, for both membranes (Figure 4-22). However, the Fujifilm membranes have a larger selectivity-solute ratio slope for calcium and sulfate, suggesting that permselectivity of the Fujifilm membranes may be more sensitive to solute ratio than the Neosepta membranes. In addition, the Fujifilm membranes have a higher limiting current density than the Neosepta membranes (i.e., they can withstand a higher operating current without a decrease in performance). A comparison of limiting current density and membrane resistance can be found in Figure 4-23.

Table 4-11. Calcium, magnesium and sulfate permselectivities of Neosepta and Fujifilm membranes for four solute ratios (Comp. 1, Comp. 2, Comp. 3, Cohen) and for all 13 analyzed BGWs. The Comp. 1, Comp. 2, and Comp. 3 values are averaged across their four tested salinities, because no trends in permselectivity with TDS are observed for either membrane.

	P_{Na}^{Ca}		P_{Na}^{Mg}		$P_{Cl}^{SO_4}$	
	Fujifilm	**Neosepta**	**Fujifilm**	**Neosepta**	**Fujifilm**	**Neosepta**
Comp. 1	0.17±0.03	0.26±0.03	0.08±0.02	0.14±0.02	0.20±0.06	0.15±0.04
Comp. 2	0.17±0.05	0.23±0.03	0.08±0.02	0.13±0.03	0.12±0.06	0.15±0.03
Comp. 3	0.20±0.04	0.27±0.04	0.08±0.02	0.17±0.03	0.23±0.08	0.20±0.06
Cohen	0.20±0.03	0.27±0.04	0.08±0.04	0.16±0.04	0.11±0.04	0.16±0.04
All BGWs	0.18±0.08	0.26±0.06	0.08±0.04	0.15±0.06	0.18±0.12	0.17±0.06

4.3.4. Implications for Desalination in Greenhouses

Our experiments confirm the monovalent selectivity of Fujifilm and Neosepta membranes, with a better Fujifilm CEM performance, in the BGW salinity range. An MSED system using either set of membranes will be capable of retaining nutrients present in the source groundwater, which would otherwise be added as fertilizer after RO treatment. This section presents a first-order estimate of MSED fertilizer savings relative to RO for BGWs with sufficient nutrient concentrations from the 2017 USGS major-ions groundwater dataset [87]. We then compare the Fujifilm and Neosepta results and conduct a case study on a 10-hectare greenhouse using MSED versus RO.

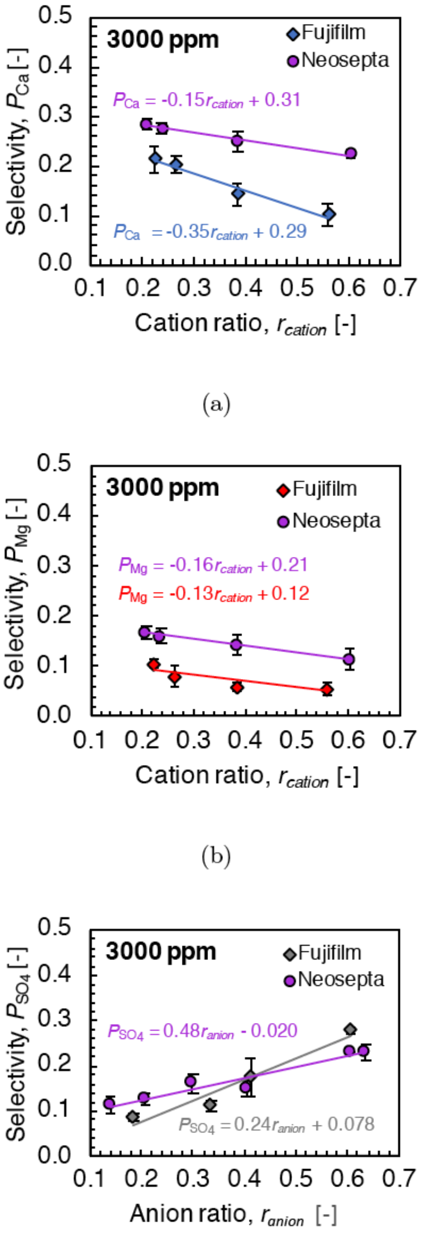

(a)

(b)

(c)

Figure 4-22. (a) Calcium, (b) magnesium, and (c) sulfate selectivity for Neosepta and Fujifilm membranes as a function of solute ratio for BGWs containing a TDS of 3,000 ppm.

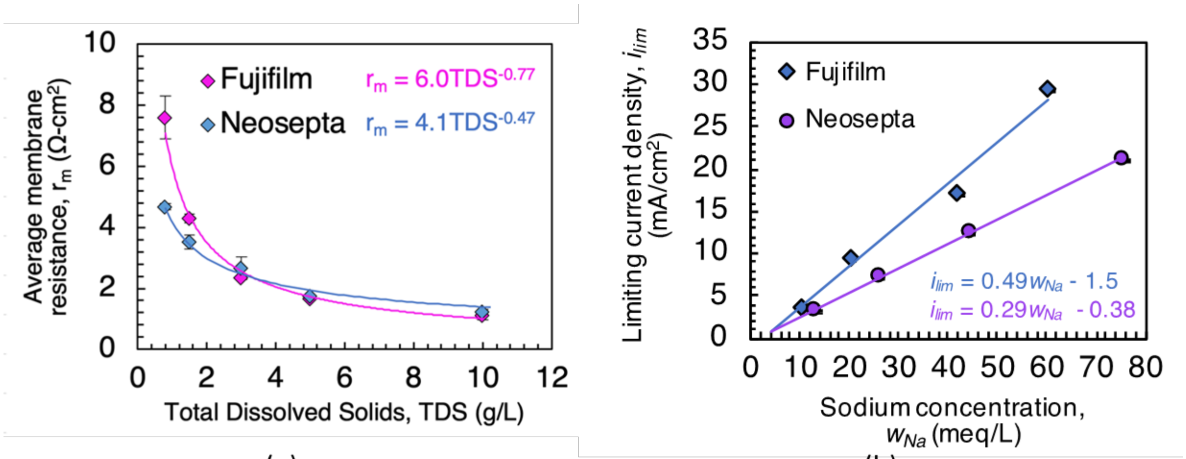

(a) (b)

Figure 4-23. (a) Membrane resistance and (b) limiting current density of Neosepta and Fujifilm membranes for various dilutions of NaCl solutions.

4.3.4.1. Fertilizer Cost Savings

MSED fertilizer cost savings are calculated for 6,000 BGWs that contain nutrient concentrations in excess of general recommendations for irrigation water quality: Ca > 150 mg/L, Mg > 50 mg/L, and/or SO_4 > 50 mg/L [92, 93]. In reality, the desired irrigation water will depend on the crop. However, we aim to provide a first-order approximation of MSED fertilizer savings independent of crop. We do not consider sulfate in our calculations of fertilizer savings, because multiple salts that compose fertilizer contain sulfate but not magnesium or calcium. Consequently, the determined fertilizer savings, based only on cations, serve as a lower bound on the nutrient savings potentially offered by MSED.

To characterize the membranes, we use the average cation permselectivities for the 13 BGW compositions. The average cation selectivities have a maximum σ of 25 percent, which may result from differences in BGW solute ratio and appears to not result from differences in BGW salinity. Consequently, the Fujifilm selectivity values for 13 diverse BGW compositions can likely be applied to BGWs across the United States. We set the final concentration of calcium, the key ion in determining fertilizer cost savings, to 150 mg/L. Equation No. 7 is applied to evaluate the final magnesium concentrations and sodium concentrations, which do not exceed 100 mg/L [94]. We then compare the final nutrient concentrations of MSED and RO, based on typical RO ion percent reductions ranging from 90 percent to 99 percent. The difference in these values is used to quantify the MSED Fujifilm savings in ion percent reductions $S_{\%,div}$ (%), final ion concentrations $S_{ppm,div}$ (mg/L), and fertilizer cost $S_{\$,div}$ (\$·ha^{-1}·yr^{-1}) relative to RO, assuming one growing season per year, in Table 4-13:

$$S_{\%,div} = 100\frac{(C_{div,i}-C_{div,f|RO})-(C_{div,i}-C_{div,f|MSED})}{C_{div,i}} \tag{8}$$

$$S_{ppm,div} = \frac{S_{\%,div}}{100}C_{div,i} \tag{9}$$

$$S_{\$,div} = (S_{ppm,div})(F_{cost,div}) \tag{10}$$

where $F_{cost,div}$ is the fertilizer cost of adding gypsum[25] or Epsom[26] to greenhouse soil.

Figure 4-24 maps the Fujifilm fertilizer cost savings $S_{\$,Ca+Mg}$ for the first row from Table 4-12 ($P_{Na,avg.}^{Ca}$, $P_{Na,avg.}^{Mg}$). MSED can generate fertilizer savings for BGWs across the United States, including agriculture centers in California's Central Valley, Iowa, and the Dakotas.

Table 4-12. MSED Fujifilm savings in ion percent reductions, final ion concentrations and fertilizer cost relative to RO for $C_{Ca,f}$ =150 mg/L and nine different cases of P_{Na}^{Ca} and P_{Na}^{Mg}(avg., +σ, -σ). For example, the first row (average P_{Na}^{Ca} and P_{Na}^{Mg}) uses the average permselectivity values. The last column includes the Neosepta fertilizer cost savings for comparison.

		Fujifilm							**Neosepta**
$P_{Na,avg.}^{Ca}$	$P_{Na,avg.}^{Mg}$	$S_{\%,Ca}$	$S_{\%,Mg}$	$S_{ppm,Ca}$	$S_{ppm,Mg}$	$S_{\$,Ca}$	$S_{\$,Mg}$	$S_{\$,Ca+Mg}$	$S_{\$,Ca+Mg}$
Avg.	Avg.	79	94	133	82	$3,587	$1,408	$4,995	$4,942
Avg.	+σ	79	93	133	81	$3,587	$1,389	$4,977	$4,915
Avg.	-σ	79	96	133	83	$3,587	$1,426	$5,013	$4,969
+σ	Avg.	77	94	133	84	$3,575	$1,435	$5,010	$4,944
+σ	+σ	77	93	133	83	$3,575	$1,416	$4,991	$4,917
+σ	-σ	77	96	133	85	$3,575	$1,453	$5,028	$4,970
-σ	Avg.	82	94	134	82	$3,600	$1,398	$4,998	$4,948
-σ	+σ	82	93	134	81	$3,600	$1,379	$4,980	$4,922
-σ	-σ	82	96	134	83	$3,600	$1,415	$5,016	$4,975

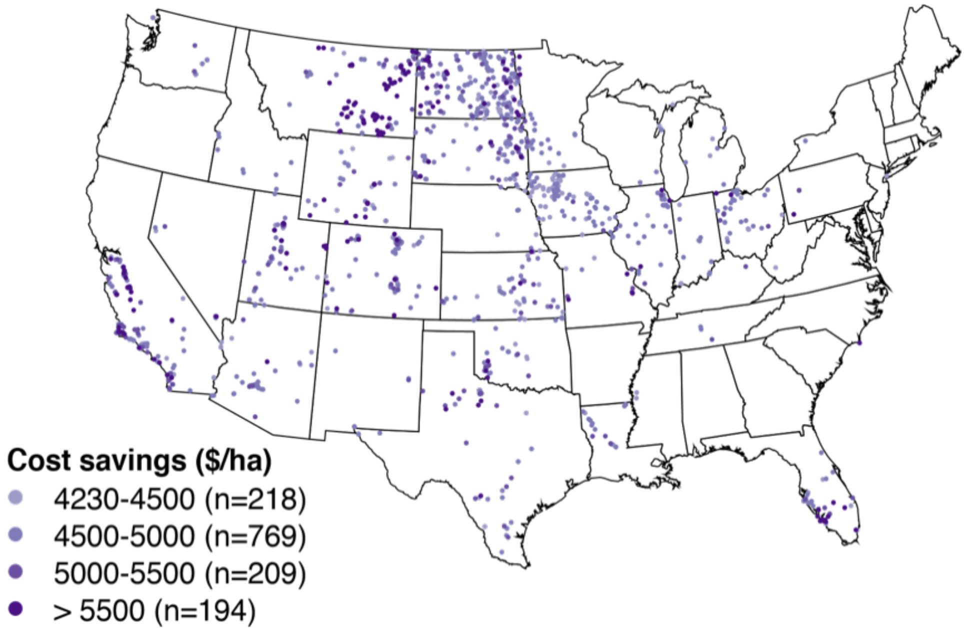

Figure 4-24. Map of Fujifilm fertilizer cost savings ($/ha) for cations in BGW samples from the USGS dataset. Each dot corresponds to a BGW sample.

4.3.4.2. Greenhouse Case Study: MSED versus RO

RO is a commodity product with lower operating costs (OpEx) and capital costs (CapEx) than MSED. Consequently, if MSED using Fujifilm or Neosepta membranes is to be implemented in greenhouses, rather than RO, MSED savings must offset OpEx and CapEx differences between the technologies within a 2-year payback period, according to greenhouse interviews we conducted [95]. We anticipate larger farms being the early adopters of this promising technology. In addition to their greater resilience to innovation, the trade-off between MSED savings and costs becomes more favorable (i.e., the payback period decreases with an increase in farm size): CapEx and OpEx grow at a decreasing rate with farm area, while MSED fertilizer savings linearly increase with farm area.

This case study compares the adoption of MSED and RO in a 10-hectare farm with source water containing 850 mg/L in TDS. All cost data for RO and MSED are obtained from Nayar et al [95]. The study assumes a desalination system capacity of 60 m^3/day-ha with a 90 percent capacity factor and 12 hrs/day of operation. We define the annual fertilizer savings as $4,995/ha, based on the average value for the Fujifilm membranes. Water savings are calculated using recovery values of 80 percent and 90 percent for RO and MSED, respectively. The net cost of the technologies after one year of operation is then evaluated as:

$$Net\ Cost\ (year\ one) = CapEx\,\frac{r(1+r)^n}{(1+r)^n-1} + OpEx - savings \tag{11}$$

where *r* corresponds to an annual interest rate of 8 percent [97] and *n* corresponds to a time period of 15 years, the life expectancy of RO and MSED systems [94]. RO savings are equal to zero. For the 10-hectare farm, the net cost of MSED is less than that of RO after 1 year of operation (i.e., the payback period for greenhouses is less than 1 year [Table 4-13]). MSED with

Fuijfilm membranes annually saves greenhouses $39,719 in fertilizer and $44,099 in fertilizer and water relative to RO.

Table 4-13. MSED and RO net costs after 1 year of operation for a 10-hectare farm, based on annual capital and operating costs, as well as fertilizer and/or water savings. The MSED net costs are negative due to the fact that the annual savings exceed the total costs. MSED savings relative to RO are equivalent to the difference in their net costs. CapEx and OpEx data are obtained from Nayar et al [94].

	MSED	RO
Annual CapEx	$16,835	$13,540
OpEx	$17,799	$10,863
Fertilizer Savings	$49,950	-
Net Cost (Year 1)	-$15,316	$24,403
Water Savings	$4,380	-
Net Cost (Year 1)	-$19,696	$28,135

5. Conclusions

A summary of the conclusions for the techno-economic comparison, characterization of the Neosepta ACS/CMS membranes, and characterization of the Fujifilm Type 16 membranes can be found below. Overall, we have proven that MSED with Fujifilm or Neosepta ion exchange membranes is a more sustainable and cost-effective desalination technology than the dominant RO for brackish water treatment in greenhouses, as a result of MSED nutrient and water savings at comparable energy consumption.

5.1. Techno-economic Comparison of MSED to RO, CRRO, ED

These conclusions assume an MSED cation savings of 15 percent. The experiments we conducted following this study reveal 80 percent cation savings for various groundwater composition. Consequently, the annual fertilizer savings of MSED determined in this techno-economic comparison provide a lower bound.

- Greenhouse operators desire simple payback periods of less than 2 years for their desalination systems.

- Greenhouses with areas under cultivation larger than 5 hectares had more corporate ownership structures and were generally early adopters of new technology. Thus, desalination system developers, especially those focusing on developing new technologies, should partner with larger greenhouses (more than 5 hectares) for piloting their technologies.
- Among the technologies RO, CCRO, EDR, and MS-EDR, RO had the lowest capital cost.
- For greenhouses with areas less than 10 hectares with groundwater salinities greater than 500 ppm, RO was the most cost-effective technology compared to CCRO, EDR, and MS-EDR. RO system component and membranes at these small capacities are more widely available and cost less. RO systems are likely to be also much easier to maintain for greenhouses with a size less than 10 hectares.
- For greenhouses with areas greater than 10 hectares:
    - Both CCRO and MS-EDR systems show great promise under the right conditions of feedwater costs, with calcium and magnesium savings possible.
    - MS-EDR systems are economically viable, irrespective of feedwater and brine disposal costs, if they can save at least 20 percent of the calcium and magnesium needed for nutrient solutions and have a membrane life of 7 years. Further research and development on brackish MS-EDR systems, especially related to membrane life and monovalent selectivity, is justified.
    - CCRO systems are economically viable if the sum of feedwater and brine disposal costs are greater than $\$0.24/m^3$.
    - EDR systems show promise if the sum of feedwater and brine disposal costs are greater than $\$0.35/m^3$ and if the groundwater has a low enough sodium concentration (≤ 78 ppm) such that the sodium concentrations in EDR product water is less than or equal to 23 ppm.
    - CCRO systems can be commercially deployed without pilot testing. However, EDR and MS-EDR systems need to be pilot tested at greenhouses with the system costs, reliability, and product water quality validated further before commercial deployment.
- For greenhouses with areas greater than 10 hectares, a feedwater salinity of 850 ppm, a feedwater cost of $\$0.32/m^3$, product water value of $\$1.05/m^3$ and an annual fertilization cost of $\$3/m^2$:
    - RO, CCRO, EDR, and MS-EDR systems had simple payback periods of 7.1, 8.4, 7.8, and 8.2 months, respectively.
    - Relative to RO, the additional investment on CCRO, EDR, and MS-EDR would pay itself back in 2.4, 3.4, and 2.1 years respectively.

5.2. MSED Membrane Characterization

5.2.1. Neosepta ACS/CMS Membranes

Neosepta membrane selectivity for monovalent ions was tested for 16 different BGW solutions in order to fully characterize the membranes and their potential for agricultural use. The following conclusions have been reached:

- Membrane permeability for monovalent ions and divalent ions is on the order of 10^{-8} m/s and 10^{-9} m/s, respectively, due to the monovalent selectivity of the membranes.
- The CEMs demonstrate for 16 BGW compositions an average calcium selectivity of 0.26±0.03, corresponding to a 3.6 to 4.6 times reduction of sodium relative to calcium in the diluate stream, and a magnesium selectivity of 0.15±0.03, corresponding to a 5.7 to 8.7 times reduction of sodium relative to magnesium in the diluate stream.
- The AEMs demonstrate for 16 BGW compositions an average sulfate selectivity of 0.17±0.03, corresponding to a 4.8 to 7.7 times reduction of chloride relative to sulfate in the diluate stream.
- The average selectivities mentioned have a maximum standard deviation of 20 percent. This variation may result from differences in BGW ionic composition and appears to not result from differences in BGW salinity. Consequently, the selectivity values determined in this study for 16 diverse BGW compositions can likely be extended to BGWs across the United States.
- A multi-ionic MSED model predicts ion transport within 8 percent of experimental data.
- The average fertilizer cost savings due to cations ranges from $4,915/ha to $4,975/ha for nine different cases of calcium and magnesium selectivity (average, +stdev., −stdev.). Farm size is a key indicator in determining the payback period for greenhouses. For a 10-hectare farm, the average calcium and magnesium selectivities applied to 6,000 BGWs across the United States yields an average annual fertilizer cost savings of $49,420. This value indicates that the adoption of MSED in place of RO will result in less than a 1-year payback period for greenhouses. Our techno-economic comparison predicts a lower MSED annual fertilizer cost savings of $15,000 for a 10-hectare farm. This difference in savings results from the study's assumption of 15 percent cation savings, compared to our experimentally determined 80 percent cation savings for various groundwater compositions.
- MSED shows great potential to be used in greenhouses. In addition to being a cost-effective technology, it is a more sustainable alternative to RO due to nutrient and water savings.

5.2.2. Fujifilm Type 16 Membranes

Fujifilm membrane selectivity for monovalent ions was tested for 13 different BGW solutions in order to fully characterize the membranes and their potential for agricultural use. The following conclusions have been reached:

- The CEMs demonstrate for 13 BGW compositions an average calcium selectivity of 0.18±0.08, corresponding to a 3.7 to 10 times reduction of sodium relative to calcium in the diluate stream, and a magnesium selectivity of 0.08±0.04, corresponding to a 8.3 to 26 times reduction of sodium relative to magnesium in the diluate stream.
- The AEMs demonstrate for 13 BGW compositions an average sulfate selectivity of 0.18±0.12, corresponding to a 3.3 to 20 times reduction of chloride relative to sulfate in the diluate stream.
- The average selectivities have a maximum standard deviation of 25 percent. This variation may result from differences in BGW ionic composition and appears to not result from differences in BGW salinity. Consequently, the selectivity values determined in this study for 13 diverse BGW compositions can likely be extended to BGWs across the United States.
- A multi-ionic MSED model predicts ion transport within 6 percent of experimental data.
- The average fertilizer cost savings due to cations ranges from $4,997/ha to $5,028/ha for nine different cases of calcium and magnesium selectivity (average, +stdev., −stdev.). Farm size is a key indicator in determining the payback period for greenhouses. For a 10-hectare farm, the average calcium and magnesium selectivities applied to 6,000 BGWs across the United States yields an average annual fertilizer cost savings of $49,950. This value indicates that the adoption of MSED in place of RO will result in less than a 1-year payback period for greenhouses.
- MSED shows great potential to be used in greenhouses. In addition to being a cost-effective technology, it is a more sustainable alternative to RO due to nutrient and water savings.

5.2.3. Membrane Comparison

- The Fujifilm CEMs show improved monovalent selectivity relative to the Neosepta CEMs. The Fujifilm calcium and magnesium average permselectivity values are 28 percent and 47 percent, respectively, less than those of Neosepta. The lower the permselectivity, the better the monovalent selectivity. Conversely, the Neosepta AEMs outperform the Fujifilm AEMs on average, although by a minimal amount. The average sulfate permselectivity is 4.1 percent greater than that of Neosepta. Overall, Fujifilm membrane performance is superior to that of Neosepta in the BGW salinity range.
- The Fujifilm membranes yield a minimal increase (less than 2 percent) in fertilizer cost savings relative to the Neosepta membranes for the nine considered permselectivity

cases. Consequently, the key consideration in MSED membrane selection becomes cost per membrane area ($/m^2 of A_m). At the lab scale (A_m less than 10 m^2), the Fujifilm membrane cost [97] is approximately $162/m^2 in comparison to the Neosepta membrane cost [96] of $503/m^2, reflecting the promise of the new Fujifilm MSED membranes.

- The minimal difference in fertilizer cost savings at the bench-scale, despite the notable difference in performance between the Fujifilm and Neosepta membranes, suggests that entirely new membranes tailored toward brackish waters like Fujifilm may not need to be developed. Cost-effective manufacturing innovations (e.g., cheaper materials) for membranes already on the market that are tailored toward higher salinities, such as the Neosepta CMS/ACS membranes, may suffice for brackish water applications. However, pilot tests in greenhouses must be conducted to ensure that the membranes perform similarly at scale.

6. Challenges and Recommended Next Steps

6.1. Challenges

The challenges for future development and adoption of this technology are similar to those faced by hard technologies in the water-food-energy space more broadly: the water and agriculture sectors are legacy industries that are resistant to change and risk-averse. A potential solution is to build a partnership with a well-established greenhouse that uses RO to treat its brackish source water, such as those in California, in order to pilot MSED and verify its selective performance at scale. Another challenge for commercialization is the automation of the MSED system to enable the tailoring of product water for particular crops. The existing ion-sensor technologies to continuously measure feedwater and product water composition have relatively large errors (around 20 percent). Feedwater composition is the key input to the developed MSED predictive model and influences membrane performance.

6.2. Recommended Next Steps

- We recommend the following next steps:
- Pilot the MSED system in a greenhouse to ensure that the experimental results scale.
- Use the MSED model to determine optimal operating conditions for MSED in real-world systems and tailor feedwaters to crop-specific needs.

7. References

These references correspond to the methods (Section 3) and results (Section 4). The introduction (Section 1) and background (Section 2) include separate reference subsections.

[1] A. Jägerskog, T. Jønch Clausen, Feeding a Thirsty World – Challenges and Opportunities for a Water and Food Secure Future. Report, 2012.

[2] G.L. Barbosa, F.D. Almeida Gadelha, N. Kublik, A. Proctor, L. Reichelm, E. Weissinger, G.M. Wohlleb, R.U. Halden, Comparison of land, water, and energy requirements of lettuce grown using hydroponic vs. Conventional agricultural methods, Int. J. Environ. Res. Public Health. 12 (2015) 6879–6891. doi:10.3390/ijerph120606879.

[3] HTF Market Intelligence Consulting Pvt Ltd, 2018-2023 Global and Regional Commercial Greenhouse Industry Production, Sales and Consumption Status and Prospects Professional Market Research Report, Edison, New Jersey, USA, 2017.

[4] D. Zarzo, E. Campos, P. Terrero, Spanish experience in desalination for agriculture, Desalin. Water Treat. 51 (2013) 53–66. doi:10.1080/19443994.2012.708155.

[5] E.A. Laate, The Economics of Production and Marketing of Greenhouse Crops in Alberta, 2011.

[6] J.B. Jones, Tomato Plant Culture: In the field, greenhouse and home garden, 1999.

[7] P.H. Gleick, The World's Water 2000–2001: The Biennial Report on Freshwater Resources, Island Press, Washington DC, 2001.

[8] S. Burn, M. Hoang, D. Zarzo, F. Olewniak, E. Campos, B. Bolto, O. Barron, Desalination techniques — A review of the opportunities for desalination in agriculture, Desalination. 364 (2015) 2–16. doi:10.1016/j.desal.2015.01.041.

[9] C. Fritzmann, J. Löwenberg, T. Wintgens, T. Melin, State-of-the-art of reverse osmosis desalination, Desalination. 216 (2007) 1–76. doi:10.1016/j.desal.2006.12.009.

[10] A. Efraty, Variable Pressure Closed Circuit Desalination, WO 2003/013704 A3, 2001.

[11] A. Efraty, R.N. Barak, Z. Gal, Closed circuit desalination — A new low energy high recovery technology without energy recovery, Desalin. Water Treat. 31 (2011) 95–101. doi:10.5004/dwt.2011.2402.

[12] K.G. Nayar, N.C. Wright, G.P. Thiel, A.G. Winter, J.H. Lienhard, Energy Requirement of Alternative Technologies for Desalinating Groundwater for Irrigation, in: Int. Desalin. Assoc. World Congr. 2015, San Diego, USA, 2015.

[13] D.M. Warsinger, E.W. Tow, K.G. Nayar, L.A. Maswadeh, J.H. Lienhard, Energy efficiency of batch and semi-batch (CCRO) reverse osmosis desalination, Water Res. 106 (2016). doi:10.1016/j.watres.2016.09.029.

[14] W.E. Katz, The electrodialysis reversal (EDR) process, Desalination. 28 (1979) 31–40. doi:10.1016/S0011-9164(00)88124-2.

[15] H. Strathmann, Electrodialysis, a mature technology with a multitude of new applications, Desalination. 264 (2010) 268–288. doi:10.1016/j.desal.2010.04.069.

[16] K.M. Chehayeb, D.M. Farhat, K.G. Nayar, J.H. Lienhard, Optimal design and operation of electrodialysis for brackish-water desalination and for high-salinity brine concentration, Desalination. 420 (2017) 167–182. doi:10.1016/j.desal.2017.07.003.

[17] D.W. Bian, S.M. Watson, N.C. Wright, S.R. Shah, T. Buonassisi, D. Ramanujan, I.M. Peters, A.G. Winter, Optimization and design of a low-cost, village-scale, photovoltaic-powered, electrodialysis reversal desalination system for rural India, Desalination. 452 (2019) 265–278. doi:10.1016/j.desal.2018.09.004.

[18] G. Saracco, M.C. Zanetti, M. Onofrio, Novel application of monovalent-ion-permselective membranes to the recovery treatment of an industrial wastewater by electrodialysis, Ind. Eng. Chem. Res. 32 (1993) 657–662. doi:10.1021/ie00016a012.

[19] B. Cohen, N. Lazarovitch, J. Gilron, Upgrading groundwater for irrigation using monovalent selective electrodialysis, Desalination. 431 (2018) 126–139. doi:10.1016/j.desal.2017.10.030.

[20] K.G. Nayar, J. Fernandes, R.K. McGovern, K.P. Dominguez, A. McCance, B. Al-Anzi, J.H. Lienhard, Cost and energy requirements of hybrid RO and ED brine concentration systems for salt production, Desalination. 456 (2019) 97–120. doi:10.1016/j.desal.2018.11.018.

[21] Y. Zhang, S. Paepen, L. Pinoy, B. Meesschaert, B. Van Der Bruggen, Selectrodialysis: Fractionation of divalent ions from monovalent ions in a novel electrodialysis stack, Sep. Purif. Technol. 88 (2012) 191–201. doi:10.1016/j.seppur.2011.12.017.

[22] M. Reig, C. Valderrama, O. Gibert, J.L. Cortina, Selectrodialysis and bipolar membrane electrodialysis combination for industrial process brines treatment: Monovalent-divalent ions separation and acid and base production, Desalination. 399 (2016) 88–95. doi:10.1016/j.desal.2016.08.010.

[23] A.E.R. Reahl, Half A Century of Desalination With Electrodialysis, 2006.

[24] N.C. Wright, A.G. Winter, Justification for community-scale photovoltaic-powered electrodialysis desalination systems for inland rural villages in India, Desalination. 352 (2014) 82–91. doi:10.1016/j.desal.2014.07.035.

[25] N.C. Wright, S.R. Shah, S.E. Amrose, A.G. Winter, A robust model of brackish water electrodialysis desalination with experimental comparison at different size scales, Desalination. 443 (2018) 27–43. doi:10.1016/j.desal.2018.04.018.

[26] B. Pilat, Water of high quality for household conditions, Desalination. 153 (2003) 405–407. doi:10.1016/S0011-9164(02)01135-9.

[27] K.G. Nayar, P. Sundararaman, J.D. Schacherl, C.L. O'Connor, M.L. Heath, M.O. Gabriel, N.C. Wright, A.G. Winter, Feasibility study of an electrodialysis system for in-

home water desalination and purification in urban India, in: Proc. ASME Des. Eng. Tech. Conf., 2015.

[28] K.G. Nayar, P. Sundararaman, C.L. O'Connor, J.D. Schacherl, M.L. Heath, M.O. Gabriel, S.R. Shah, N.C. Wright, A.G. Winter, Feasibility study of an electrodialysis system for in-home water desalination in urban India, Dev. Eng. 2 (2017) 38–46. doi:10.1016/j.deveng.2016.12.001.

[29] H. Kawate, K. Miyaso, M. Takiguchi, Energy Savings in Salt Manufacture by Ion Exchange Membrane Electrodialysis, Sixth Int. Symp. Salt. 2 (1983) 471–479.

[30] U. Yermiyahu, A. Tal, A. Ben-Gal, A. Bar-Tal, Rethinking Desalinated Water Quality and Agriculture, Science (80-.). 318 (2007) 920–921.

[31] A. Ben-Gal, U. Yermiyahu, S. Cohen, Fertilization and blending alternatives for irrigation with desalinated water., J. Environ. Qual. 38 (2009) 529–536. doi:10.2134/jeq2008.0199.

[32] G. Saracco, M.C. Zanetti, Ion transport through monovalent-anion-permselective membranes, Ind. Eng. Chem. Res. 33 (1994) 96–101. doi:10.1021/ie00025a013.

[33] G. Saracco, Transport properties of monovalent-ion-permselective membranes, Chem. Eng. Sci. 52 (1997) 3019–3031. doi:10.1016/S0009-2509(97)00107-3.

[34] FUJIFILM Manufacturing Europe B.V, Personal Communication to Kishor Nayar, (2019). https://www.fujifilmmembranes.com/about-us.

[35] R.K. McGovern, S.M. Zubair, J.H. Lienhard, The benefits of hybridising electrodialysis with reverse osmosis, J. Memb. Sci. 469 (2014) 326–335. doi:10.1016/j.memsci.2014.06.040.

[36] H.-J. Lee, F. Sarfert, H. Strathmann, S.-H. Moon, Designing of an electrodialysis desalination plant, in: Desalination, 2002: pp. 267–286. doi:10.1016/S0011-9164(02)00208-4.

[37] A. Al-Karaghouli, L.L. Kazmerski, Energy consumption and water production cost of conventional and renewable-energy-powered desalination processes, Renew. Sustain. Energy Rev. (2013). doi:10.1016/j.rser.2012.12.064.

[38] Cuesta Roble Greenhouse Vegetable Consulting, International Greenhouse Vegetable Production - Statistics, Mariposa, CA, 2017. https://www.cuestaroble.com/statistics.htm.

[39] Vermont Natural Resources Council, Appendix B: Water pricing in other U.S. states, in: Tax. Vermont's Groundw., Vermont Natural Resources Council, 2013. http://vnrc.org/wp-content/uploads/2013/11/Appendix-B.pdf.

[40] L. Dale, Clarifying and Quantifying Current and Near-Term Groundwater Pumping Energy Use and Costs in California, in: 2016 Epic Symp., Lawrence Berkley National Laboratory, 2016: p. 15. https://www.energy.ca.gov/research/epic/documents/2016-12-01_symposium/presentations/1-07_Californias_Groundwater_Pumping-The_Energy_Perspective.pdf.

[41] United States Department of Agriculture, Irrigated Agriculture in the United States, Dataset 3. Average irrigation statistics (by water source) and purchased water cost statistics (per acre or per acre-foot), 2017. https://www.ers.usda.gov/webdocs/DataFiles/83358/Set 3. Average irrigation statistics (by water source) and purchased water cost statistics.

[42] Water in the West, Understanding California's Groundwater, 2019. http://web.stanford.edu/group/waterinthewest/documents/Rechargev4.pdf.

[43] Metropolitan Water District of Southern California, VENTURA COUNTY WATERWORKS DISTRICT NO. 1 WATER RATES & MONTHLY SERVICE CHARGES COMMODITY, Ventura County, 2018. http://www.mwdh2o.com/2018 Background Materials/Ventura County Waterworks Districts Rates 2018.pdf.

[44] Forever Pure, Brackish Water Reverse Osmosis System Price List For TDS < 5000 mg/l, 2010. http://www.frantechasia.com/company_images/BWRO Various Configurations Specifications and Price list -2010.pdf.

[45] Pure Aqua Inc., Personal Communication to Kishor Nayar, (2017). https://www.pureaqua.com/commercial-brackish-water-reverse-osmosis-bwro-systems/.

[46] US Water Systems, US Water Systems 2000 GPD AR-5-2000, (2017). https://www.uswatersystems.com/us-water-2-000-gpd-american-revolution-commercial-reverse-osmosis-system-ar-5-2000.html (accessed July 10, 2017).

[47] Lubron Waterbehandeling B.V, Lubron Water Technologies, (2018). http://www.lubronwaterbehandeling.nl.

[48] Ampac USA, Personal Communication to Kishor Nayar, (2017).

[49] Desalitech, Personal Communication to Kishor Nayar, (2019).

[50] E.T. Sajtar, D.M. Bagley, Electrodialysis reversal: Process and cost approximations for treating coal-bed methane waters, Desalin. Water Treat. 2 (2009) 284–294. doi:10.5004/dwt.2009.259.

[51] R.K. McGovern, A.M. Weiner, L. Sun, C.G. Chambers, S.M. Zubair, J.H. Lienhard, On the cost of electrodialysis for the desalination of high salinity feeds, Appl. Energy. 136 (2014) 649–661. doi:10.1016/j.apenergy.2014.09.050.

[52] K.G. Nayar, J. Fernandes, R.K. McGovern, B.S. Al-Anzi, J.H. Lienhard, Cost and energy needs of RO-ED-crystallizer systems for zero brine discharge seawater desalination, Desalination. 457 (2019) 115–132. doi:10.1016/j.desal.2019.01.015.

[53] K.G. Nayar, Improving Seawater Desalination and Seawater Desalination Brine Management, Massachusetts Institute of Technology, 2019.

[54] Suez Water Technologies & Solutions, RO Tools: Cost of Operations, (2019). https://rotools.suezwatertechnologies.com/Cost-Of-OperationsNo Title (accessed March 16, 2019).

[55] DesalData, DesalData Projects, (2019). https://www.desaldata.com/projects (accessed May 22, 2019).

[56] P. Dlugolkecki, B. Anet, S. J. Metz, K. Nijmeijer, M. Wessling, Transport limitations in ion exchange membranes at low salt concentrations, Journal of Membrane Science 346 (1) (2010) 163–171.

[57] H. Strathmann, Ion-exchange membrane separation processes, Vol. 9, Elsevier, 2004.

[58] G. M. Geise, A. J. Curtis, M. C. Hatzell, M. A. Hickner, B. E. Logan, Salt concentration differences alter membrane resistance in reverse electrodialysis stacks, Environmental Science & Technology Letters 1 (1) (2013) 36–39.

[59] Firdaous, J. Maleriat, J. Schlumpf, F. Qu´ em´ eneur,´ Transfer of monovalent and divalent cations in salt solutions by electrodialysis, Separation Science and Technology 42 (5) (2007) 931–948. arXiv:https://doi.org/10.1080/01496390701206413, doi:10.1080/01496390701206413.URL https://doi.org/10.1080/01496390701206413.

[60] Ameridia Innovative Solutions, Inc., Personal communication to Yvana Ahdab (2019). URL http://www.eurodia.com/index.php/en/the-eurodia-group.

[61] Agvise Laboratories, Soil amendments (2019).

[62] Agricultural Service Laboratory, Fertility recommendations: Small area (square footage) (2019).

[63] Amazon.com, Inc., Product: Calcium sulfate dihydrate - gypsum - caso42h2o - 5 pounds. URL: https://www.amazon.com/Calcium-Sulfate-Dihydrate-%20Gypsum-CaSO42H2O/dp/B008LEV0V0/ref=sr_1_8?keywords=gypsum&qid=1566234006&s=gateway&sr=8-8

[64] Amazon.com, Inc., Product: Epsoak epsom salt - 5 lbs. magnesium sulfate usp. URL. https://www.amazon.com/Epsoak-Epsom-Salt-Magnesium-%20Sulfate/dp/B004N79BYC/ref=asc_df_B004N79BYC/?tag=hyprod%2020&linkCode=df0&hvadid=198090695510&hvpos=1o1&hvnetw=g&hvrand=8657695814199950374&hvpone=&hvptwo=&hvqmt=&hvdev=c&hvdvc%20mdl=&hvlocint=&hvlocphy=9002000&hvtargid=pla-380366446553&psc=1

[65] U. Yermiyahu, A. Tal, A. Ben-Gal, A. Bar-Tal, J. Tarchitzky, O. Lahav, Rethinking desalinated water quality and agriculture, Science 318 (5852) (2007) 920–921. arXiv:https://science.sciencemag.org/content/318/5852/920.full.pdf, doi:10.1126/science.1146339.

[66] E. Will, J. Faust, Irrigation water quality for greenhouse production, Agricultural Extention Service, The University of Tennessee (1999).

[67] U.S. Department of Agriculture, 2007 census of agriculture (2007). URL https://www.nass.usda.gov/Publications/AgCensus/2007/Online_Highlights/Ag_Atlas_Maps/Farms/Land_in_Farms_and_Land_Use/07-M079.php

[68] K. G. Nayar, J. H. Lienhard, Brackish water desalination for greenhouse agriculture: Comparing the costs of RO, CCRO, EDR, and monovalent-selective EDR, Desalination 475 (2020) 114188.

[69] T. Tetreault, SBA loan rates 2019 – current interest rates and how they work (2019). URL https://fitsmallbusiness.com/sba-loan-rates/

[70] United Nations, World Water Development Report 2020: Water and Climate Change. 2020; https://unesdoc. unesco.org/ark:/48223/pf0000372985.locale=en, Accessed June 10, 2020.

[71] Hunter, M. C.; Smith, R. G.; Schipanski, M. E.; Atwood, L. W.; Mortensen, D. A. Agriculture in 2050: Recalibrating Targets for Sustainable Intensification. BioScience 2017, 67, 386–391, DOI: 10.1093/biosci/bix010.

[72] Foley, J. A five-step plan to feed the world. https://www.nationalgeographic.com/foodfeatures/ feeding-9-billion/, Accessed May 15, 2020.

[73] Stanton, J. S.; Anning, D. W.; Brown, C. J.; Moore, R. B.; McGuire, V. L.; Qi, S. L.; Harris, A. C.; Dennehy, K. F.; McMahon, P. B.; Degnan, J. R.; Böhlke, J. Brackish groundwater in the United States. U.S. Geological Survey Professional Paper 1833 2017, 185, DOI: https://doi.org/10.3133/pp1833.

[74] Cohen-Tanugi, D.; Grossman, J. C. Water desalination across nanoporous graphene. Nano letters 2012, 12, 3602–3608, DOI: https://doi.org/10.1021/nl3012853.

[75] Song, L.; Schuetze, B.; Rainwater, K. Demonstration of a High Recovery and Energy Efficient RO System for Small-Scale Brackish Water Desalination. 2012; https://www.twdb.texas.gov/innovativewater/ desal/projects/texastech/doc/texas_tech_final_rpt.pdf, Accessed July 12, 2019.

[76] Strathmann, H. Electrodialysis, a mature technology with a multitude of new applications. Desalination 2010, 264, 268–288, DOI: https://doi.org/10.1016/j.desal.2010.04.069.

[77] Kawate, H.; Miyaso, K.; Takiguchi, M. Energy savings in salt manufacture by ion exchange membrane electrodialysis. Sixth International Symposium on Salt. Toronto, Canada, 24-28 May 1983, Vol. II, pp. 471–479.

[78] Saracco, G.; Zanetti, M. C. Ion transport through monovalent-anion-permselective membranes. Industrial & Engineering Chemistry Research 1994, 33, 96–101, DOI: https://doi.org/10.1021/ie00025a013.

[79] Saracco, G. Transport properties of monovalent-ion-permselective membranes. Chemical Engineering Science 1997, 52, 3019–3031, DOI: https://doi.org/10.1016/S0009-2509(97)00107-3.

[80] Luo, T.; Abdu, S.; Wessling, M. Selectivity of ion exchange membranes: A review. Journal of Membrane Science 2018, 555, 429–454, DOI: https://doi.org/10.1016/j.memsci.2018.03.051.

[81] Jiang, W.; Lin, L.; Xu, X.; Wang, H.; Xu, P. Physicochemical and electrochemical characterization of cation-exchange membranes modified with polyethyleneimine for elucidating enhanced monovalent permselectivity of electrodialysis. Journal of Membrane Science 2019, 572, 545–556, DOI: https://doi.org/10.1016/j.memsci.2018.11.038.

[82] Ahdab, Y. D.; Rehman, D.; Lienhard, J. H. Brackish water desalination for greenhouses: improving groundwater quality for irrigation using monovalent selective electrodialysis reversal. Journal of Membrane Science 2020, DOI: https://doi.org/10.1016/j.memsci.2020.118072.

[83] Chen, G.; Wei, K.; Hassanvand, A.; Freeman, B.; Kentish, S. Single and binary ion sorption equilibria of monovalent and divalent ions in commercial ion exchange membranes. Water Research 2020, 175, 115681, DOI: https://doi.org/10.1016/j.watres.2020.115681.

[84] Ahdab, Y. D.; Thiel, G. P.; Böhlke, J.; Stanton, J.; Lienhard, J. H. Minimum energy requirements for desalination of brackish groundwater in the United States with comparison to international datasets. Water Research 2018, 141, 387–404, DOI: https://doi.org/10.1016/j.watres.2018.04.015.

[85] Rehman, D.; Ahdab, Y.; Lienhard, J. H. Improving groundwater quality for irrigation using monovalent selective electrodialysis. IDA World Congress on Desalination and Water Use . Dubai, UAE, 20-24 Oct. 2019. No. IDAWC19-Rehman. https://dspace.mit.edu/handle/1721.1/124385.

[86] Qi, S.; Harris, A. Geochemical Database for the Brackish Groundwater Assessment of the United States: Data Release; U.S. Geological Survey, 2017; DOI: https://doi.org/10.5066/F72F7KK1.

[87] Ayers, R. S.; Westcot, D. W. Water quality for agriculture; Food and Agriculture Organization of the United Nations, 1985; Vol. 29.

[88] Cobban, B.; Faller, K. Electrodialysis and electrodialysis reversal: M38; American Water Works Association, 1995; Vol. 38.

[89] McGovern, R. K.; Weiner, A. M.; Sun, L.; Chambers, C. G.; Zubair, S. M.; Lienhard, J. H. On the cost of electrodialysis for the desalination of high salinity feeds. Applied Energy 2014, 136, 649–661, DOI: https://doi.org/10.1016/j.apenergy.2014.09.050.

[90] Firdaous, L.; Malériat, J.; Schlumpf, J.; Quéméneur, F. Transfer of Monovalent and Divalent Cations in Salt Solutions by Electrodialysis. Separation Science and Technology 2007, 42, 931–948, DOI: 10.1080/01496390701206413.

[91] Yermiyahu, U.; Tal, A.; Ben-Gal, A.; Bar-Tal, A.; Tarchitzky, J.; Lahav, O. Rethinking Desalinated Water Quality and Agriculture. Science 2007, 318, 920–921, DOI: 10.1126/science.1146339.

[92] Will, E.; Faust, J. PB1617-Irrigation Water Quality for Greenhouse Production. 1999; http://trace. tennessee.edu/utk_agexcomhort/5, Accessed Aug 7, 2019.

[93] Nayar, K. G.; Lienhard, J. H. Brackish water desalination for greenhouse agriculture: Comparing the costs of RO, CCRO, EDR, and monovalent-selective EDR. Desalination 2020, 475, 114188, DOI: https://doi.org/10.1016/j.desal.2019.114188.

[94] Alpha chemicals, Product: Calcium Sulfate Dihydrate - CaSO4*2H2O. https://alphachemicals.com/ calcium_sulfate, Accessed July 17, 2019. PowerGrow Systems, Product: Epsom Salt - Agricultural Grade. https://www.powergrowsystems.com/products/epsom-salt-magnesium-sulfate-agricultural-grade? variant=40175466190, Accessed July 17, 2019.

[95] Tetreault, T. SBA Loan Rates 2019 – Current Interest Rates and How They Work. 2019; https:// fitsmallbusiness.com/sba-loan-rates/, Accessed Jan 10, 2020. FUJIFILM

[96] Ameridia Innovative Solutions, Inc., Daniel Bar, Personal Communication to Yvana Ahdab. 2019; http:// www.eurodia.com/index.php/en/the-eurodia-group, Accessed June 15, 2019.

[97] Manufacturing Europe B.V., Jeroen van Nunen, Personal Communication to Yvana Ahdab. 2020; https://www.fujifilmmembranes.com/, Accessed June 15, 2019.

[80] Luo, T.; Abdu, S.; Wessling, M. Selectivity of ion exchange membranes: A review. Journal of Membrane Science 2018, 555, 429–454, DOI: https://doi.org/10.1016/j.memsci.2018.03.051.

[81] Jiang, W.; Lin, L.; Xu, X.; Wang, H.; Xu, P. Physicochemical and electrochemical characterization of cation-exchange membranes modified with polyethyleneimine for elucidating enhanced monovalent permselectivity of electrodialysis. Journal of Membrane Science 2019, 572, 545–556, DOI: https://doi.org/10.1016/j.memsci.2018.11.038.

[82] Ahdab, Y. D.; Rehman, D.; Lienhard, J. H. Brackish water desalination for greenhouses: improving groundwater quality for irrigation using monovalent selective electrodialysis reversal. Journal of Membrane Science 2020, DOI: https://doi.org/10.1016/j.memsci.2020.118072.

[83] Chen, G.; Wei, K.; Hassanvand, A.; Freeman, B.; Kentish, S. Single and binary ion sorption equilibria of monovalent and divalent ions in commercial ion exchange membranes. Water Research 2020, 175, 115681, DOI: https://doi.org/10.1016/j.watres.2020.115681.

[84] Ahdab, Y. D.; Thiel, G. P.; Böhlke, J.; Stanton, J.; Lienhard, J. H. Minimum energy requirements for desalination of brackish groundwater in the United States with comparison to international datasets. Water Research 2018, 141, 387–404, DOI: https://doi.org/10.1016/j.watres.2018.04.015.

[85] Rehman, D.; Ahdab, Y.; Lienhard, J. H. Improving groundwater quality for irrigation using monovalent selective electrodialysis. IDA World Congress on Desalination and Water Use . Dubai, UAE, 20-24 Oct. 2019. No. IDAWC19-Rehman. https://dspace.mit.edu/handle/1721.1/124385.

[86] Qi, S.; Harris, A. Geochemical Database for the Brackish Groundwater Assessment of the United States: Data Release; U.S. Geological Survey, 2017; DOI: https://doi.org/10.5066/F72F7KK1.

[87] Ayers, R. S.; Westcot, D. W. Water quality for agriculture; Food and Agriculture Organization of the United Nations, 1985; Vol. 29.

[88] Cobban, B.; Faller, K. Electrodialysis and electrodialysis reversal: M38; American Water Works Association, 1995; Vol. 38.

[89] McGovern, R. K.; Weiner, A. M.; Sun, L.; Chambers, C. G.; Zubair, S. M.; Lienhard, J. H. On the cost of electrodialysis for the desalination of high salinity feeds. Applied Energy 2014, 136, 649–661, DOI: https://doi.org/10.1016/j.apenergy.2014.09.050.

[90] Firdaous, L.; Malériat, J.; Schlumpf, J.; Quéméneur, F. Transfer of Monovalent and Divalent Cations in Salt Solutions by Electrodialysis. Separation Science and Technology 2007, 42, 931–948, DOI: 10.1080/01496390701206413.

[91] Yermiyahu, U.; Tal, A.; Ben-Gal, A.; Bar-Tal, A.; Tarchitzky, J.; Lahav, O. Rethinking Desalinated Water Quality and Agriculture. Science 2007, 318, 920–921, DOI: 10.1126/science.1146339.

[92] Will, E.; Faust, J. PB1617-Irrigation Water Quality for Greenhouse Production. 1999; http://trace. tennessee.edu/utk_agexcomhort/5, Accessed Aug 7, 2019.

[93] Nayar, K. G.; Lienhard, J. H. Brackish water desalination for greenhouse agriculture: Comparing the costs of RO, CCRO, EDR, and monovalent-selective EDR. Desalination 2020, 475, 114188, DOI: https://doi.org/10.1016/j.desal.2019.114188.

[94] Alpha chemicals, Product: Calcium Sulfate Dihydrate - CaSO4*2H2O. https://alphachemicals.com/ calcium_sulfate, Accessed July 17, 2019. PowerGrow Systems, Product: Epsom Salt - Agricultural Grade. https://www.powergrowsystems.com/products/epsom-salt-magnesium-sulfate-agricultural-grade? variant=40175466190, Accessed July 17, 2019.

[95] Tetreault, T. SBA Loan Rates 2019 – Current Interest Rates and How They Work. 2019; https:// fitsmallbusiness.com/sba-loan-rates/, Accessed Jan 10, 2020. FUJIFILM

[96] Ameridia Innovative Solutions, Inc., Daniel Bar, Personal Communication to Yvana Ahdab. 2019; http:// www.eurodia.com/index.php/en/the-eurodia-group, Accessed June 15, 2019.

[97] Manufacturing Europe B.V., Jeroen van Nunen, Personal Communication to Yvana Ahdab. 2020; https://www.fujifilmmembranes.com/, Accessed June 15, 2019.